



UNIVERSITY OF AGDER
FACULTY OF ENGINEERING AND SCIENCE

OFFSHORE WIND POWER TECHNOLOGY
DEVELOPMENT AND TESTING OF A DOWNSCALED PITCH CONTROLLED
WIND TURBINE

MASTER THESIS, SPRING 2015

BY

ANITA BRATBAK
HÅVARD FRØLAND

SUPERVISOR:
GEIR HOVLAND

This master's thesis is carried out and approved as a part of the education at the University of Agder. However, this does not imply that the University is responsible for the methods that are used or the conclusions that are drawn in this thesis.

MAY 20, 2015

FACULTY OF ENGINEERING AND SCIENCE
DEPARTMENT OF ENGINEERING SCIENCES
UNIVERSITY OF AGDER

Abstract

The energy demand of the world increases day by day, and at the same time people become more aware of the impact fossil energy sources have on the climate. This leads to an increased focus on renewable energy sources, such as wind power, which has been pointed out as an important contributor to the production of renewable energy. In recent years the focus has shifted from land based wind farms towards the possibilities of the large energy potential that exist in the open ocean along the coast line.

The background of the thesis is motivated by the increased focus on offshore wind power technology. State of the art technology in the field of floating offshore wind power was reviewed in the first part in addition to relevant background theory regarding design and operation of wind turbines. The main objective has been to develop and test a downscaled pitch controlled wind turbine. A pitch mechanism was designed to turn the blade pitch angle to a given angle with a stepper motor. The stepper motor transfers rotational movement with a leading screw to translational movement of a sliding mechanism. The sliding mechanism rotates the angle of the blade shaft to the optimal calculated angle. Control of the stepper motor is achieved by a PLC step drive and a ladder diagram describing the desired functionality. Optimized pitch angles are calculated and implemented as a function with the current wind speed as input. The wind speed is measured with an anemometer and connected to the PLC as an analogue signal. From the PLC the signals are logged with an OPC server and processed in Excel.

The wind turbine was tested on the campus roof top. The cut-in speed was as expected, and the turbine require between 3 and 5 m/s to start to rotate depending on the angle of the wind, while cut-out speed is around 17 m/s, due to high risk of malfunction and destruction of parts or components. The voltage was measured to be around 150-250 mV at optimal wind speed 9 m/s and the maximum obtained shaft speed generated about 280 mV. More extensive testing should be performed in order to obtain more reliable results and complete verify the model. Some improvements has been discussed, including implementing a gearbox, redesigning the blades with a different profile as well as material. A proper test site with more easily controllable wind speeds is preferable.

Preface

The present thesis, entitled “Development of Motion-Compensated Controller for a Floating Wind Turbine” is the final work on a two year master’s degree in Mechatronics and Renewable Energy. The work with the master’s thesis was carried out at UiA, Department of Engineering, during the spring of 2014. The problem text was formulated by ourselves in cooperation with supervisor Professor Geir Hovland, and is intended to mark the beginning of more bachelor and master projects at UiA involving wind energy in the future.

The report primarily consists of two main parts. In the first part, relevant theory explained and methods used during the work is discussed. The second part contains the analyses performed, and corresponding results with relevant discussions, as well as further work and improvements of the model. The figures presented in this thesis is self-produced, if otherwise not mentioned.

Several persons has in various degree helped and guided us, during the work with the present thesis. Without their contribution, the work would have been a lot harder and the result far worse. We are especially grateful to our main supervisor, Professor Geir Hovland, for the opportunity to work with wind turbines, for invaluable guidance and interesting discussions. We would also like to thank him for providing us with an interesting and inspiring subject for this thesis. Program Coordinator Stein Bergsmark, deserves many thanks for help and guidance with the report.

We would also like to thank Post-Doc Knut Berg Kallestad for help with developing the 3D model and 3D printing. He has always an open door, answered all over questions and given valuable guidance with the design of the test model. A huge thanks to the lab engineers of UiA, especially Roy Werner Folgerø, Carl Thomas Duus and Jan Andreas Holm who always helped when the need was great. Peter Hugh Middleton helped us with various design improvements and guidance regarding the gearbox and for that we are grateful. The schools maintenance staff deserves many thanks for lending us equipment as well as allow us to use the roof top as our main test site, both night and day. Our fellow students at mechatronics and renewable energy also deserves our gratitude for support and helpful advices during difficult decisions and times with particularly high workload, in addition to creating a good working environment.

Our best wishes to all readers. We hope you like our work.

Grimstad, May 20, 2015

Anita Bratbak

Håvard Frøland

Nomenclature

In the tables below some important symbols are defined and explained. Symbols are in addition explained in the text.

Symbol	Meaning
α	Angle of attack [$^{\circ}$]
β	Pitch angle [$^{\circ}$]
η	Gearbox efficiency [-]
ρ	Density of the air [-]
ω	Angular velocity [rad/s]
Ω	Tip speed [m/s]
a	Induction factor [-]
a'	Angular induction factor [-]
A	Area [m^2]
A	Projected airfoil area [m]
C_l	Lift coefficient [-]
C_d	Drag coefficient [-]
C_m	Pitching moment coefficient [-]
c_p	Power coefficient [-]
c_T	Thrust coefficient [-]
c	Scale factor [-]
C	Chord [-]
dr	The circular element [m]
$H_{\frac{1}{3}}$	Significant wave height [m]
I	Current [A]
i	Gear ratio [-]
j	Rank number [-]
k	Shape factor [-]
M_F	Torque on [Nm]
M_S	Torque on low speed shaft [Nm]
N	Section number [-]
P_{calc}	Calculated power from generator [W]
P_{mech}	Available wind power [W]
P_{wind}	Theoretical wind power [W]

r	Distance from center to the circular element [m]
$T_{\frac{1}{3}}$	Significant wave period [t]
U	Free stream velocity [m/s]
U	Voltage [<i>Volt</i>]
v_0	Unaffected wind speed [$\frac{m}{s}$]
v_w	Wind speed [m/s]
z_0	Ground roughness [m]
z_1	Measuring height [m]
z_2	Hub height [m]

Abbreviations

In the tables below some important abbreviations are defined and explained. Abbreviations are in addition explained first time they occur in the text.

Abbreviation	Meaning
BET	Blade Element Theory
CV	Control Volume
DAQ	Data Acquisition
FAST	Fatigue, Aerodynamics, Structures and Turbulence
FOWT	Floating Offshore Wind Turbine
HAWT	Horizontal Axis Wind Turbine
MT	Momentum Theory
OPC	Open Platform Communications
PLC	Programmable Logic Controller
SKF	Svenska Kullagerfabriken
RPM	Revolution per minute
TSR	Tip Speed Ratio
VAWT	Vertical Axis Wind Turbine
WTG	Wind Turbine Generator

List of Figures

2.1	An example Weibull distribution of measured wind at a given location	8
2.2	Waves approaching shallow water	9
2.3	Definition of waves, downward crossing [1]	9
2.5	Waves parameters	10
2.6	Aerodynamic properties of an airfoil	11
2.7	The principle of stall in aerodynamics	12
2.8	The principles of the momentum theory	13
2.9	The principles of the blade element theory	14
2.11	Power curves for different control strategies	21
2.12	Description of airfoil with relevant parameters	23
2.13	Fixed turbine setup	23
2.14	Feedback control structure of the pitch controller	24
2.15	Yaw control system	25
2.18	A photo from the transportation process of the Hywind turbine [2]	29
2.19	Two different floating offshore wind turbine design: HiPRWind Project [3] and the WindFloat project [4]	31
2.20	The floating structure of the Fukushima FORWARD Project [5]	31
2.21	A screen capture from the SIMO software [6]	32
2.22	Degrees of freedom for an offshore floating wind turbine platform	34
2.23	The Stewart platform located at UiA, [7]	35
3.1	Concept of Test Turbine Model	37
3.2	Shape of the blade sections	38
3.3	Wind turbine test model: Structure of the blade	38
3.4	Wind turbine test model: Gear and Pinions	38
3.6	The stepper motor from RS components connected to the Siemens Simatic et200s PLC via 1-Step-Drive from Phytron	40
3.7	Test turbine model: Pitch mechanism	41
3.8	Test turbine model: Lift mechanism	42
3.9	Test turbine model: Slider mechanism	43
3.10	Positioning of bearings and slider mechanism	43
3.11	Bearing between the gear and the lift mechanism	44
3.12	Bearing between main shaft and the support structure	44
3.13	Bearing between the support structure and the main shaft	45
3.14	The tower structure for the wind turbine	46
3.15	Welding robot from ABB at the University	46
3.16	The finished print of the bevel gears in housing	47
3.17	The main body mounted on the tower structure with the plc placed below on the bracing	48
3.18	Final model with PLC	48

3.19	Stepper motor support structure	49
3.20	Mounting of the blades	49
3.21	Support rig of the blades	50
3.22	The LabVIEW program developed to log the data from the generator	51
3.23	Relationship between voltage and rotational speed in the generator	51
3.24	Link positions, all dimensions given in mm and degrees	52
3.25	The stepper motor used in this project	53
3.26	The relationship between the blade angle and the linear screw distance.	56
3.27	The relationship between the wind speed and a optimized pitch angle	57
3.28	Flowchart showing the main operations of the PLC program.	58
3.29	Descision block for achieved windspeed.	59
3.30	Function call for the direction and number of steps for the step drive.	59
3.31	Function call that tracks the slider position.	60
3.32	The function call which tracks when the number of steps needed to pitch the blades has been met.	60
3.35	Forces acting on the turbine blades	68
3.36	Forces acting on the bevel gears	69
3.37	Forces acting on the bevel gears	70
3.38	Forces acting on the support rig	70
3.39	Forces acting on the support rig	71
3.40	Forces acting on the tower main shaft	71
3.41	Forces acting on the tower construction	72
4.1	Overview of test site	73
4.2	Schematic diagram of the test setup	74
4.3	Experimental test setup	74
4.4	The LabVIEW program developed to log the wind measurements	75
4.5	Setup of a PI system	76
4.6	The Relationship between generated voltage and wind speed	78
4.7	The Relationship between generated voltage and wind speed	78
4.8	Relationship between shaft speed and voltage of the generator	78
4.9	Relationship between tipshaft speed and voltage of the generator	79
4.10	The calculated shaft speed at wind speeds from cut-in to cut-out	81
4.11	The calculated tip speed at wind speeds from cut-in to cut-out	81
4.12	Measuring current and voltage of test model generator	83
4.13	The calculated power with respect to rotational speed	84
4.14	Voltage generated between 5 and 10 m/s wind speed	85
4.15	The gearbox selected for this application [8]	86

List of Tables

3.1	Design Specification of Wind Turbine	37
3.2	Data for stepper motor 440-470	39
3.3	Gear parameters	41
3.4	Pinion parameters	42
3.5	Values for beta and deviation	55
3.6	List of networks and functions therein.	61
3.7	Device configuration in PLC.	62
3.8	Maximum Power Coefficient	64
3.9	Turbine design parameters from 0 m/s to rated wind speed	66
3.10	Turbine design parameters for operation during wind speeds above the rated wind speed	67
4.1	Tags created PI System Management Tools for logging in the PI Server	77
4.2	Test run of stepper motor in the lab.	80
4.3	Test run of stepper motor in the lab.	80
4.4	Design Specification of Wind Turbine	84

Contents

Abstract	i
Preface	ii
Nomenclature	iii
Abbreviations	v
List of Figures	vi
List of Tables	viii
Table of Contents	xi
1 Introduction	1
1.1 Purpose and Scope	1
1.2 Motivation	2
1.3 Problem Definition	3
1.3.1 Research Questions	3
1.3.2 Limitations	3
1.4 Solution Strategy	3
1.5 Report Outline	4
2 Theoretical Background	5
2.1 Environmental Aspects	5
2.1.1 Wind Properties	5
2.1.2 Wind Distribution	7
2.1.3 Waves	8
2.2 Aerodynamics	11
2.2.1 Blade Element Momentum Theory	12
2.3 Wind Turbines	15
2.3.1 Inside The Wind Turbine’s Main Body	15
2.3.2 Wind Turbine Operation	19
2.4 Wind Turbine Control	20
2.4.1 Fixed Pitch	23
2.4.2 Stall Control	23
2.4.3 Pitch Controller	24
2.4.4 Yaw Controller	24
2.5 State of The Art: Floating Offshore Wind Turbine Devices	25
2.5.1 Platform Topologies and Anchoring Systems	26
2.5.2 Prototypes and Design Concepts	29

2.5.3	Design Tools and Simulation Programs	32
2.5.4	The Future of Offshore Wind: Challenges	32
2.6	Motion-Compensation	34
2.6.1	Stewart-Platform	34
3	Methods and Tools	36
3.1	Wind Turbine Test Model Design	36
3.1.1	Concept	36
3.1.2	Blades	37
3.1.3	Stepper Motor	39
3.1.4	Pitch Control System	40
3.1.5	The Selection and Location of Bearings	43
3.2	Experimental Setup	45
3.2.1	Assembly of the Turbine	45
3.2.2	Optimized Functions For PLC: Control of Stepper	51
3.2.3	Programmable Logic Controller	57
3.3	Wind Turbine Design Calculations	63
3.3.1	Optimized β	64
3.4	Load Considerations	68
3.4.1	Forces Acting on The Blades	68
3.4.2	Loads Acting on The Gears	69
3.4.3	Loads Acting on Other Parts	70
3.4.4	Friction	72
4	Results and Discussion	73
4.1	Testing	73
4.1.1	The Test Site	73
4.1.2	Test Setup	73
4.1.3	Logging Results	75
4.2	Test Model	77
4.2.1	From Cut-in Speed to Rated Speed	77
4.2.2	The Pitch Controller	79
4.3	Verification of the Test Model	80
4.3.1	Calculations	81
4.3.2	Improvement of Power Coefficient Calculations	81
4.3.3	Calculation of c_p : Test Model	82
4.4	Improvements	85
4.4.1	Gearbox	85
4.5	Summary of Results	86
5	Conclusion and Further Work	88
	Bibliography	89
	Appendices	91
A	Component Information	92
A.1	Stepper Motor	92
A.2	Generator	100
A.3	Gearbox	103

B Material and Printer Specification	107
B.1 High Definition Printer	107
B.2 Standard Definition Printer	111
C Programmable Logic controller	114
C.1 Step-script	115
C.2 Step-drive	116
C.3 Complete program	127
D Technical Drawings	138

Chapter 1

Introduction

Wind power production is the technology of converting the energy in the air movement to usable mechanical energy, and subsequently electrical energy. This project is intended to be the first step of increased focus on research of offshore floating wind turbines at the University of Agder at bachelor and master level. A prototype of a wind turbine with a pitch controller mechanism controlled by a PLC step drive is to be constructed. In future projects the model can be tested when mounted on the Stewart platform located in the school's lab area. This chapter consider the background and the motivation for the selected topic as well as the problem definition, research questions and limitations regarding the thesis as well as the structure of the report.

1.1 Purpose and Scope

Project scope of this master thesis includes a review of state-of the art technology and common challenges in the field of offshore wind turbines, specifically focusing on floating offshore wind turbines in the theory part. Floating wind turbines have a large potential to increase the level of green energy in the world, as explained later.

The experimental part of the project includes a downscaled model of a wind turbine with an electrical pitch controller. A mechanical mechanism is to be design to turn the blades to a given position. This mechanism is controlled by a hybrid stepper motor generating the necessary motion to turn the angle of the blades. From the pitching system it is possible to calculate the number of steps required based on the design configuration. The model of the wind turbine is designed in SolidWorks and printed in a 3D-printer where the most critical parts was printed with low tolerance and high definition. The majority of the parts are made of the plastic material used in the 3D-printer. However, some of the components such as bearings and tower structure, are steel parts.

The turbine built in the project is designed as a pitch controlled wind turbine. As mentioned before a stepper motor is installed to control the pitch angle. The stepper motor is controlled with the help of a Programmable Logic Controller (PLC) program. The controller is designed to turn the pitch angle based on the given wind speed and the number of steps needed to achieve the correct angle. An optimal pitch angle is calculated with common formulas and known parameters from the test model. The wind turbine is tested on the roof top of the school during different wind conditions, to obtain the characteristics of the wind turbine such as cut-in and cut-out speed, including verifying the functionality of the pitch controller. Hand calculations should be included to verify the model.

SolidWorks, LabVIEW, Open Platform Communications (OPC) server and PLC is used due to the students being familiar with the programs and the setup from earlier courses. Former relevant

subjects include wind power, control theory, linear multi-variable control, robotics, kinematics, dynamics and control and Industrial IT.

1.2 Motivation

Wind power technology is not exactly a new idea, as there are many different historical claims that wind machines which harness the power of the wind, date back beyond the time of the ancient Egyptians [9]. The world's energy consumption from the beginning of the 18th century when the industrial revolution started and until today has increased at a tremendous degree. Most of the energy comes from sources like oil and coal, which has a negative impact on the environment. Therefore, the world looks to more sustainable and climate friendly energy production methods are emphasized among researchers as a solution to problems regarding future energy shortage and threats from climate change. Wind power has a large potential as a source for clean energy due to the unlimited availability. Especially in deep water area outside the coast, many opportunities for building of large scale wind farms are plausible.

Offshore wind power has proven to be a renewable energy source with a high potential, and the use of wind energy in general has grown rapidly in recent years due to increased focus regarding climate changes and increased oil prices. The North Sea and other seas have very good environmental conditions for harvesting the wind resources, ready to cover the need for electricity for the increasing population on earth. This is technology for future generations and can replace fossil fuels like oil, gas and coal to achieve the goal of a reducing the climate changes. However, offshore wind power is without doubt one of the most expensive energy generating technologies when large scale deployment is considered.

Considering the investments it is always beneficial to find new ways to reduce the cost and increase the efficiency. In recent years, a large number of offshore wind farms with fixed foundations have been installed in Europe. However, in 2007 the Norwegian company Hydro (now Statoil-Hydro) launched their HYWIND project, a study of floating wind turbines to increase efficiency and reduce the cost compared to fixed installations.

The floating wind farms can be installed further out in deep water where the wind is steadier and stronger, making it possible to achieve a larger and more constant production of electricity. The visibility offshore is lower and the absence of ship lanes restrictions is a great advantage to exploit the available space. However, compared to a fixed foundation wind turbine, a floating turbine may sustain rougher winds, waves and heavier weather conditions, which can be difficult to control. If the energy price from wind turbines in the coming years is to be competitive with other power production methods, a cost reduction is needed in addition to increase the energy gain. To decrease energy cost, it is beneficial to increase the turbine size and use well defined control system to gain as much power as possible from the wind. The reason for developing motion controllers as well as improved pitch controllers for offshore wind turbines is to minimize the impact of the waves and winds which occasionally can be very large in rough weather conditions. To increase the efficiency of the wind turbine the blade-pitch control strategy is important.

Some of the motivation behind this project is to contribute to the research at University of Agder(UiA) on offshore wind turbines, which is a very interesting subject for future research and project work, both for bachelor thesis, master thesis and doctoral thesis.

1.3 Problem Definition

In this project, a test model of a pitch controlled wind turbine is to be designed and developed, modelled in SolidWork, printed in 3D and mounted on a steel plate with a corresponding tower structure. The pitch mechanism is designed to be powered by a stepper motor to be able to turn the angle of the blades. A controller is modelled with a programmable logic controller to turn the stepper motor. The An OPC server is utilized to log the data in Excel. The functionality of the model should be verified.

1.3.1 Research Questions

- RQ 1. Conduct review of state of the art technology and challenges related to offshore wind turbines, with special focus on floating devices.
- RQ 2. Build the pitch controlled wind turbine model in SolidWorks and print in 3D for testing.
- RQ 3. Develop a PLC-program for the step drive to control the pitch mechanism of the model with a hybrid stepper motor.
- RQ 4. Preform test during different wind conditions and evaluate the results from the test model. Study how the change in wind speed, shaft speed and tip speed affect the voltage output of the test wind turbine. Verify with hand calculations.
- RQ 5. Test the functionality of the pitch controller and the PLC program controlling the stepper motor.
- RQ 6. If time allows, compare the result of the test model and the simulated model with offshore conditions. The test model will be mounted on top of the Stewart platform in order to simulate offshore conditions.

1.3.2 Limitations

Since this work includes building of a downscaled prototype of a pitch-controlled wind turbine, there will always be some uncertainties considering the functionality of the design. The improvements done to the design of the prototype will be limited by the time and resources available. Cost is not considered in this project. The main goal of the project is to build and test the pitch controlled wind turbine. The Stewart platform testing will only be executed if time allows it, and may or may not be performed in accordance with the supervisor.

The results obtained from testing will be based on voltage output at different wind speeds and pitch angles. Adequate wind resources is important to obtain good testing conditions for the wind turbine, and normally Grimstad provides good wind conditions at this time of the year. If the wind conditions during the test period proves to be insufficient, alternative wind resources such as a wind tunnel or a leaf blower may be a possibility. The testing methods may be changed in accordance with the supervisor.

1.4 Solution Strategy

The main goal of the project is achieved by building a physical test model based on a design developed in SolidWorks, and controlled with the PLC. To streamline the development process, the model and the PLC program is developed simultaneously. The parts for the test model will mostly

be plastic material of various quality from the printer, but also some steel components when this is considered necessary. The model will be built with a pitch system consisting of a stepper motor programmed in PLC through 1-Step-Drive from Phytron, using TIA portal V12. The results from the test model is logged with OPC server. The simulated model will obtain its results by testing over a range of simulated wind speeds. Initially, the testing will be based on onshore wind turbine conditions. The results found from these tests will be validated with the simulated model as well as hand calculations. Finally, if time allows the model will be tested with offshore conditions on a Stewart platform.

Every week a progress meeting with the main supervisor will be held to ensure that problems was taken care of as soon as possible.

1.5 Report Outline

Chapter 2 considers the theoretical aspects of this thesis essential for the reader to understand floating wind turbines. Topics related to other aspects of the thesis are also outlined.

In Chapter 3, the methods and tools used are described and explained in detail. The experimental wind turbine setup is widely illustrated in addition to description of each stage of the process.

Chapter 4 include all the obtained results. Simulated results are presented and explained with graphs, figures, tables and descriptive text. This chapter also evaluates and discusses the results obtained from the simulations and experiments.

Chapter 5 present the conclusion of the presented work, along with suggestions regarding modifications and further work and analysis in the area of the topic.

Chapter 2

Theoretical Background

This chapter consider important theoretical aspects of the thesis. The chapter contains an introduction to the environmental aspects of wind turbines. The wind is introduced as a renewable resource in abundance and the different approaches of calculating the various properties in the wind at a given site. Next section covers the aerodynamic aspect of the wind turbines, before the components of the wind turbine is explained in detail. Then a brief study of the operational considerations, before going deeper into the state-of-the-art devices used in offshore wind turbine industry. The last section covers motion compensation and topics related to the Stewart platform.

2.1 Environmental Aspects

This section covers the environmental aspect of wind turbine operation. The external forces acting on a wind turbine is determined by this aspect. To understand the concept of a wind turbines it is beneficial to know how the wind and waves behave and affect the turbine.

2.1.1 Wind Properties

Wind is the movement of air across the surface of the Earth, flowing from areas of high pressure to areas of lower pressure. This is caused by the uneven heating of the atmosphere by the sun, the irregularities of the surface and rotation of the Earth. When air is heated up the density reduces, thus lowering the pressure. This makes the warmer air rise up and above the cooler air, which results in pressure differentials. This in combination with the rotation of the planet, drags the atmosphere and creates turbulence. Eventually, this results in a constantly varying pattern of winds at different speeds scattered across the surface of the Earth. This wind flow, or motion energy, when harvested by modern wind turbines, can be used to generate electricity.

The term wind power describes the process by which the wind is used to generate mechanical energy or electricity. Wind turbines convert the kinetic energy in the wind into mechanical energy. This mechanical energy can be used for specific tasks (such as grinding or pumping water) or a generator can convert this mechanical energy into electric energy. The power in the wind depends on the wind speed and is proportional to both the wind speed cubed and the rotor area. The general formula for this kinetic energy, in its unperturbed state is given in Equation (2.1) [10].

$$P_{wind} = \frac{1}{2} \cdot \rho \cdot A \cdot v_w^3 \quad (2.1)$$

where

- ρ = Density of the air [$\frac{kg}{m^3}$]
 A = Area of the turbine blades [m^2]
 v_w = Wind speed [$\frac{m}{s}$]

Equation 2.1 is very important since it tells us that the maximum available power increases with the cube of the wind speed and only linearly with the density and area. The available wind speed at a given site is usually first measured over a period of time before a project is started because of the importance of the wind speed. Power from the wind as given by Equation (2.1) is just a theoretical maximum value. The actual kinetic energy that can be extracted is considerably lower. The actual power depends on several factors like blade design, generator and rotor used, friction as well as other electrical losses. There is also a physical limit to the (amount of) power that can be extracted from the wind, which is independent of wind turbine design, according to Betz's Law. This law states that no turbine can extract more than $\frac{16}{27}$ (or 59.3%) of the kinetic energy in wind. The factor $\frac{16}{27}$ (or 0.593), is the maximum extraction factor for the power coefficient (c_p). This is the maximum upper limit and its called the Betz limit. Thus multiplication of the kinetic energy with c_p gives the mechanical energy as given by Equation (2.2) [11]. The c_p coefficient is given by Equation (2.3), and this leaves the tip speed (λ) and the pitch angle (β) as the main design parameters. [12]

$$P_{mech} = c_p \cdot (\lambda, \beta) \cdot \frac{1}{2} \cdot \rho \cdot A \cdot v_w^3 \quad (2.2)$$

where

$$c_p = C_1 \cdot (C_2 - C_3 \cdot \beta^2 - C_4) \cdot e^{C_5} \quad (2.3)$$

where

- c_p = Power coefficient [-]
 C_1 = 0.5 [-]
 C_2 = $\frac{r}{\lambda}$ [-]
 C_3 = 0.022 [-]
 C_4 = 5.6 [-]
 C_5 = $-0.17 \cdot \frac{r}{\lambda}$ [-]
 β = Pitch angle [-]
 λ = Tip speed ratio [-]

The propeller thrust of the wind turbine can be calculated from Equation (??), and it can be seen that the power is defined as the thrust times the velocity of the wind, if the coefficient is disregarded [13].

$$T_{wind} = C_t \cdot \frac{1}{2} \cdot \rho \cdot A \cdot v_w^2 \quad (2.4)$$

where

C_t = Thrust coefficient [-]

An important factor when calculating wind speeds is the ground roughness, dependent on vegetation and other environmental obstacles, which greatly influence wind speeds and power extraction. Above the ground, in the undisturbed air layers of the geostrophic wind, approximately 5 km up, wind speed is supposed to be unaffected by the roughness. Wind speed changes between these two extreme values, is referred to as vertical wind shear. The logarithmic wind profile estimation for vertical wind shear is used in flat terrain with a neutrally stratified atmosphere. According to the logarithmic wind profile, the wind speed at a height z above ground level is given by Equation (2.5). [11]

$$v_w = v_0 \cdot \frac{\ln \frac{z_2}{z_0}}{\ln \frac{z_1}{z_0}} \quad (2.5)$$

where

v_0 = Unaffected wind speed [$\frac{m}{s}$]
 z_0 = Ground roughness [m]
 z_1 = Measuring height [m]
 z_2 = Hub height [m]

2.1.2 Wind Distribution

The study of variations in wind characteristics at particular turbine location is essential for implementation of wind power as in the design of machines and energy systems, as well as for economic feasibility. The variations in wind speeds and geographic characteristics of locations makes it challenging. To cope with these issues, engineers make use of statistical analysis, meteorology and correlation of measurements of time series. The increasing development in wind power has led to more sophisticated data handling techniques and computer modelling for wind distribution studies. Weibull and Rayleigh analysis are the most commonly used analysis techniques to compute power available from wind at particular location using the basic measured data of the wind distribution.

The Weibull Distribution

A common way to represent measured wind data in a wind flow model is by fitting the measured wind data into a probability distribution function. This will simplify the calculations and at the same time give accurate predictions of wind flow and calculations of energy production. The most common distribution applied for wind energy purposes is the Weibull distribution which is used to express the probability for a certain wind speed to occur, shown in Equation (2.6). An example of a Weibull distribution is given in Figure 2.1.

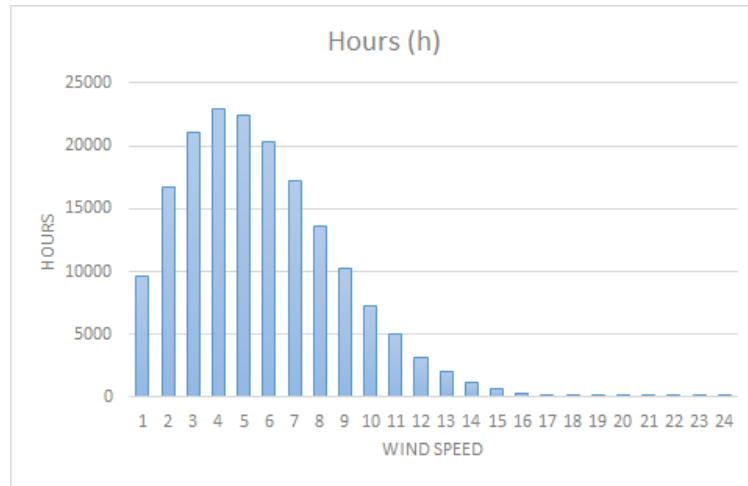


Figure 2.1: An example Weibull distribution of measured wind at a given location

$$h(v) = \frac{k}{c} \cdot \left(\frac{v}{c}\right)^{k-1} \cdot e^{-\left(\frac{v}{c}\right)^k} \quad (2.6)$$

where

$h(v)$ = The frequency of occurrence of wind speed [–]

v_w = Wind speed [m/s]

k = The dimensionless shape factor which describes the form and width of the distribution [–]

c = The scale factor which is closely related to the wind speed at the location [m/s]

The Rayleigh Distribution

Wind characteristics are essentially location specific and the performance of wind turbines vary if the actual wind distribution at the location differ from the standard distribution. One special case of Weibull distribution commonly used in wind energy projects is the Rayleigh distribution, is defined when the k parameter equals 2 and is commonly applied when no information of the site specific distribution is known. [11]

2.1.3 Waves

Waves and sea currents, which essentially is energy passing through water, have a great impact on an offshore wind turbine, both floating and fixed foundations. The forces of the waves affect the lifetime of the turbine as well as the dynamic response. There exist many theories and equations to describe waves and loads from waves. However, some theories fits better for larger waves than other and some fits better for greater water depths. This means that the location need to be taken into account when performing calculations regarding wave loads. Waves consist of numerous reasons, such as movement of continental plates, tidal water and wind. Wind creates waves due to difference in velocity and density between the two fluids, air and water [14]. This creates small waves with different pressure on each side of the wave. High air pressure push the surface of the water downwards, while low air pressure move the surface upwards and the wind transfer energy to the increasing waves. When the amplitude of the wave increase due to steady winds over time, the wind will transfer energy more effectively and larger waves are created. Water particles move in a decreasing orbital pattern down in the ocean. As long as we are in deep oceans (>100m), or

the depth is greater than twice the wavelength, we can neglect the friction from the bottom. This will have a significant impact on the wave energy in shallow waters ($<100\text{m}$). As we can see from the figure the pattern of movement also becomes more elliptical [1].

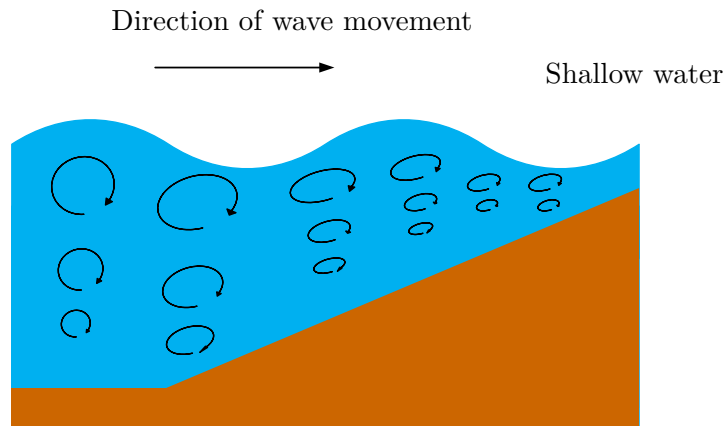


Figure 2.2: Waves approaching shallow water

It is not easy to describe a wave because of its unpredictable and complex nature. They are a product of many factors: wind duration, depth, wind velocity, pressure, and temperature. In deep ocean, waves can propagate over a distance of several hundred kilometres and maintain their characteristics. A wave is defined in [1] as the profile of the surface elevation between two successive downward or upward zero-crossings, as seen in Figure 2.3 and 2.4. Waves behave stochastic as the amplitude, length and period of the waves change constantly, which makes it hard to predict the next wave. However there exist many simplified methods.

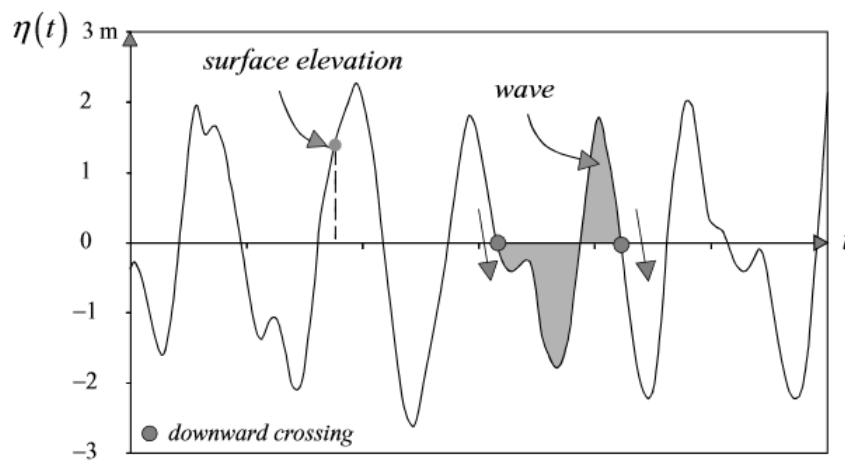


Figure 2.3: Definition of waves, downward crossing [1]

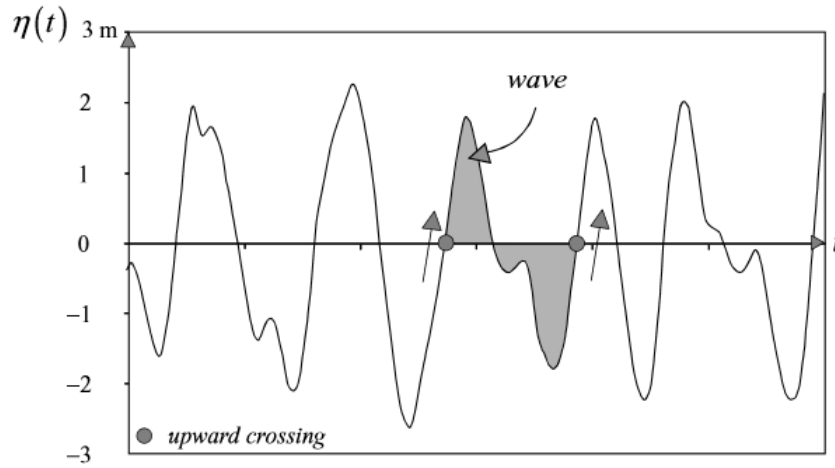


Figure 2.4: Definition of waves, upward crossing [1]

The wave height, H , is defined as the distance between the highest and lowest surface elevation in a wave. However, usually the term significant wave height is used to define the wave height for a certain period of time. Significant wave height is the mean of the highest one-third of waves in the wave record, as seen in Equation (2.7) [14].

$$H_{\frac{1}{3}} = \frac{N}{1/3} \cdot \sum_{j=1}^7 \frac{N}{3} \cdot H_j \quad (2.7)$$

where j must not be confused with the sequence number since it is the rank number which means that $j = 1$ is the highest waves and $j = 2$ is the second highest wave. N is the number of waves during the period of time, usually 20 minutes. The period of the wave, T , is defined as the time from the start of the wave to the end of the wave, or the interval between one zero-crossing and the next. In the same way as for wave height, the significant wave period can be estimated based on years of research. The significant wave period is calculated as seen in Equation (2.8) and is defined as the mean period of the highest one-third of waves.

$$T_{\frac{1}{3}} = \frac{N}{1/3} \cdot \sum_{j=1}^7 \frac{N}{3} \cdot T_{0,j} \quad (2.8)$$

Where j is defined as the rank number, as seen before, whereas T_0 is the zero-crossing period. The wave length, λ is the horizontal distance between two zero-crossings. All parameters are seen on Figure 2.5.

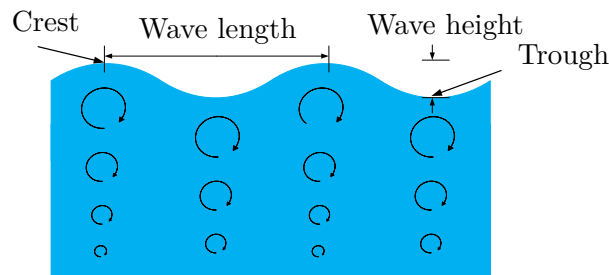


Figure 2.5: Waves parameters

2.2 Aerodynamics

This section describes elementary aerodynamic theory and terms, as well as the blade element momentum theory for wind turbines. To understand the potential of the wind turbine it is important to know some of the aerodynamic theory behind and some of the common terms used.

The oldest models of wind turbine design relied mostly on the force of the wind to push the blades into motion to capture the energy. Today modern wind turbines take advantage of more advanced aerodynamic principles to capture the energy of the wind. Kinetic energy is converted by the wind turbine, into rotational energy which is then extracted as electrical energy by a generator. This conversion is caused by aerodynamic forces. As seen in Figure 2.6, the lift and drag force are the two forces that act on the rotor when the blades rotate.

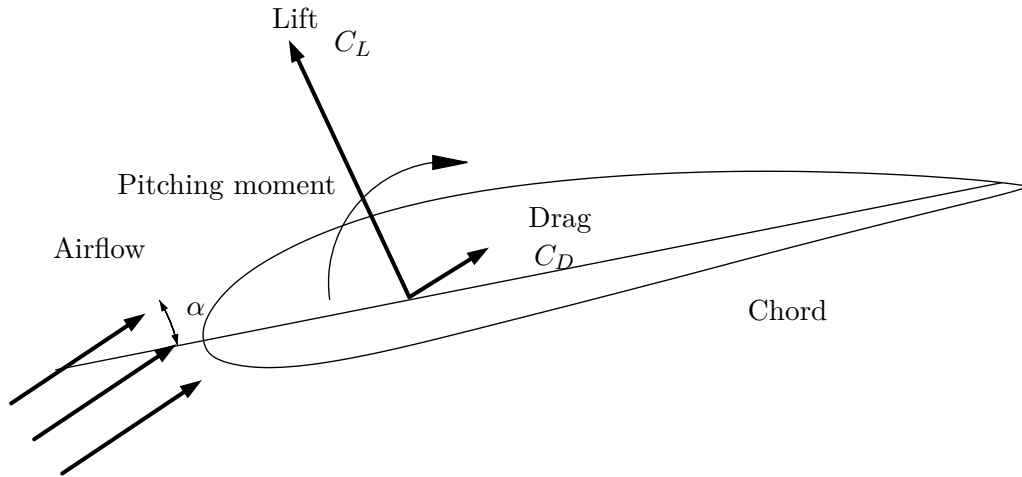


Figure 2.6: Aerodynamic properties of an airfoil

The lift force is defined as the force acting perpendicular to the direction of the wind and is a consequence of the unequal pressure between the upper and lower airfoil surfaces. The drag force on the other hand, acts parallel to the direction of the wind flow. Viscous friction forces at the foil surface as well as unequal pressure creates the drag force. The drag force increases when the angle of attack, the angle of the airflow on the blade is increasing, until the point of stall. Horizontal turbine blades are shaped like an airplane wing and utilize the same principles to convert movement of the wind to mechanical energy. The pitching moment is defined as the moment around an axis perpendicular to the cross-section of the airfoil. Lift is created due to the fact that the air would need to travel longer on the upper side of the blade, and thereby faster, to reach the end of the blade to meet the wind travelling from the lower side of the blade. A low pressure zone is created in the upper side of the blade and the blade is sucked in the downwind direction, which is known as the phenomena lift. This phenomena is taken advantages of when designing airfoils as well as turbine blades. [15] In Equations (2.9), (2.10) and (2.11) the lift, drag and pitching moment coefficients defined.

$$C_l = \frac{L}{0.5 \cdot \rho \cdot U^2 \cdot c} \quad (2.9)$$

$$C_d = \frac{D}{0.5 \cdot \rho \cdot U^2 \cdot c} \quad (2.10)$$

$$C_m = \frac{M}{0.5 \cdot \rho \cdot U^2 \cdot c \cdot A} \quad (2.11)$$

where

C_l	=	Lift coefficient [-]
C_d	=	Drag coefficient [-]
C_m	=	Pitching moment coefficient [-]
A	=	Projected airfoil area [m]
c	=	Chord [-]

The angle of attack is, as the name suggests, the attacking angle of the wind on the blade or the angle between the chord line and an vector representing the direction of the wind. In Figure 2.6, the angle of attack and other terms outlined. An important term in wind turbine theory is the stall which is defined as a sudden reduction in the lift when the angle of attack increases too much. Usually, the critical angle of attack is around 15 degrees [11], but depends on the type of fluid, foil and the Reynolds number. The stalling of a airfoil causes the important effect known as turbulence, where the air whirls around in an irregular vortex, as seen in Figure 2.7. Turbulence is a flow regime categorized by constant and chaotic property changes and despite much research in the topic still hard to grasp for scientist and researchers. In turbine design engineers can take advantage of the stall phenomenon when designing the blades.

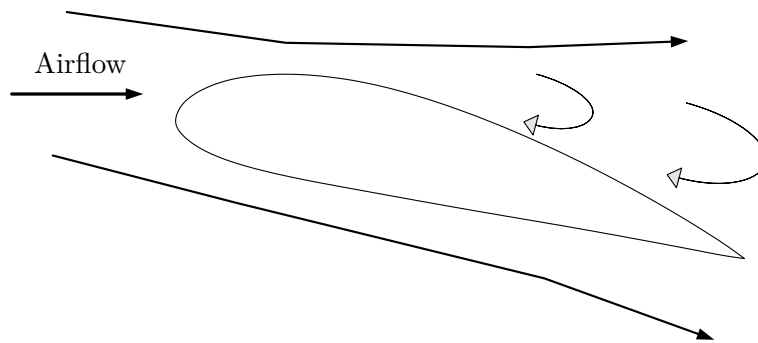


Figure 2.7: The principle of stall in aerodynamics

2.2.1 Blade Element Momentum Theory

In the wind industry, the blade element momentum theory (BEM) is used to calculate the loads acting on a wind turbine, and many computer programs take advantage of this theory as well. This theory is a combination of the blade element theory (BET) and the momentum theory(MT). In the BET theory the forces at a section of the blade is analysed as a function of blade geometry. The momentum theory is used to describe the fluid dynamics of an ideal actuator with a mathematical model. In this theory, also called actuator disk theory, utilize a control volume (CV) analysis of the forces, at the blade, based on the conservation of linear and angular momentum. When these two theories are combined, the result relates blade shape to the rotor's ability to extract power from the wind. [13]

The momentum theory explains the physics behind the stages from kinetic energy to mechanical torque. More than hundred years ago, Rankine and Froude developed models to predict the performance of propellers, before Betz extended their work to also include a turbine rotor. The key idea is conservation of momentum to calculate the forces and flow conditions on a rotor with infinite number of blades. An air stream passing through a cross sectional area contains the same amount

of momentum on both sides, which means that the air speed is reduced to extract energy from the air stream. As said the velocity is decreased and thereby the pressure will increase after the propeller. However, the pressure of the surroundings will not increase, which entail that the air stream expands to create equilibrium. Then the velocity will increase gradually to velocity if the air stream is equal to the surroundings.

Betz found through his work a relationship between optimal power extraction and the relative velocity between the free stream velocity and the velocity behind the actuator disk. In theory it is assumed that a control volume, as seen in Figure 2.8, where the boundaries are the surface of a stream tube and four station shown. Station 1 is upstream of the turbine, number 2 is just before the blades, number 3 just after the blades and 4 downstream of the blades. Applying linear momentum conservation to the CV with radius r and thickness dr gives the thrust contribution as seen in Equation 2.12. For a ideal rotor it can be found that the axial velocity in the wake could be expressed in terms of the axial induction factor a and the speed U as $(1 - 2a)U_0$, seen in Figure 2.8 [13]. The induction factor is a number defining the relationship between the velocity of the wind before and after the turbine rotor.

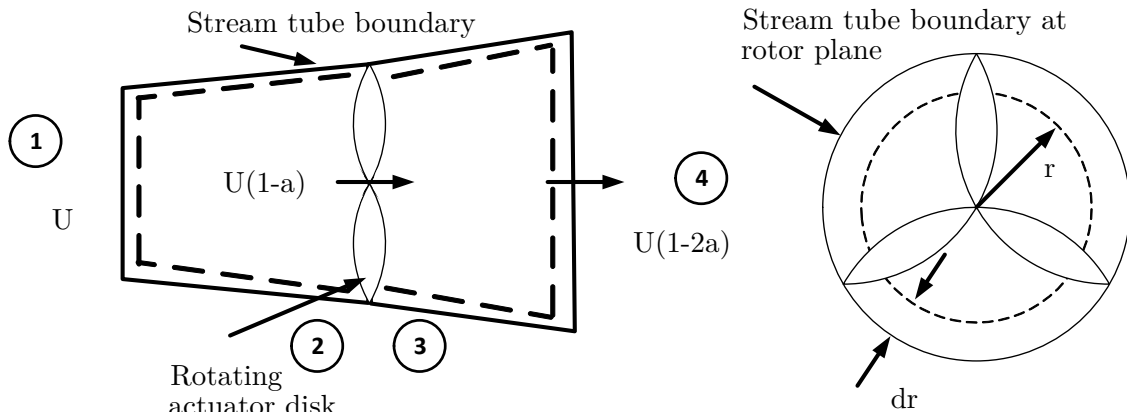


Figure 2.8: The principles of the momentum theory

$$dT = \rho \cdot U^2 \cdot 4 \cdot a \cdot (1 - a) \cdot \pi \cdot r \cdot dr \quad (2.12)$$

where

- U = Free stream velocity [m/s]
- ρ = Density of the air [-]
- a = Induction factor [-]
- r = Distance from center to the circular element[m]
- dr = The circular element [m]

In a similar way, from the conservation of angular momentum the differential torque, Q , imparted to the blades can be obtained from Equation 2.13.

$$dQ = 4 \cdot a' \cdot (1 - a) \cdot \rho \cdot U \cdot \pi \cdot r^3 \cdot \Omega \cdot dr \quad (2.13)$$

where

a' = Angular induction factor [-]

ω = Angular velocity [-]

Both the induction factors as well as the density is unknown, which gives two equations with several unknown parameters. To solve this matter, the blade element theory is used. In the blade element theory, the blade is assumed to be broken down into N several sections or elements, usually between ten and twenty, in order to determine the forces acting on these small parts. C_l , C_d and α is used to express the forces on the blades of a wind turbine. Then all the forces are integrated along the blade and one revolution of the rotor to obtain the forces and moments produced by the entire rotor. This theory relies on two key assumptions [13]

1. No aerodynamics interactions between different blade elements, i.e. what happens at one element cannot affect the other.
2. The forces acting on the blade elements are determined by lift and drag coefficients, and are constant on each annular element. This corresponds to a rotor with an infinite number of blades.

With the given assumptions, it is shown that each of the blade elements will experience a slightly different flow as each of them has different rotational speed, chord length and a twist angle. Figure 2.9 refers to the principles of the blade element theory and displays the main variables.

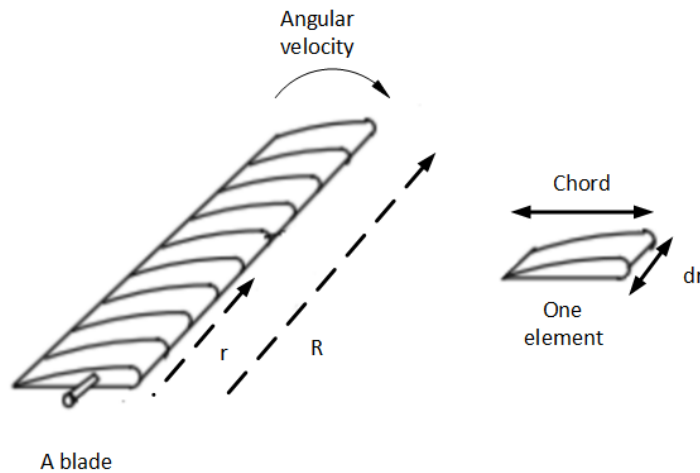


Figure 2.9: The principles of the blade element theory

Prandtl's tip-loss factor F is introduced to correct the assumption of an infinite number of blades seen in Equation (2.14) and (2.15). The vortex system in the wake differs for a rotor with a finite number of blades from a rotor with an infinite number of blades. [15]

$$F = \frac{2}{\pi} \cos^{-1} \cdot (e^{-f}) \quad (2.14)$$

where

$$f = \frac{B}{2} \cdot \frac{R - r}{r \cdot \sin\phi} \quad (2.15)$$

where

- B = Number of blades [-]
R = Overall radius of the rotor [m]
r = Local radius [m]

And thus the thrust and the torque can be computed as in Equations (2.16) and (2.17).

$$dT = \rho \cdot U^2 \cdot 4 \cdot a \cdot (1 - a) \cdot \pi \cdot r \cdot F \cdot dr \quad (2.16)$$

$$dQ = 4 \cdot a' \cdot (1 - a) \cdot \rho \cdot U \cdot \pi \cdot r^3 \cdot \Omega \cdot F \cdot dr \quad (2.17)$$

2.3 Wind Turbines

To understand how a wind turbine is assembled, a short description of all the components of a wind turbine will be given. The concepts of wind turbine operation will also be discussed in this section. Fundamental aspects of floating offshore wind turbines (FOWT) will be further explained and discussed in Section 2.5.

2.3.1 Inside The Wind Turbine's Main Body

The wind turbine is a power generating system depending on many different components. In this section the components in a pitch controlled wind turbine will be studied to give the reader insight in what components are needed for power production, including how the parts work.

Rotor

The rotor is composed by three components; hub, blades and a spinner. The blades mounted onto the hub are shaped like air plane wings in order to use the principle of lift to turn the wind energy into mechanical energy. For a typical utility-scale wind turbine three high-technology blades are commonly used, although the number of blades can vary from two to six. The blades are one of the most critical aspects for a wind turbine and considered a strategic component by wind turbine original equipment manufacturers. The blades are made of laminated materials, such as composites, balsa wood, carbon fibre, and fibreglass. These materials have a high strength and a low weight. In order to generate lift, which causes the rotor to turn, the materials mentioned are moulded into air foils and adapted to achieve the best dynamic qualities. The blades also often include material to protect against lightning strikes. They are bolted onto the hub, with a pitch mechanism interposed to allow the blade to rotate about its axis to take advantage of varying wind speeds. [16]

The hub is commonly made of ductile cast iron and is one of a wind turbine's heaviest components. The hub is designed to be rigid yet able to absorb a high level of vibration. The hub is covered by a nose cone. The nose cone is designed primarily with aesthetics in mind but can provide some protection from the environment for the hub. The nose cone is manufactured with composites similar to those used for the blades. [17]

The blades are mounted in different ways depending on the wind turbine. There are two main types, horizontal axis wind turbine (HAWT) and vertical axis wind turbine (VAWT). HAWT is preferred, and dominates the current international surge in wind energy capacity. [10]. The turbines can be configured in two different ways regarding the rotor position with respect to the tower, upwind and downwind. The upwind configuration is the most commonly chosen. The principal advantage of

this configuration is that the tower shadow effect is much less for the same blade-tower spacing, reducing both dynamic loads on the blade and rhythmic noise effect. Set against this is the need to take great care to avoid the risk of blade-tower strikes with upwind machines, requiring accurate prediction of blade deflections under turbulent wind loading [17]. The downwind configuration of a HAWT has some disadvantages which often result in a higher cost. This due to a larger wind velocity deficit and significantly higher blade fatigue, which usually is reduced by choosing a more costly nacelle solution. However, such a configuration allows the use of very flexible blades without the risk of tower strike. Such blades benefit by being less severely unloaded by the tower shadow, because wind loading deflects them further from the tower in the first place [17]. The number of blades is most commonly two or three. When determining the number of blades, the factors mentioned must be taken into account. [17]

- Performance
- Loads
- Cost of rotor
- Impact on the drive train cost
- Noise emission
- Visual appearance

Some of these factors are strongly influenced by rotational speed and rotor solidity, and the ideal relationship between these parameters and the number of blades will be briefly considered in this section. For the blade design to be successful, it must satisfy a wide range of objectives, some of which are in conflict [17]. These objectives can be summarized as follows:

- Maximize annual energy yield for the specified wind speed distribution
- Limit maximum power output (in the case of stall regulated machines)
- Resist extreme and fatigue loads
- Restrict tip deflections to avoid blade/tower collisions(in the case of upwind machines)
- Avoid resonance
- Minimize weight and cost

Rotor diameter is determined mostly based on cost analysis and the wind conditions at the site. The larger the rotor diameter is, the higher tip speed ratio λ . A too high λ is unwanted, due to the higher level of noise that occurs at high tip speed. The issue of what size of turbine produces energy at minimum cost has been fiercely debated for a long time. Protagonists of large machine cite economies of scale and the increase in wind speed with height in their favour. From the other camp, the 'square-cube law', whereby energy capture increases as the square of the diameter, whereas rotor mass (and therefore cost)increases as the cube, is advanced argument against [17].

Pitch Drive

In larger wind turbines, pitch control systems with sensors are preferred. The pitch system is critical in larger wind turbines as a safety subsystem and as well as for optimizing the power production. The sensor is placed in the hub and exchange information between the pitch controller placed in the nacelle and the controller which contains the total overview. The pitch system is placed in the front of the nacelle, the most critical part of the wind turbine, in order to protect it from lightning and electromagnetic compatibility issues. Based on the data obtained from the sensors the angle of the blades can be altered. The pitch system is crucial in order to harness the energy in the wind when the wind goes above rated wind speed, as external influence can lead to fatal consequences for the turbine. The pitch system controls the pitch angle of the blades, in order to generate the same amount of power as generated at the rated wind speed. It also avoids damage by reducing fatigue loads. Normally, the pitch system can pitch the blades to function at wind speeds up to 30 m/s, depending on the given size of the turbine and the location. The drive is a only a part of this system, which usually consists of wind vane, anemometer and different sensors. [18]

Nacelle

The rotor attaches to the nacelle, which sits atop the tower and encloses the various components. The nacelle of a wind turbine is the box-like compartment that sits atop the tower and is connected to the rotor. The nacelle contains the majority of the approximately 8000 components of the wind turbine, such as the gearbox, generator, main frame, etc. The nacelle housing is made of fibreglass and protects the internal components from the environment. The nacelle cover is fastened to the main frame, which also supports all the other components inside the nacelle. The main frames are large metal structures that must be able to withstand large fatigue loads. [17]

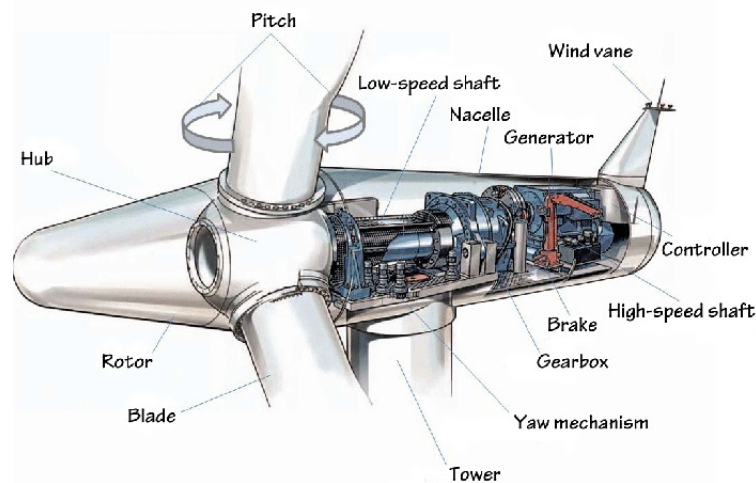


Figure 2.10: The major components of a wind turbine. Source

Gearbox

For converting the mechanical energy into electricity, the generator is the main component. When the main shaft is rotating with the rotor, the RPM is quite low, as one would expect with such a large rotating mass. Inside the nacelle of a typical wind turbine, the rotor drives a large shaft into a gearbox, which steps up the revolutions per minute to a speed suitable for the electrical generator. A wind turbine gearbox must be robust enough to handle the frequent changes in torque caused

by changes in the wind speed. It also requires a lubrication system to minimize wear. Wind turbines have either induction or permanent-magnet generators, depending on the model being sold. Induction generators are common and require a gearbox as described. [16]

Some wind turbines avoid the gearbox completely and use a direct drive system. A direct drive system connects the rotor directly to a permanent-magnet generator. This is quite common in turbines which have a rated power output below 10kW. These turbines avoid the mechanical problems associated with a gearbox, but require heavier and more expensive generators in order to produce electricity from the rotating shaft based on the actual rotational speed of the blades.

In general the main shaft of wind turbines run at low rotational speed compared to most motors and generators. The rotor turns the low-speed shaft at speeds ranging from 20 RPM large turbines to 400 RPM on residential units. Transmission gears increase the speed to the 1200-1800 RPM required by most generators to efficiently produce electricity. Equation 2.18 displays the effect which is the relationship between the input torque on the low speed shaft and the output torque on the high speed shaft.

$$M_S = \eta_{GB} \cdot i \cdot M_F \quad (2.18)$$

where

$$\begin{aligned} M_S &= \text{Torque on low speed shaft [Nm]} \\ \eta &= \text{Gearbox efficiency [-]} \\ M_F &= \text{Torque on [Nm]} \\ i &= \text{Gear ratio [-]} \end{aligned}$$

Generator

Further into the nacelle the generator is located. The generator size is dependent on the gearbox and the location of the wind turbine, whether there are much strong winds or calmer wind conditions. The generator converts the rotational mechanical energy produced by the rotor shaft into electric energy. As the winds vary at times, the production becomes irregular, and the need for a battery bank and a dump load is necessary. The most commonly used generator is a unidirectional synchronous permanent magnet generator. Different designs produce either direct current or alternating current. The electricity may be used by nearby appliances, stored in batteries or transferred to the power grid. [11]

Controller

A computer system runs self-diagnostic tests, starts and stops the turbine, and makes adjustments as wind speeds vary. A remote operator can run system checks and enter new parameters via modem. Blades can be rotated to reduce the amount of lift when wind speeds become too high. To control the functioning of the wind turbine, it is fitted with a number of sensors to read the speed and direction of the wind, the levels of electrical power generation, the rotor speed, the blades pitch angle, vibration levels, the temperature of the lubricants and other variables. A computer processes the inputs to carry out the normal operation of the turbine, with a safety system which can override the controller in an emergency. The control system protects the turbine from operating

in dangerous conditions and ensures that the power generated has the proper frequency, voltage, and current levels to be supplied to the grid. [19]

Wind Vane

Detects wind direction and passes it along to the controller, which adjusts the “yaw”, or heading, of the rotor and nacelle. The wind vane is used in a combination with an anemometer which measures the wind speed and passes it along to the controller.

Yaw Drive

All turbines have a yaw drive system to keep the rotor facing into the wind and to unwind the cables that travel down to the base of the tower. The yaw drive system usually consists of an electric or hydraulic motor mounted on the nacelle which drives a pinion mounted on a vertical shaft through a reducing gearbox. The yaw drive system also has a brake in order to be able to stop a turbine from turning and stabilize it during normal operation. The yawing of the wind turbine is used to turn the wind turbine into the wind to harness the energy, and turn away from the wind when it reaches maximum power output.

Tower

The nacelle and generator are mounted on top of a tall tower to allow the blades to take advantage of the best winds. Because wind speed increases with height, taller towers allow turbines to capture more energy. The power available to a wind turbine is proportional to the cube of the wind speed. Therefore, a 10 % increase in wind speed would result in a 33 % increase in available wind power. Towers are typically made of three or four tubular steel sections coated with paint and sealants and joined by flanges and bolts. Currently, the most common wind turbine towers is usually about 80 to 100 meters tall. Most towers come with load lifting systems with load-bearing capacity of more than 200 kilograms. When estimating the wanted power output and the forces that will affect the wind turbine, the tower is of large importance. When constructing a tower different aspects such as height, soil and mooring, if necessary, must be taken into account. When using a higher tower the power output will increase, as mentioned earlier. However, a higher tower also have higher requirements for stability and effects of forces induced by wind and waves. [10]

The blocking of the air flow by the tower results in regions of reduced wind speed both upwind and downwind the tower. This reduction is more severe for tubular towers than for lattice towers and, in the case of tubular towers, is larger on the downwind side because of flow separation. As a consequence, designers of downwind machines usually position the rotor plane well clear of the tower to minimize the interference effect [17].

2.3.2 Wind Turbine Operation

The turbine starts operating when the wind speed exceeds the cut-in wind speed. The power captured by the turbine increases with the wind speed. At some wind speed the rated operation is set, and the generating power reaches the maximum turbine power. If the wind speed continues to rise, the generator output power remains constant at the design limit. Due to safety consideration, the turbine is shut down at speeds exceeding cut-out wind speed. [20]

Cut-in and cut-out wind speed

The range of operational wind speeds is limited by the cut-in and the cut-out wind speeds. The turbine remains stopped beyond these limits. Below cut-in wind speed, the available wind energy is too low to compensate for the operation cost and losses. Most analysts agree that lowering the cut-in speed from the common 4.5 m/s contributes little to total energy generation. [11]

Above cut-out wind speed, the turbine is shut down to prevent from structural overload. Constructing the turbine robust enough to support the underlying mechanical stresses under very high wind conditions would be completely uneconomical. In fact, even though wind speeds above cut-out speed contain are powerful, their contribution to the annual average energy is negligible. The rating of the turbine arises from a compromise between available energy and manufacturing costs. For instance, designing the turbine to extract all the available energy up to cut-out wind speed would lead to an increment in the cost per kW. Wind speeds above rated wind speed are not frequent enough to justify the extra sizing of the turbine required to capture power above rated. [19]

Rated wind speed and design wind speed

The rated wind speed is where you reach the maximum power output. Above this wind speed the pitch angle control comes into place in order to keep the energy production constant at rated power. The design wind speed is based on the probability density function of the wind speed. It is with this parameter it can be calculated which range of wind speeds that is most beneficial to operate with the maximum value of C_p at a given site.

2.4 Wind Turbine Control

This section covers basic topics regarding control of wind energy conversion systems. Control is an important part of the modern wind industry, because controlling a wind turbine enables a better use of the turbines capacity and increase the lifetime of the complete installation. One of the best known and greatest challenges associated with wind power is without a doubt the unpredictable character of the wind. Even at wind sites with steady high speed wind, there are variations in speed and direction of the wind which affect the ability of the wind turbine to deliver power during the day. This is why wind turbines, both large and small ones, require a reasonably good control system, which track changes in wind direction and speed of the rotor, and thereby adjust orientation, blade angle and gearing to gain the desired output. The main purpose of controlling a turbine is [21]:

1. Prevent damage to the wind turbine
2. Prevent damage to the load
3. Maximize power production

The following control configurations can be used to manage the functionality of the turbine throughout the ideal power curve, as shown in Figure 2.11.

1. Fixed speed - Fixed pitch
2. Fixed speed - Variable pitch
3. Variable speed - Fixed pitch
4. Variable speed - Variable speed

Before continuing with the current topic, all configurations will be explained briefly. Configuration number four, a variable-speed variable-pitch turbine, is the only one of the control strategies that theoretically can achieve the ideal power curve. This configuration is a combination of number two and three, which resemble the ideal power curve at rated speed and before rated speed respectively. Fixed speed operation implies a maximum output power at one or two wind speeds, so these turbines has limited options when it comes to active control of the turbine. The generator is directly coupled to the power grid, which causes a fixed rotational speed. Passive control is used to prevent that rated power is not exceeded, but it would be impossible to follow the ideal power curve. In this project the turbine is of type two, fixed-speed variable-pitch. After reaching rated power, the pitch control mechanism is activated, to limit the power output to rated power.

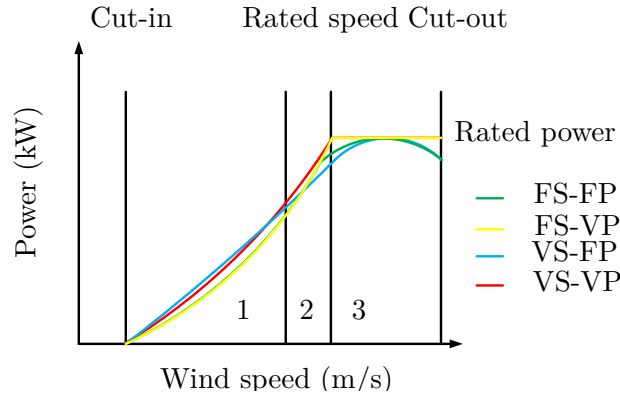


Figure 2.11: Power curves for different control strategies

In a wind turbine, the rotor blades can either be rigidly mounted on the rotor hub at a fixed pitch angle, or through a variable pitch mechanism. The interaction of the rotor blades with the oncoming wind results in the development of an aerodynamic torque T_a , as shown in Equation (2.19), which rotates the rotor. In this section, both fixed pitch and variable pitch is discussed.

$$T_a = \frac{P_a}{\omega} \quad (2.19)$$

where

$$\begin{aligned} T_a &= \text{Torque generated by the wind turbine [Nm]} \\ P_a &= \text{Power generated by the wind turbine [Nm]} \\ \omega &= \text{Rotational speed of the rotor [rad/s]} \end{aligned}$$

The pitch angle β is the angle at which the blade surface contacts the wind. Pitch angle control is the most common means for adjusting the aerodynamic torque of the wind turbine when wind speed is above rated speed. This kind of control is required in conditions above the rated wind speed when the rotational speed is kept constant, in order to prevent the input mechanical power to exceed the design limits. Below rated wind speed, the pitch setting should be at its optimum value to give maximum power [13]. Before discussing more wind turbine control, a few more aerodynamics principle is outlined.

In Equation (2.20) the relationship that gives the wind's angle of attack α on the rotor blades can be studied.

$$\alpha = \phi - \beta \quad (2.20)$$

where

- ϕ = The angle between the local flow direction and the rotor plane [°]
- β = Pitch angle [°]

The pitch angle β is measured between the chord and the rotor plane, as shown in Figure 2.12. Note that the chord length and the pitch angle may vary along the blade, i.e. they may be functions of the radial distance of the blade element to the axis of rotation [13]. The c_P has its maximum when β is at a small angle, ideally zero. Forces acting on the blade can be resolved in tangential and axial components. The tangential forces describe the torque on the rotor, and the axial forces describe the thrust on the rotor hub. The forces the air blade experiences are expressed in Equation (2.21) as drag force, and Equation (2.22) as lift force.

$$F_d = 0.5 \cdot C_d(\alpha) \cdot \phi \cdot v^2 \cdot A \quad (2.21)$$

$$F_l = 0.5 \cdot C_l(\alpha) \cdot \phi \cdot v^2 \cdot A \quad (2.22)$$

where

- C_d = Drag coefficient
- C_l = Lift coefficient
- v = Wind speed [m/s]
- A = Area swept by rotor [m²]

Where the lift c_l and drag c_d coefficients are dependent of the attack angle (α). As previously mentioned an increase of β , decreases α , thus decreasing the forces acting on the blade. We see in Figure 2.12 how an increase of β , would decrease α . The lift-to-drag ratio is determined by the angle of attack of the blades, i.e. the blades' angle with respect to the apparent wind, its shape and its aspect ratio.

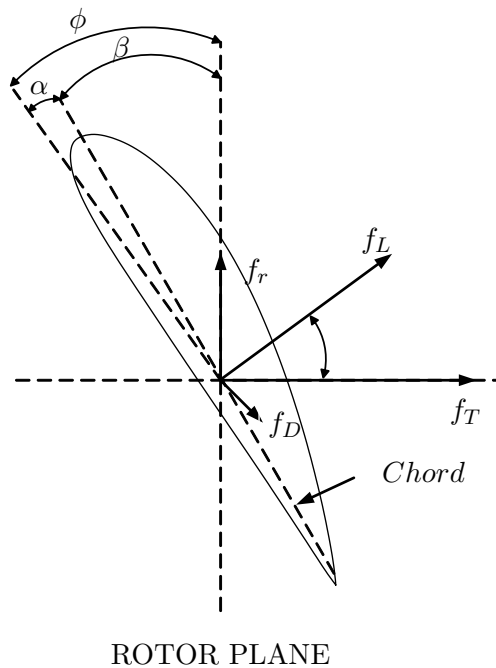


Figure 2.12: Description of airfoil with relevant parameters

2.4.1 Fixed Pitch

The fixed blades require little maintenance and can harness the energy in the wind across a wide range. At one point the maximum power is reached, and the wind turbine have to yaw out of the wind. There are several methods of controlling the fixed pitch turbine. By yaw control, stall control and a special technique which determines the operating point of the wind turbine by using the measured rotor speed and power. The only way to decelerate the turbine is through the generator which can lead to an over-power situation.

In most cases, the fixed pitch wind turbine includes any turbines in the range >10 kW rated power output. This is due to the fact that a pitch controlled system is more costly to produce, and the market for small-scale wind turbines is mostly common household or farms, which prefer a low maintenance system.

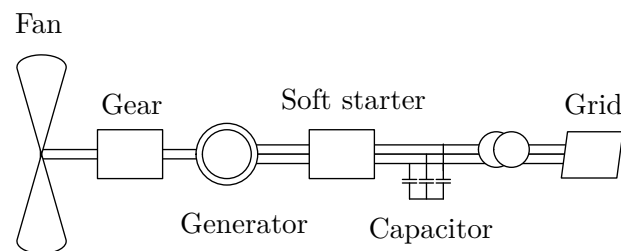


Figure 2.13: Fixed turbine setup

2.4.2 Stall Control

The earlier explained aerodynamic condition known as stall can be catastrophic for an aircraft, but for a wind turbine it can have both positive and negative implications. Stall control take advantage of the phenomena and deliberately use it to limit the amount of power captured by

the rotor during high wind speeds, to prevent damage of the turbine. In the early 1980s Danish wind turbine technology used passive stall control. The blades stall at a certain wind speed which increase the angle of attack above 14 - 15 degrees, and create a turbulent vortex which limit the rotor power[CITE]. However, passive stall control gives a very limited form of control, but since the eighties more sophisticated control options has been developed. A variable-pitch configuration, allows very effective active stall control in which the blades are turned around the lateral axis to give a smooth transition from normal power generation to limited power generation. The blades can also be pitch the other way to a negative angle of attack, known as feathering.

2.4.3 Pitch Controller

In a wind turbine, the rotor blades can either be rigidly mounted on the rotor hub at a fixed pitch angle, or through a variable pitch mechanism. The pitch controlled wind turbines are used in turbines in the range of <10 kW. For larger wind farms and offshore wind turbines the pitch control is greatly desired, as it can harness energy in the wind above rated wind speed. Compared to the fixed pitch wind turbine, which has mainly the stall regulation for generating mechanical energy, the pitch controlled turbine can change its angle of attack in order to adjust the aerodynamics torque of the wind turbine when wind speed is above rated wind speed. This kind of control is required in conditions above the rated wind speed when the rotational speed is kept constant, in order to prevent the input mechanical power to exceed the design limits. Below rated wind speed, the pitch setting should be at its optimum value to give maximum power. A pitch-controlled wind turbine may operate at a fixed pitch until a certain nominal power is generated. For higher wind speeds the blades are pitched in a given standard-angle with the leading edge into the wind in order to maintain this nominal power. Therefore, the power curve of a pitch-controlled wind turbine is absolutely flat after the nominal power has been reached.

The pitch control can be hydraulic, electric or a hybrid system which uses both. The electric control requires more monitoring, but one can avoid the maintenance problem of leakage in the hydraulic system. A more modern mechanical approach is the passive pitch control. This pitch control was introduced to passively govern the pitch blades at high RPM. The governor has masses connected to spring-loaded links that swing in and out depending on the RPM of the rotor. During high RPM, they swing outwards, increasing the pitch angle of the rotor and slowing it down. As RPM decreases, the springs pull back on the links which decrease the pitch of the blades. A block diagram showing the function of a pitch controlled wind turbine can be seen in Figure 2.14.

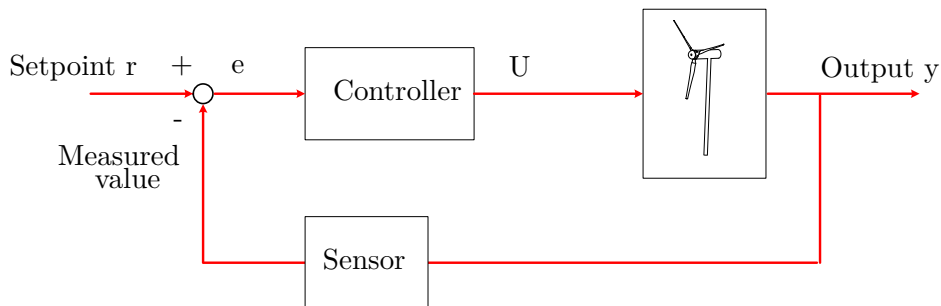


Figure 2.14: Feedback control structure of the pitch controller

2.4.4 Yaw Controller

Rotation in yaw refers to rotation of the entire rotor around its horizontal axis. Already in the mid-18th century, the first windmills had some sort of yaw mechanism to turn the nacelle. Now

most commercial and non-commercial wind turbines has a yaw mechanism installed, used to turn the rotor blades against the wind direction at all times. If the rotor is not aligned perpendicular to the direction of the wind, it has a yaw error which implies that a lower part of the wind energy will pass the rotor area [13].

A yaw controller can either be passive or active, depending on which type of technology used to achieved the desired result. The simplest type of yaw control is achieved through passive yaw control systems which use the wind force to rotate the nacelle in the direction of the wind. Typically, roller bearings is used to connect the tower and the nacelle. A tail fin is mounted on the top of the nacelle which aims to apply a torque to turn the entire nacelle in such a way that the rotor is pointing in the direction of the wind. This kind of yaw control is suitable for small scale wind turbines. More advanced control capabilities is provided if an active yaw controller is implemented. The feature which differentiates an active yaw controller system from a passive, is the mechanical mechanism included inside the nacelle that produces torque in order to revolve the nacelle to a suitable position according to current wind parameters [19]. A typical yaw controller as seen in Figure 2.15, consist of a bearing mechanism joining the nacelle and the tower structure, a yaw drive (including a motor and a gearbox), a controller and a yaw brake to provide counter torque. Usually a wind sensor is installed to detect the direction of the wind, and this is the signal input to the controller. Then the system aligns the rotor with the wind direction and thereby minimize the yaw angle error.

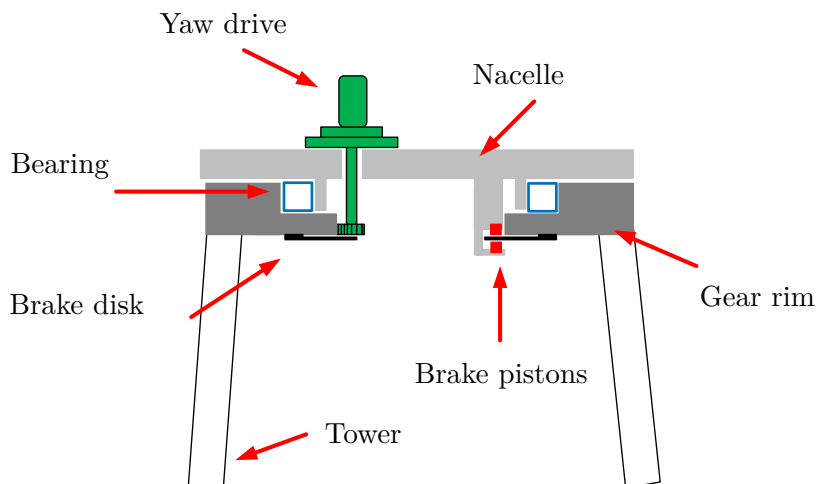


Figure 2.15: Yaw control system

2.5 State of The Art: Floating Offshore Wind Turbine Devices

In this section the state of the art on floating offshore wind turbines is presented. First some general consideration about floating turbine topology and anchor system, while the second part consider some of the developed concepts tested in a real environment as well as future challenges.

In recent years it as been a significant growth of offshore wind farms which have been installed all over Europe, especially in The North Sea outside the cost of United Kingdom and in Skagerak outside the cost of Denmark. However, these wind farms have a fixed foundation, which is considered to be encouraged weaker and less steady winds, restricted by ship lanes and less economical potential than floating turbines [6]. Off the coast of countries like Japan, China, USA, Spain and Norway large wind resources exist in much deeper water than the current standard. In these locations it is not feasible with support structures fixed to the bottom of the ocean. There is without doubt

a large economical potential in floating offshore wind turbines (FOWTs) due to the wide range of possible locations and smaller devices, but these topic will not be addressed in this project. [22] However, the realization of this large potential requires cost efficient, reliable and optimized control designs to compete with other energy resources.

As early as in 1972, Professor William E. Heronemus from University of Massachusetts, introduced the visionary concept of large-scale offshore floating wind turbines. However, the topic was not taken by mainstream researchers until the wind industry was well established in the mid 90's [23] due to an increasing oil industry and the high cost of development work.

2.5.1 Platform Topologies and Anchoring Systems

The design of a wind turbine with regards to the foundation is very important, as the wind turbine will experience several forces offshore. In this section we will study the stability contributed by the chosen foundation and tower design. This design takes into account the forces generated by wind loads and wave motion and other structural design criteria such as buckling, deflection, stress and natural frequency. The best method for determining these forces are calculated using dynamic models, which account for the wind inflow, aerodynamics, elasticity, and controls of the wind turbine along with incident waves, sea current, hydrodynamics, platform and mooring dynamics of the floater.

The concrete base of a conventional offshore wind turbine is replaced by a floating structure, which needs to withstand pitch, roll and heave motion from the waves within reasonable limits. This floating base structure will also need to provide enough buoyancy in order to support the weight of the wind turbine. In practice, floating structures has been in use for decades in the marine and offshore industries, which gave inspiration to the developing of floating structures for wind turbines. The actual platform configurations may vary widely from platform to platform and usually determined by a static stability analysis. [24]

When designing a floating turbine, a concept of either multiple- or single-turbine floaters is possible, as seen in Figure 2.16. A multiple-turbine concept consists of a single platform with several turbine towers. This is done in order to decrease anchor costs and provide increased wave stability. To benefit from such a structure, the spacing between the turbines must be optimized in order to maintain the efficiency. There are also considerations that needs to be taken into account during placement of the turbines in force direction. When the direction of the wind change, the turbines need to yaw with the wind or stop producing energy until the direction shifts back to the prevailing direction. As for multiple-turbine concepts, there are a variety of possible single-turbines concepts, which is a combination of the selected platform topology previously listed and the selected anchoring system [24].

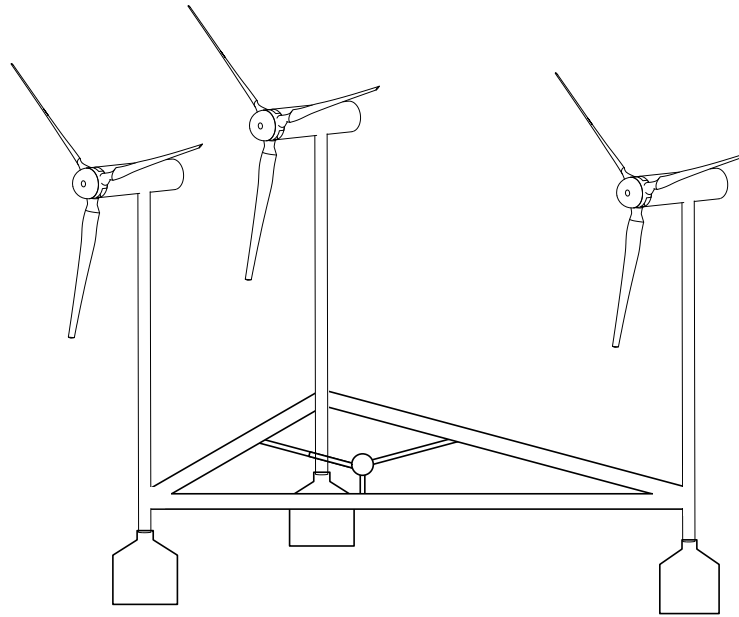


Figure 2.16: Multiple platform concept

In general all platforms, both multiple and singular turbine floaters, can be divided into three categories based on the given principle used to achieve static stability of the wind turbine construction. In reality all floating wind turbines are hybrid designs that gain stability from all three categories. The three categories and a general description of the main principles are:

1. **Ballast:** In this configuration stability is achieved by using ballast weights which are hung below a buoyancy tank located directly under the wind turbine. This approach creates a righting moment of inertia and high inertial resistance to pitch and roll movement, as well as enough draft to offset heave motion.
2. **Mooring Lines:** This category includes all types of floating platforms using mooring lines as the main method to achieve static stability. A concept called the tension leg platform use this concept to obtain righting stability of the platform structure[CITE].
3. **Buoyancy:** As seen in Figure 2.17, these types of platforms achieve stability through the use of distributed buoyancy. To obtain a righting moment of inertia, the weighted water plane area is used, the same principle that are used to keep a barge floating.

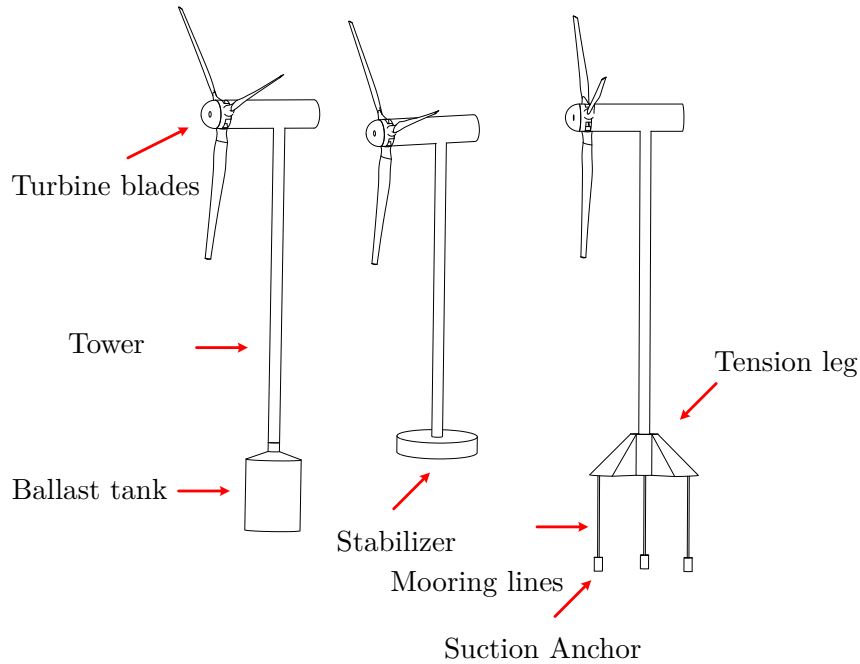


Figure 2.17: Three main platform topologies for floating wind turbines

The structural design depends on the depth of the water, and it is common to have land-based turbines with a concrete pile in the ground, or a guyed wire tower. In offshore cases the common approach is to have a monopole structure in depths of 0 - 30 meters, this is considered shallow water and allows for this foundation. At transitional depths of 30 - 60 meters the tripod foundation is common. At deepwater floating, the depths are 60 - 900 meters and in these cases the foundation is mooring lines which is attached to the seabed and a floating foundation some meters below mean sea level.

Different anchoring systems are used depending on the bottom soil conditions in the area of the wind turbine location, and whether it is shallow or deep water. Often the three different types are combined. The soil and bottom is of great importance, and this factor leads to individual design of the anchor system for each site, at least for permanent installations. Of importance is also the direction of the applied force, the direction of the wind, which influences the holding capacity of an anchor. Different anchor systems take advantage of the conditions at the given site. Even though not all single turbine platform used mooring systems to achieve static stability, they may use mooring to keep the turbine construction in place. The three most commonly used mooring systems, catenary mooring, taut-leg mooring and vertical tension legs, have been used for several years in the oil and ship industry. All three systems are represented in Figure 2.17. For a wind turbine, where horizontal forces acts so far above the center of buoyancy, it is important to maintain the stability of the turbine with a sufficient anchor system. Catenary systems has some problems maintaining stability against overturning due to the low acting center of buoyancy. However, when combined with ballast the system can provide stability and this system has in fact been used in the successful Hywind concept, discussed later. When the water depth increase, taut-leg mooring systems is advantageous due to the fact that less and shorter mooring lines are needed. Vertical tension legs are a subset of taut-leg mooring systems. Deciding on one concept or another is always a trade-off between complexity, selected anchors and turbine cost as well as the environment and other factors.

2.5.2 Prototypes and Design Concepts

Over the past twenty years, many design concepts of FOWT have been proposed and many prototypes are available on the market. However, not very many concepts have been tested under real life conditions. In this subsection some of the most promising available design concepts and prototypes are described.

HYWVIND - A Floating Wind Turbine Concept

The Hywind turbine developed by Norsk Hydro, now Statoil, is one of the most successfully tested next generation offshore deep-water floating large-capacity wind turbine concept. Previously, the installation of large wind turbines has only been on land or in shallow water close to the shore. However, the Hywind turbine is located in The North Sea 10 km West of Karmøy, North of Stavanger in Norway. This concept is the world's first full-scale floating turbine installed for testing and demonstration. Figure 2.18 is a photo from the transportation of the Hywind turbine.



Figure 2.18: A photo from the transportation process of the Hywind turbine [2]

With this turbine Statoil combines its offshore experience from the oil and gas industry with technologies from the wind industries. The Hywind turbine size is 2.3 MW, the turbine height (from sea level to nacelle) is 65 m and the rotor blade diameter is 82.4 m. At the selected site the water depth is 200 m, which is a common water depth outside the coast of Norway [CITE]. The turbine was constructed by Siemens wind power division and mounted on a floating tower construction with ballast stabilized design, described earlier in Section 2.5. Regarding the anchoring system of the Hywind concept, three slack anchored mooring lines keep the floating turbine in place. The 3-point catenary mooring system is described in Section 2.5.

The intention of the project is to test how different wave and wind conditions affect the structure of the turbine and its components. This allows further development of the design through optimization of the output power, and thereby reduce the cost, an essential part of commercializing the turbine. In 2009, the Hywind turbine was assembled. From Finland the floating substructure was towed to Åmøyfjorden, where it was raised to a vertical position. In Dusavika outside Stavanger, the wind turbine was pre assembled in two parts. The tower, the nacelle and the rotor was connected with the tower accounted for one part while the blades and the hub the second assembly. Both part was transported to Åmøyfjorden where the wind turbine was lifted in place and mounted on the substructure. The test period started in 2009 and lasted for 2 years. Since then, Statoil has started working on a pilot park i Scotland with five 6 MW turbines. [2]

The most innovative and important feature of Hywind is the active damping pitch control system. Normal procedure for a pitch controlled land based wind turbine is to adjust the blade pitch in such a way that constant power is generated for a relative wind speed above the rated wind speed of the turbine. However, for a floating concept this may not be as simple due to the tendency of increased negative damping of the tower motion. Hywind's active damping system utilizes the velocity of the tower structure to optimize the pitch in the system, with respect to damping of the tower motion as well as well as keeping the power output at constant level.

The HiPRWind Project

The High Power, High Reliability Offshore Wind Technology is an EU funded research and development project started in 2010, to contribute to the development of renewable resources in the offshore wind industry. The project focused on very large cost-efficient floating wind systems and farms to take advantage of unused deep water areas all around the world. Originally the project was intended to test a prototype on 50 m depth in the Bay of Biscay to deliver data to researchers. Due to funding problems, the project stranded. However, The Norwegian University of Science and Technology (NTNU) and the Norwegian company that designed the floating structure, intend to transport the prototype floating structure to Trondheim to test the wind turbine, and continue research and development on offshore wind. As of today it is not known when and if the prototype is transported to Trondheim. The design of the structure can be seen in Figure 2.19a.

WindFloat

This floating concept is developed by Principle Power and the turbine by Vestas. A full-scale prototype was tested offshore 5 km outside the coast of Portugal in 2011. The WindFloat is a three-legged floating foundation structure for multimegawatt FOWTs. It is designed to accommodate a wind turbine, approximately 5 MW or larger, on top of one of the legs. The platform is intended to be used with onshore turbines which simplifies the design process significantly, as no new turbine part has to be developed. As Hywind this platform structure was also based on design previous tested in the oil and gas industry. The floating structure itself along with the wind turbine was completely assembled and commissioned onshore before being transported to the test site outside Aguacadoura. This significantly reduces the cost of deployment significantly compared to other structures which require lift operation of heavy constructions offshore. [4] A subsea cable delivers electric power to the local grid, and last summer the test turbine past the 10 GWh threshold for total energy produced. The project have been extended to include test sites outside Maine and Oregon. An illustration of WindFloat can be seen in Figure 2.19b.

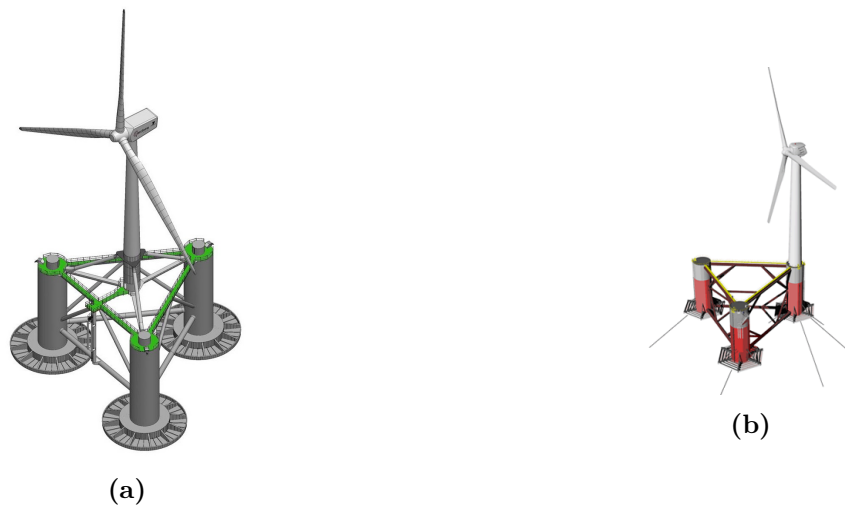


Figure 2.19: Two different floating offshore wind turbine design: HiPRWind Project [3] and the WindFloat project [4]

FORWARD: Fukushima Mirai

Japan started developing alternative energy sources after the Fukushima nuclear melt-down in March 2011. This project is called Fukushima FORWARD, and the intention is to install a wind farm outside the coast of Japan and bring the local community of Fukushima a step forward and recover from the incident. So far three wind turbines and a power station have been installed. The first construction of a compact semi-sub floater for a 2 MW downwind turbine was completed in May 2013. This floater is a three-legged structure with an extra beam in the middle connected to each other. Ballast tanks are located on the bottom of each leg [25].

In June 2013 the turbine was assembled on top of the floating structure and after a commissioning test the construction was towed to the test site where it began generating power in November the same year. Figure 2.20 shows the floating structure at the construction site.



Figure 2.20: The floating structure of the Fukushima FORWARD Project [5]

2.5.3 Design Tools and Simulation Programs

A short introduction to design tools and simulation programs for floating turbines will be given in this paragraph. Currently, the design tools and software to simulate floating offshore wind turbines has become more and more technically advance and accurate. In large-scale projects, programs such as FAST, HydroDyn, TurbSim, AeroDyn, SIMO/RIFLEX, ADAMS and 3DCharm have been used to simulate the different conditions and situations that may occur during offshore production [6]. SIMO/RIFLEX is developed by researcher at NTNU.

FAST, Fatigue, Aerodynamics, Structures and Turbulence, is a publicly available simulation tool for horizontal axis wind turbines, which initially was developed for the conventional analysis of fixed-bottom wind turbines. Later on, the FAST code has been extended to also include analysis of floating offshore wind turbines. The FAST code can combined with the two packages AeroDyn and HydroDyn to include four categories: analysis, structural dynamics, aerodynamics, hydrodynamics and mooring lines. The HydroDyn packages apply the Airy wave theory to calculate the wave kinematics with free-surface corrections [26]. The forces of mooring lines are represented using a quasi-static mooring system module. This module represent the weight of the mooring lines in fluid, the stretching of the lines and the friction at seabed.

SIMO is used to model and simulate offshore structures, and this simulation tool is also extended to include floating wind turbines. This is done by adding an external model to simulate the aerodynamic forces of the rotor. RIFLEX is coupled with SIMO to include dynamic of analysis of mooring lines among other [6]. A picture from the simulation tool can be seen in Figure 2.21.

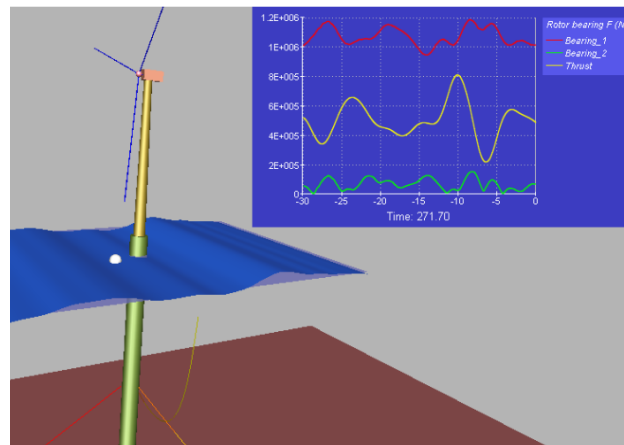


Figure 2.21: A screen capture from the SIMO software [6]

2.5.4 The Future of Offshore Wind: Challenges

The main challenge of floating offshore wind installations is to reduce the cost of development, operation and maintenance, in order to reduce the threshold for investments in the technology. The possibility of mass production will lower the cost considerably, but require simple systems. As well as the cost aspect of the challenge, some technical challenges will be discussed. Among these challenges are dimensions, wave loads, stability, motion response and anchorage.

When designing an offshore floating wind turbine it is necessary to think of the new mechanical constraints which affect the nacelle and the rotor. The motion of the selected floating structure will affect the performance of the wind turbine and vice-versa. If the concept is economically feasible, the mass of the floating structure is not much larger than the mass of the wind turbine. [22] Due

to this fact, the rotational movement of the rotor and the conversion of kinetic energy to electricity will affect the floating structure. The current trend is also to design taller wind turbines to catch the more effective higher wind speeds, which causes small pitch and roll rotations that result in large motion at the location at the nacelle. The same effect can be seen for velocities and accelerations which cause a large load on some of the most sensitive components. The large load on structural components, increases the importance of designing constructions that can handle the increased load, which will invariably increase cost. It is also important to gain stability of the structure during its entire lifetime in rough weather conditions.

As for most large scale wind turbines the installation process is a complex and time consuming process. When installing a wind turbine at sea, the water and weather conditions are of great importance. From the Hywind installation, two main challenges can be outlined; the water depth, and the conditions of the waves and swells. To upend and assemble the structure a sufficient water depth is required. This was not an issue at the assembly point for Hywind, but would be in other areas where the water is shallower. Close to shore or if there are some shallow passages offshore on the way to the the destination point of the wind turbine this may cause trouble. To assemble such a large structure as the Hywind turbine involves very large forces, and the effect of waves and swells increase the impact on the turbine and the constructions used to upend the turbine. It is necessary with low winds and low waves for a sufficient period of time. This restricts the installation period to the summer months in the respective parts of the world, which is unfortunate since time and time delays increase the cost. Also the assemble process need to be optimized to assemble structures safely, efficiently and economically.

To install a wind turbine construction and take advantage of the energy in the wind effectively requires a lot of work, but usually more than one turbine is located in the same area in a wind farm. A wind farm can include 10 - 100 turbines or more. One issue that needs to be addressed is how the transportation of multiple turbines to the destination point can be done efficiently. There is no doubt it is complicated to transport a 80 meter turbine mounted on the top of a 100 m substructure. This is an important question for the future, as Statoil plans to locate large wind farms outside the coast of Scotland.

As for all structures and especially rotating structures, maintenance is required to ensure a safe and reliable operation. Sometimes large and heavy components, such as the blades, need to be replaced. Then it should be easy and cost efficient to perform the operation itself as well as the transportation of the components. Stability needs to be maintained during the maintenance period as well. Other issues related to the maintenance is the possibility of corrosion due to the corrosive environment and fatigue due to the constant impact of waves, wind and rotating components. In areas where the temperature goes below zero, the possibility of ice formation on the blades must be considered.

Multiple turbines in a wind farm create a complex flow field since the turbines affect each other. In other words, it is not beneficial to place a wind turbine in the shadow of one of the other turbines, due to loss of mechanical energy as the wind field is distorted. To avoid these circumstances some of the towers can have an increased hight, but wind farms are carefully planned and all these issues are taken into account. However, despite the challenges in the coming years it is expected that the offshore wind industry will increase significantly.

2.6 Motion-Compensation

A motion compensator is, as the name suggest, a device that compensates for any undesirable effect of the relative motion between two connected objects, for example the wind turbine and the surrounding water. The motion compensator usually compensates for the effect of motion in all directions, both linear and rotational. An offshore wind turbine has six degrees of freedom which means that it can move in all six directions. The three linear motion are heave, sway and surge and the three rotational motions are pitch, roll and yaw. Heave is the up and down motion along the linear vertical axis, sway is the side to side motion along the lateral axis, while surge is front to back motion along the longitudinal axis. Pitch motion can be defined as the motion around the lateral axis which in terms of a wind turbine, means turning the angle of the blade. The roll motion occurs around the longitudinal axis, while the yaw motion occurs around the normal axis, i.e. the axis along the wind turbine tower. All motions are illustrated in Figure 2.22.

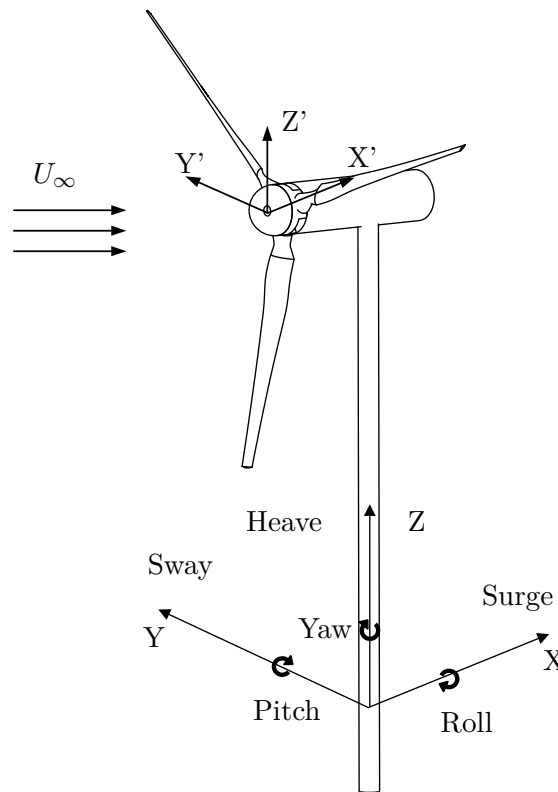


Figure 2.22: Degrees of freedom for an offshore floating wind turbine platform

2.6.1 Stewart-Platform

University of Agder has two Stewart platforms to be used for scientific purposes situated in the lab area. A Stewart platform is a robot mechanism that incorporates six prismatic actuators to be able to simulate motion in all directions. The prototype was designed by D. Stewart, and described in a paper for the first time in 1965 [27]. The mechanism he built consisted of a triangular platform supported by ball joints, connected with three legs adjustable in length. The adjustable legs was then connected to ground through a two-axis joint. Eric Gough, another researcher of the same period, suggested an improvement with the use of six linear actuators in parallel, which was similar to a tyre test machine he had designed some years earlier. In the paper the Stewart platform is described as a mechanism which has six degrees of freedom, controlled in any combination by six motors, each at a given distance from the ground. Initially it was designed to simulate flight

conditions in order to generate general motion in space to be used for pilot training purposes. It has since been used in numerous applications in the field of robotics.

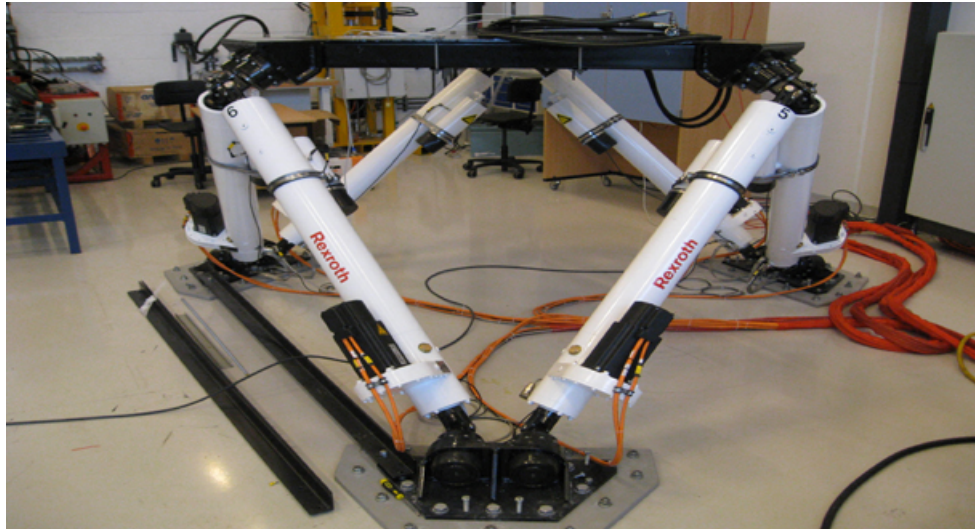


Figure 2.23: The Stewart platform located at UiA, [7]

The design of the platform has been subjected to modifications since the first models, but the concept is still the same. Currently, a Stewart platform consists of a base and a platform connected together with six extendible legs, each leg with spherical joints at both ends.

Chapter 3

Methods and Tools

This chapter describes the methods and tools utilized in order to finalize the project description presented in Chapter 1. All models and procedures are described and illustrated to give the reader a good understanding of the project. The chapter is divided in different subsections to easily get an overview of the different parts. The first part consider the making of the test model, while the second part consider the experimental setup and the functionality of the pitch controller. In the third section, force calculations regarding the blades as well as other components affected by forces have been carried out. The final section considers the simulated part of the project.

3.1 Wind Turbine Test Model Design

In this section the wind turbine test model is described. All parts are explained and widely illustrated with descriptive figures from the CAD model and photos to ensure that the reader understand the different concepts. Moreover, all choices taken regarding the feasibility of the design is explained and justified.

3.1.1 Concept

A small scale wind turbine model is designed in SolidWorks. The different components are 3D-printed using a ProJet 3510 HD printer, and later assembled to test and optimize the pitch controller mechanism. The main shaft as well as the bearings, screws, washer and nuts are made of steel. All other parts are plastic materials from the 3D printer. The concept of this model includes a mechanism to pitch the angle of the blades to the desired position relative to the wind speed. The pitch angle for wind turbine blades is described in detail in Chapter 2. A stepper motor is used to provide the rotation needed to move the slider mechanism in order to rotate the blades to the desired angle provided by the control system. The stepper motor is connected to a PLC-controller developed for providing the desired angle. Figure 3.1 shows the final setup of the wind turbine with the main components inside the nacelle, the rotor mechanism, the tower and the base. The modelled parts shall be mounted on a steel plate, which means that some of the parts might not be printed, as they are not needed. However, they are included in the figure to illustrate an example set up. Illustrative photos of the final concept can be seen in the experimental set up section.

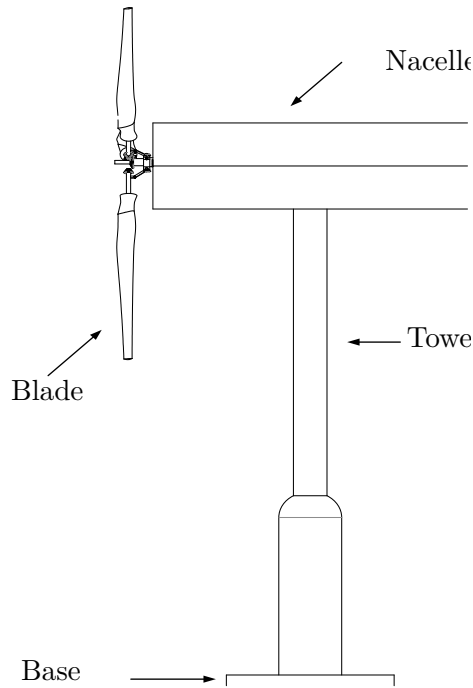


Figure 3.1: Concept of Test Turbine Model

Specifications of the test model are listed in Table 3.1.

Table 3.1: Design Specification of Wind Turbine

Parameter	Value
Hub height	1060 [mm]
Hub diameter	165.77 [mm]
Hub length	82.885 [mm]
Length of main shaft	1050 [mm]
Length of blade	478.86 [mm]
Rotor diameter	1200 [mm]
Pitch in start position	0 [°]
Slider mech. movement distance	106 [mm]
Tower height	1005 [mm]
Tower width	300 [mm]

3.1.2 Blades

The blade is modelled after NACA4415, provided from the UIUC Airfoil Coordinates Database. In Figure 3.2, the shape of the foil is shown and important values can be seen in Table 3.1. To transform the shape of the foil to a blade, the blade is divided in ten section, with a different chord length and a different angle. With this approach the blade will get a smooth surface.

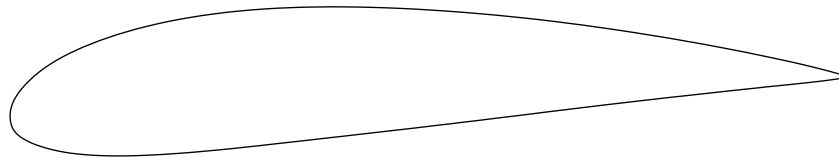


Figure 3.2: Shape of the blade sections

The total length of the blade is 478.86 mm, the distance from rotor center to the beginning of the blade is 146 mm and the diameter of the blade connection section is 40 mm. It can be observed that the distance between the rotor center and the beginning of the blade is quite long, and this is done to be able to extend the blade length as well as some space, if modifications are required.

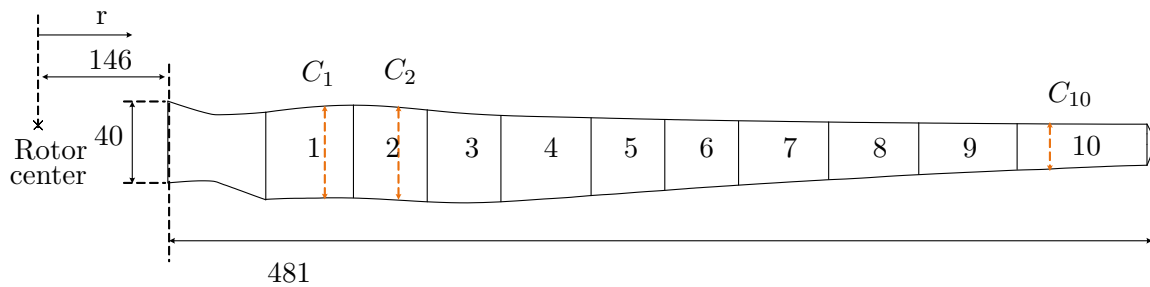


Figure 3.3: Wind turbine test model: Structure of the blade

The idea of this setup is to be able to control the pitch angle of the blades simultaneously in order to achieve greater output power. Bevel gears are used to transfer the linear motion of the slider mechanism to rotation of the blades. A link mechanism turns the blades, and the pinions follows the track of the gear head. The design ensure that the motion is transferred, and at the same time limit, the changes in pitch angle to prevent too large angles. Figure 3.4 shows the the gear and the three pinions rotating around. In the middle of the gear shaft, the main shaft of the wind turbine is connected. The main shaft is rotated when the wind rotates the blades, and mechanical power is created from the wind energy.

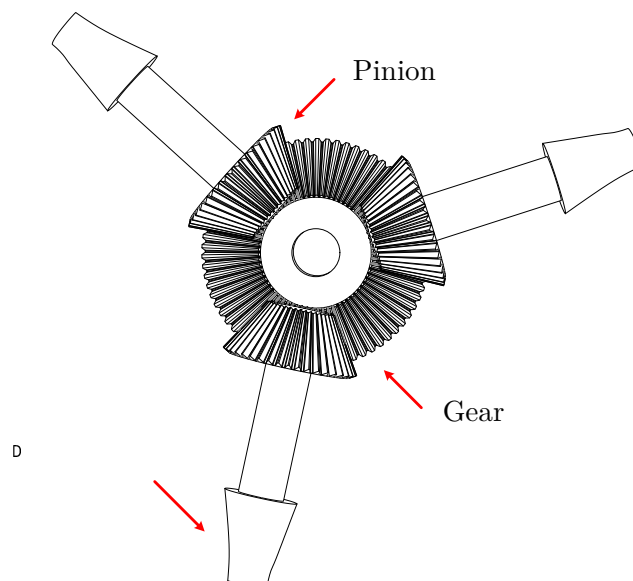


Figure 3.4: Wind turbine test model: Gear and Pinions

3.1.3 Stepper Motor

In order to precisely control and track the pitch angle of the blades, we use a stepper motor which is programmed in Siemens PLC. The drive mounted on the PLC is a 1-Step-Drive from Phytron. The program enables pulses to the stepper motor, thus we can program and monitor the pitching system as it changes based on the pitch angle as a function of different wind speeds.

The stepper motor used in this project is the 440-470 stepper motor delivered by RS Components. The stepper motor is a pulse driven electric motor which is suitable for motion control in many different areas of application. The 440-470 is a 8-wire unipolar stepper motor. The main parameters for its task is the current rating and the degrees the motor rotates per pulse. The current rating is considered as a unnecessary powerful motor is unwanted for the small-scale test model. The deg/step relationship is vital to precisely control the pitch angle. The specifications for the stepper motor are shown in the data sheet from Phytron, an excerpt of the most important data is shown in Table 3.2.

Table 3.2: Data for stepper motor 440-470

Specification	Value
Current Rating	4.5 [A]
Frame Size	82.6 x 82.6 [mm]
Holding Torque	2200 [mNm]
Number Of Wires	8 [-]
Resistance Per Phase	0.56 [Ω]
Shaft Diameter	9.5 [mm]
Step Angle	1.8 [$^\circ$]
Stepper Motor Type	Hybrid [-]
Voltage Rating	2.5 [V]

For different drive requirement, the windings can be connected either in series or in parallel. The configuration of the stepper motor used in this project is unipolar, and the windings for the motor is connected in parallel, which is standard for this model. The motor is further connected to the PLC as a 4-lead stepper motor as shown in Figure 3.5.

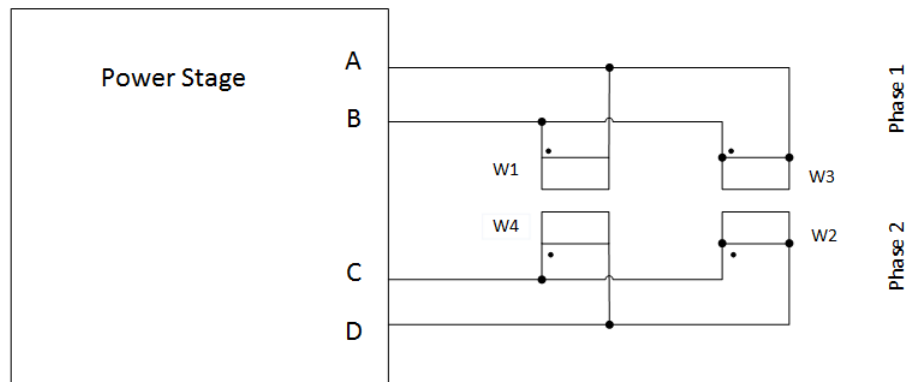


Figure 3.5: Wiring scheme for 1-Step-Drive module. In this project a 8 lead stepper motor is connected in parallel as a 4-lead.

The connection from the stepper motor to the 1-Step-Drive on the PLC is shown in Figure 3.6. The motor provided for this project was connected properly in advance, so the main focus was to design the program and establish a satisfying pitch control.

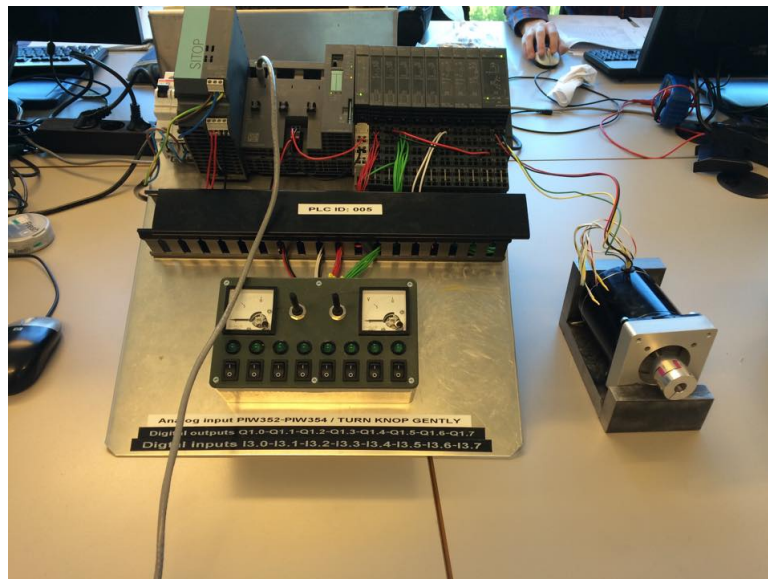


Figure 3.6: The stepper motor from RS components connected to the Siemens Simatic et200s PLC via 1-Step-Drive from Phytron

3.1.4 Pitch Control System

The pitching system consists of a screw with a rotating nut, a slider and a lift mechanism connected with two links. With the help of the nut, which is connected to the lower hole of the slider, the screw transfers rotational motion to the slider mechanism. When the slider is moved back and forth, the link mechanism is moved accordingly. This motion contributes to the pitching of the blade angles, controlled by the bevel gears connected to the pinions, link mechanism and main shaft, as shown in Figure 3.7. Here are all the components that constitute the pitching system are shown and named.

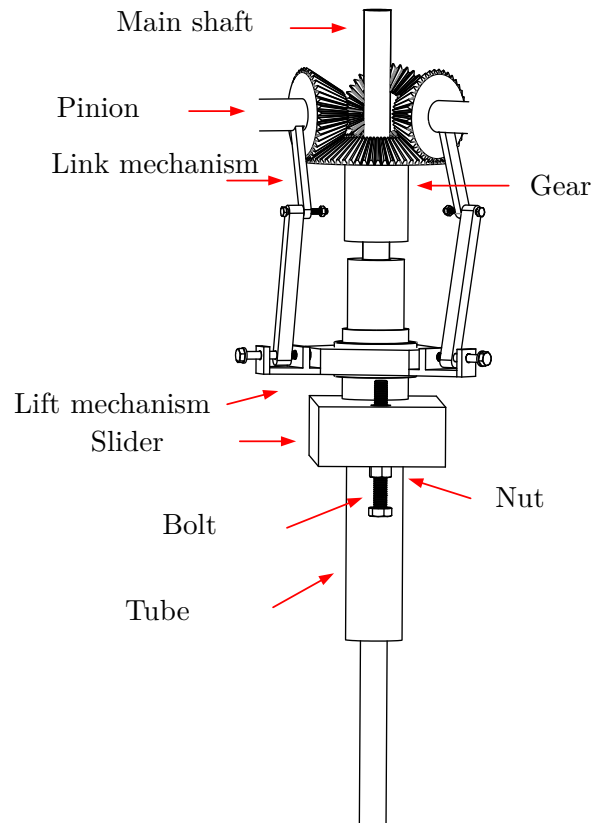


Figure 3.7: Test turbine model: Pitch mechanism

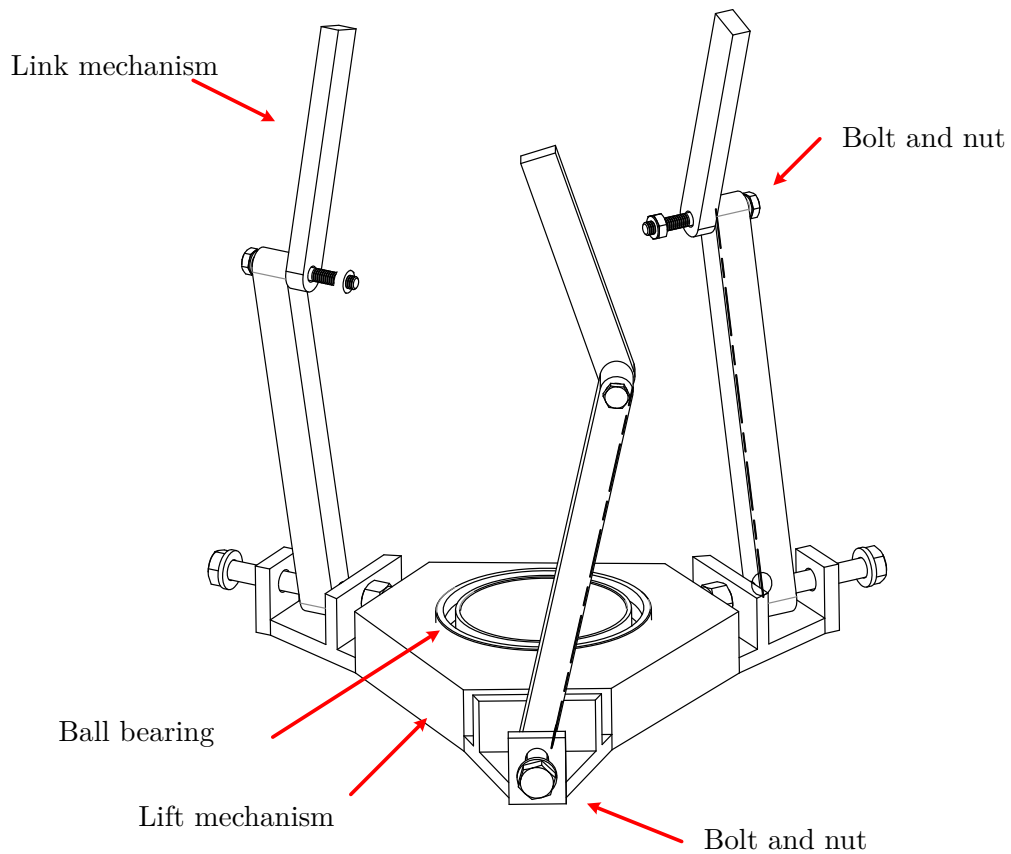
Figure 3.8 shows the lift mechanism connected with the links. The links are fastened to the lift mechanism with bolts and nuts. It is seen that it is the upper part of the link that gives the rotational motion. The gear is fitted inside the middle hole in the middle the lift mechanism, while the link mechanism is connected to the three pinions. In table 3.3 and 3.4, the selected size, number of teeth and other parameters in connection with the gear and the pinion is shown. The module indicates the size of the gear, which is the reference diameter of the gear divided by the number of teeth. The gear ratio is 1.75.

Table 3.3: Gear parameters

Parameter	Value
Module	1.75 [mm/teeth]
Number of teeth	70 [-]
Pressure Angle	20 [°]
Face width	35 [mm]
Hub diameter	50 [mm]
Nominal shaft diameter	20 [mm]

Table 3.4: Pinion parameters

Parameter	Value
Module	1.75 [mm/teeth]
Number of teeth	40 [-]
Pressure Angle	20 [°]
Face width	35 [mm]
Hub diameter	25 [mm]
Nominal shaft diameter	20 [mm]

**Figure 3.8: Test turbine model: Lift mechanism**

The stepper motor is connected to the rotating screw as shown in Figure 3.9. When the screw rotates the l-shaped slider mechanism moves linearly and the tube connected to the lift mechanism rotates the pitch angle.

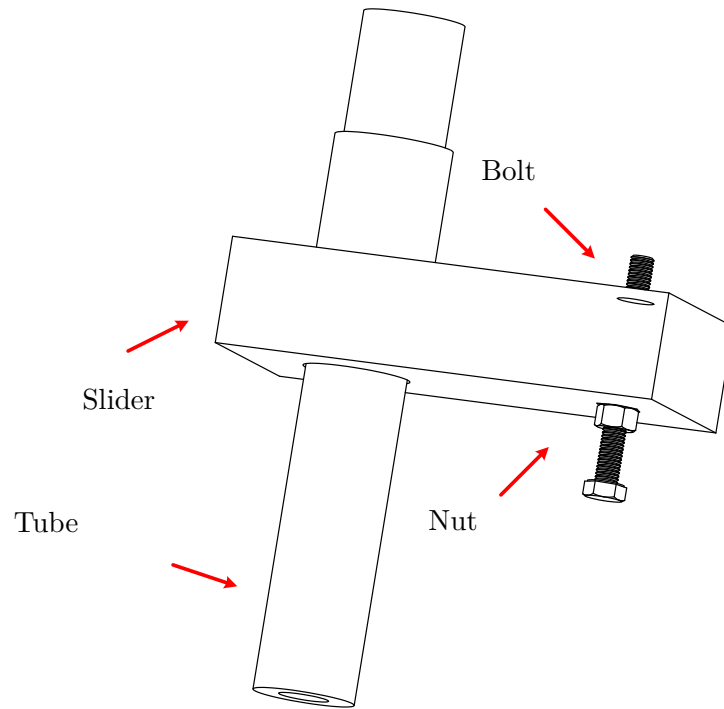


Figure 3.9: Test turbine model: Slider mechanism

3.1.5 The Selection and Location of Bearings

To ensure that all parts rotate smoothly and stabilizes the nacelle components on the tower structure, bearings are included in the design. The selection of bearings are based on expected torque and force requirements as well as available dimensions. All bearings are selected from the SKF bearing catalogue. In Figure 3.10, the position of all bearings are marked with red arrows.

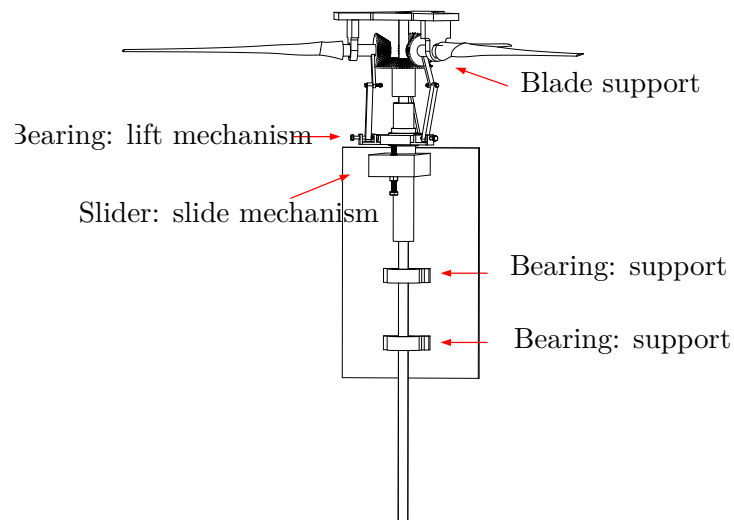


Figure 3.10: Positioning of bearings and slider mechanism

The lift mechanism rotates when the blades rotate, but is also required to move linearly along the lateral axis. To achieve this, the lift mechanism is mounted on the slider. However, to avoid rotation of the slider, a deep groove ball bearing (single row) is located between the gear and the lift

mechanism to allow the gear to rotate freely. The bearing is of type 61810-RS, and all dimension and tolerances can be seen in Figure 3.11. RS means that it is lubricated and covered with rubber coating. A single plastic tube is fitted between the slider and the main shaft to avoid the need for more bearings. Between the tube and slider a relatively small tolerance is kept in order to insure a smooth sliding.

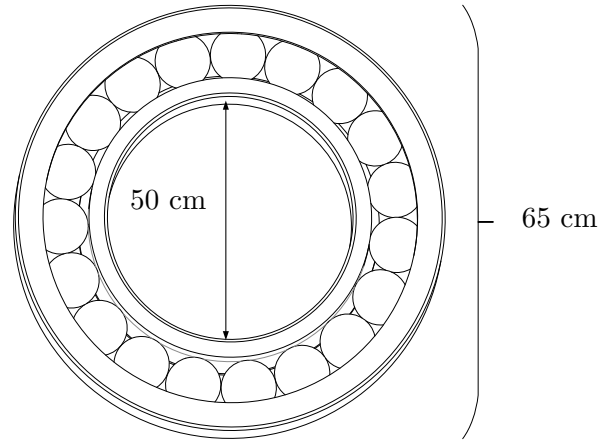


Figure 3.11: Bearing between the gear and the lift mechanism

To support the components inside the nacelle as well as to ensure the rotating of the main shaft, two bearings are included between the main shaft and a support structure mounted on a horizontal steel plate. The bearings of type 6005-RS are glued to the support plate with epoxy. All the dimensions can be seen in Figure 3.12.

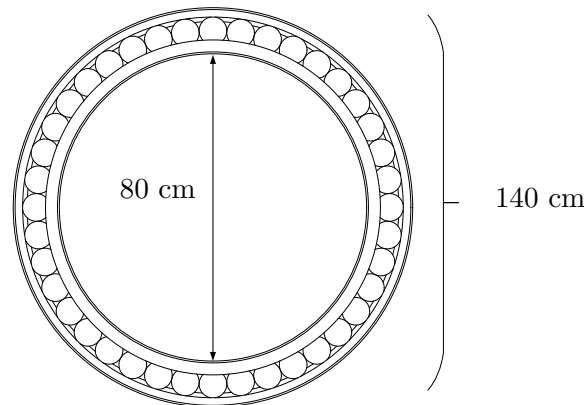


Figure 3.12: Bearing between main shaft and the support structure

To keep the blades in correct position a support mechanism is connected to the main shaft, and a total of three bearings are utilized to ensure the rotational movement of the blades. The three bearings are connected to the blades to support the blades as well as allowing free rotational movement of the blades, as seen in Figure 3.10. Dimensions of the bearing can be seen in Figure 3.13

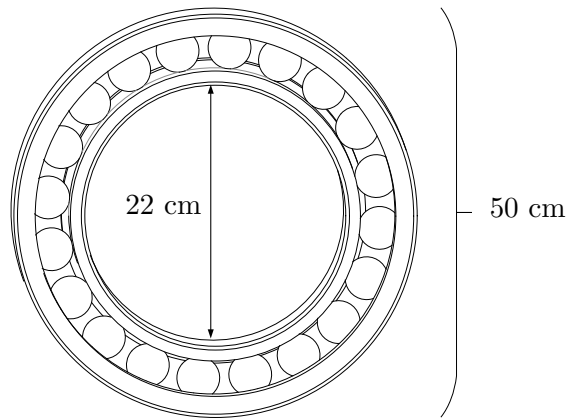


Figure 3.13: Bearing between the support structure and the main shaft

Most components of the test model are made of plastic, while the bearings are made of steel and therefore a potential problem could be the linear movement of the bearings during operation. The bearings are press fitted, but a small edge is included to prevent unintentionally sliding of the bearings. However, plastic could never withstand as much force as steel or a different metal.

3.2 Experimental Setup

In this project, the main goal is to build a pitch controlled wind turbine based on optimal pitch angle from the given wind speed and validate the results with calculations. The approach will be explained as well as the design of the downscaled test model, including the programming of the pitch control. In order to get the model working properly, calculations for the pitch angle was carried out. These calculations will be described in this chapter. Finally the validation and testing of the wind turbine will be shown.

3.2.1 Assembly of the Turbine

The assembly of the test model wind turbine requires a lot of preparation. In this section we will explain each step of the process, from the design of the parts in 3D-modelling parts shown in the previous chapter to the final plastic parts assembled in the test model. Most of the parts are modelled in SolidWorks and printed using plastic material. However, crucial components such as the turbine foundation and main shaft are made of steel material.

The prototype model is mostly made of two different types of plastic from the two 3D-printers used to produce the components. However, the printers also print with different methods which gives a large difference in quality. The high definition printer produce massive components which gives them high density and relatively high weight compared to the component of the other printer. The standard printer (see Appendix B.2) produces components with a solid surface, while inside plastic material is layered up in a zigzag pattern with air in between. This gives the components a much lower density and thereby much lighter than the massive components. This way the wind turbine was built in the lighter components where this was possible, and high definition where this was needed. The main shaft, the bearings, the slider mechanism fixed to the tower structure and the tower structure itself is made of steel.

Foundation

The foundation of the wind turbine, or the wind turbine tower, is an important component that needs to be stable and strong in order to handle the forces from the rotational motion from the wind turbine. For this reason, the entire set up of the tower is made of steel parts. The tower structure is shown in Figure 3.14.



Figure 3.14: The tower structure for the wind turbine

The tower is assembled by the use of a welding robot from ABB, shown in Figure 3.15. With the robot, the upper plate and the bottom plate could easily be welded to the legs, which was also the case for the bracing structure. This made the tower structure strong and stable, as well as the possibility for human error during assembly was reduced. A simple program used for the welding robot makes it possible to accurately weld the components together.

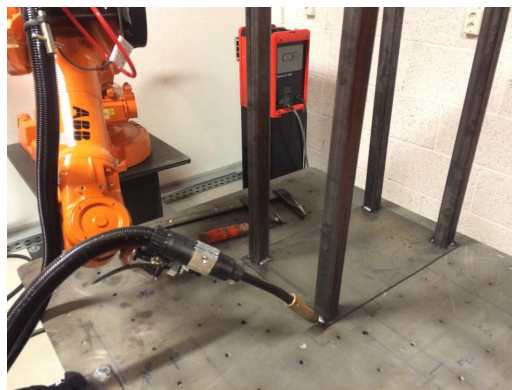


Figure 3.15: Welding robot from ABB at the University

The tower structure is made of a steel plate with dimensions 300 mm x 500 mm x 4 mm with four hollow metal legs welded to each corner of the steel plate. A second steel plate of the same material, but with a larger thickness, is welded to the other side of the legs forming a sandwich structure. A robot can weld faster than manual welding and prevents too much damage of the thin steel plate as there is less time to heat the material. To support the PLC placed beneath the main body of the test model, four metal pieces is welded between the legs. The bracing steel both supports the entire structure as well as creating a platform for the PLC. As the cables from the motor to the PLC is of limited length (30 cm), the bracing structure has to be welded in an appropriate height. A slider mechanism is mounted on the steel plate, which makes it possible for the stepper motor to move the pitch mechanism back and forth.

Main Body

The main body as shown in Figure 3.10 consists of two bearing casings, the slider connected to the mechanical pitch mechanism as well as the electric stepper motor and a tube that encloses the main shaft through the slider. The pitching of the blades will be prompted by the bevel gears connected to the main shaft. In Figure 3.16 the assembly of the three pinions are shown. These will be bonded to the supporting plate in front of the blades and also connected to the large bevel gear, keeping them tight in position.



Figure 3.16: The finished print of the bevel gears in housing

All the bearings used in the prototype is press fitted. Since the bearings are made of steel and the surrounding components are made of plastic, epoxy is a reasonable choice to fasten the bearings in the casings. All surfaces are cleaned sufficiently with acetone before assembly. The turbine is assembled from the rear, starting with the support structure for the casings, before assembling the rest of the components. The bearing houses and part of the mechanical slider mechanism is shown in Figure 3.17.

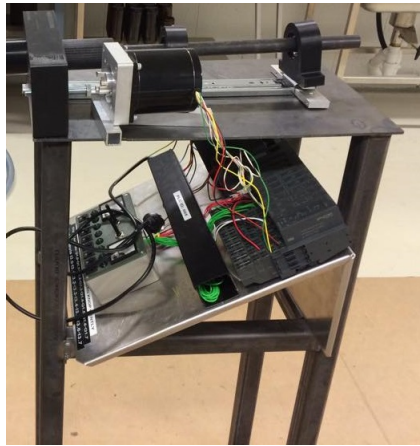


Figure 3.17: The main body mounted on the tower structure with the plc placed below on the bracing

The final model is shown in Figure 3.18. Here the model is mounted to the tower structure, with the programmable logic controller placed below the turbine on the bracing structure. The assembly of the complete turbine is done mostly by using epoxy and locktite to attach the different parts. By gluing the parts together like this, the model becomes more rigid, and the level of tolerance due to vibrations is high.

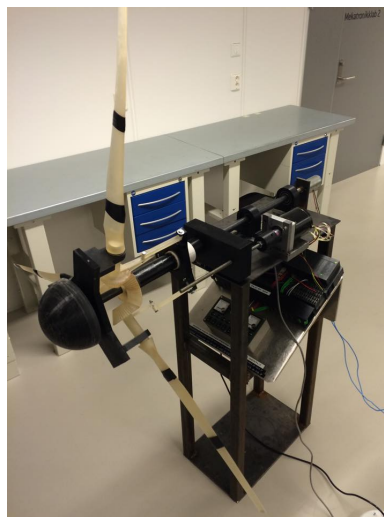


Figure 3.18: Final model with PLC

The frame built to keep the stepper motor from moving is shown in Figure 3.19.

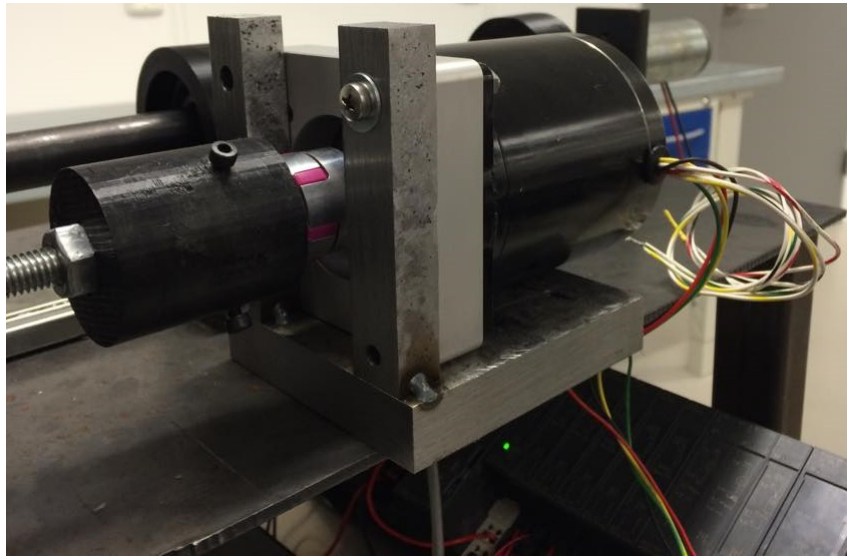


Figure 3.19: Stepper motor support structure

Blades

Next step is to assemble the blades. The blades were divided in three parts since the dimension of the printer is too small to fit the entire blade at once, as it is 478.86 mm. On each side of the blades either a tap or a hole was made on the end of each blade in order to enable a simple assembly. After cleaning the surface, a two component Loctite glue is used to bond the blade together, as seen in Figure 3.20.



Figure 3.20: Mounting of the blades

The taps give the blades a some additional strength, which is needed, as the blade is printed in

three parts. At the root of the blade the pinion is mounted as well as the support structure to prevent the blade from falling out of position. Bearings are mounted inside the support structure as previously described to allow the blades to rotate freely. The complete support structure consist of a rigid support rig, which ensures the stability of the rotor. The finished assembly of the rotor is shown in Figure 3.21, where the supporting plate is connected to the shaft and rotates along with the blades. All technical drawings can be found in Appendix D.

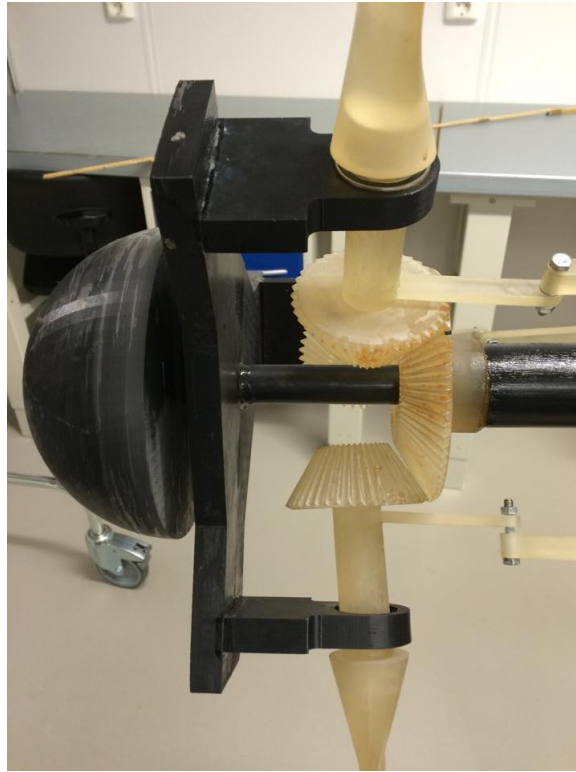


Figure 3.21: Support rig of the blades

Power Generation

A generator is connected directly to the main shaft of the wind turbine. A DC brush motor from Kählig Antriebstechnik GmbH is provided by UiA, and the data sheet can be found in Appendix A.2. To measure the voltage, the generator is connected to the same analogue signal detector as mentioned before to be able to log the data from the generator in LabVIEW. The program developed in LabVIEW, as seen in Figure 3.22, log the data in a txt-file which easily can be implemented in MATLAB.

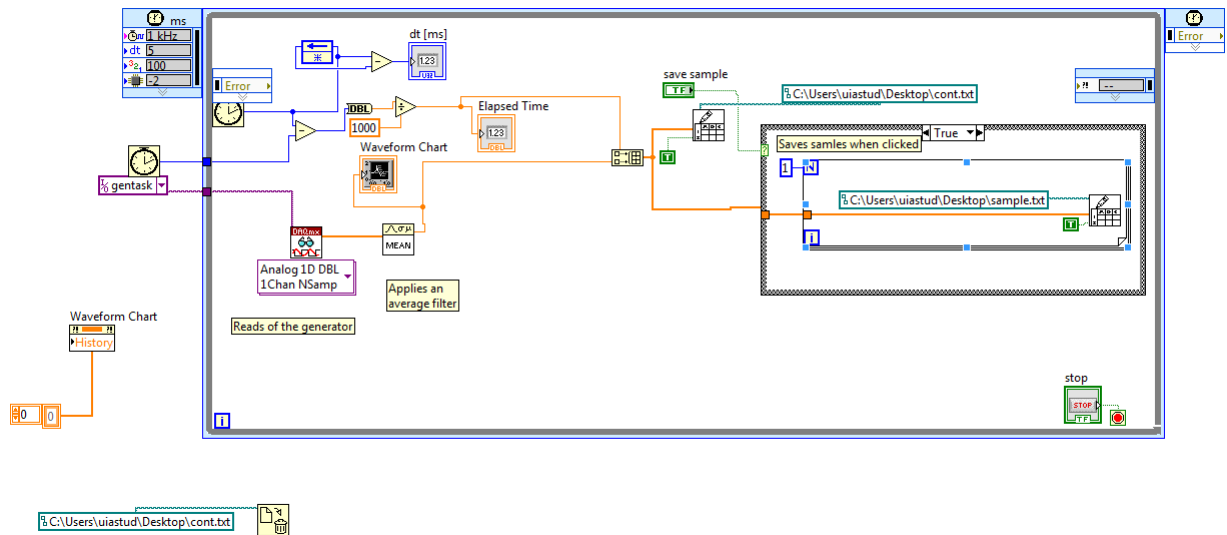


Figure 3.22: The LabVIEW program developed to log the data from the generator

The generator was tested with an electrical drill to see if the relationship between voltage and rotational speed indeed was linear and thereby verify the functionality. As seen in Figure 3.23, the relationship is linear, as expected.

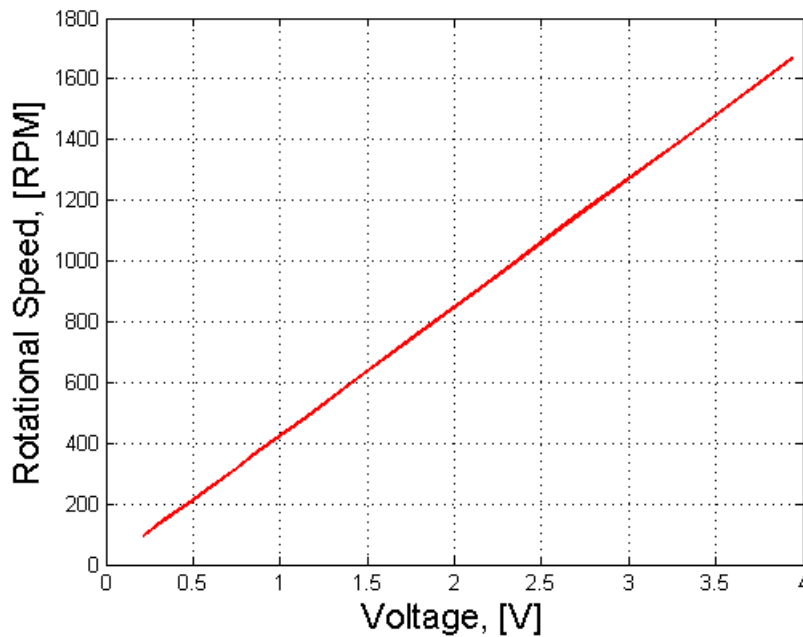


Figure 3.23: Relationship between voltage and rotational speed in the generator

3.2.2 Optimized Functions For PLC: Control of Stepper

The stepper motor is controlled by the PLC with a ladder diagram. To determine the number of steps required to turn the angle to the optimal angle.

1. A function determining the optimal pitch angle from the wind speed corresponding to the size of the test turbine. The wind speed is the input variable.

2. A function determining the distance travelled by the screw in order to achieve the given pitch angle. The Pitch angle is the input variable of the function.
3. A function determining the number of steps required to achieve the distance travelled.

The method used to calculate the pitch angle utilize some of the principles from [ref] and [ref]. The angle of the pinions is the same as angle as the pitch angle of the blades. It is necessary to calculate this angle in order to find out the distance the slider would need to move to turn the blades to a given position, as well as preventing the link mechanism to move out of position and break. In addition it is necessary to find out how many steps the change in position requires. When calculating the pitch angle, three main positions are considered, and then curve fitting is used to find the rest of the angles and a suitable function. The three positions are the start position(initial angle of the blades), the middle position and the end position(max pitch angle), which are shown in Figure 3.24. Dimensions and angles are shown for all three positions. If the pitch angle can be controlled, the power output can be optimized compared to a fixed pitch wind turbine which usually have one or two fixed speeds and cannot rotate the blades along the lateral axis. Most large scale turbines (more than 10 MW) nowadays have electric pitch controlled blades.

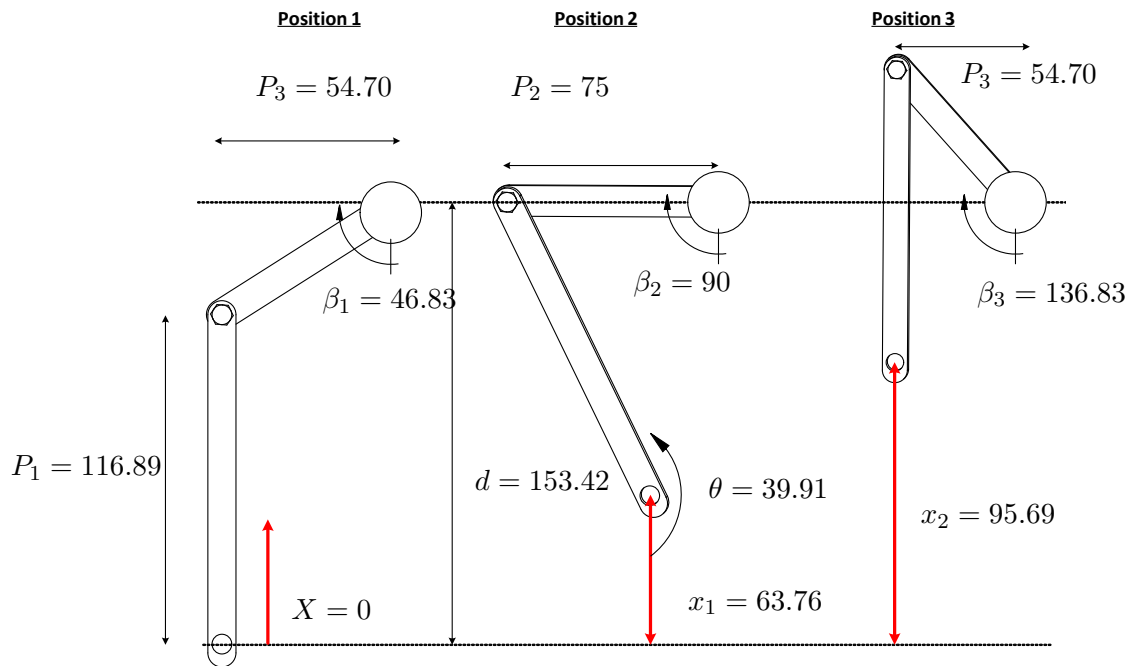


Figure 3.24: Link positions, all dimensions given in mm and degrees

The test model has a mechanical construction, described in the previous section, to turn the angles. It is beneficial to use a hybrid stepper motor because it is possible to calculate the linear movement of the slider based on the rotational movement of the given hybrid stepper motor RS 440-470. Technical specifications can be found in Appendix x. Since the stepper motor is of type hybrid with a step angle of 1.8° , it is capable of delivering much higher working torques and stepping rates than a permanent magnet motor with 7.5° and 15° step angles, which is important for positioning. The given step angle means that the shaft angle moves 1.8° for each step from the stepper motor. This gives 200 steps per revolution.



Figure 3.25: The stepper motor used in this project

The linear distance of the screw can be described as a function of the shaft angle and number of steps. A M10 standard screw has a pitch of 1.5 mm, which is quite large for this particular use. Preferably a small pitch is wanted since then it is a smaller pitch angle difference corresponding to the achieved linear motion and consequently a higher precision. Equation (3.1) and (3.2) gives the representation of the linear distance based on number of steps.

$$X = \frac{\text{thread pitch}}{360^\circ} \cdot \alpha = \frac{1.5}{360^\circ} \cdot \alpha \quad (3.1)$$

$$\alpha = P_\alpha \cdot S = 1.8 \cdot S \quad (3.2)$$

where

X	=	Screw linear distance [mm]
thread pitch	=	Standard pitch of M10 [mm]
α	=	Shaft angle [°]
P_α	=	Step angle [°]
S	=	Step [-]

Since the distance will be the input, the equation is inverted and can be seen in Equation 3.3.

$$S = \frac{360 \cdot x}{\text{Screw thread} \cdot P_\alpha} \quad (3.3)$$

In addition to the calculation of the linear position, the pitch angle is required to be calculated as a function of the linear motion. A mathematical representation of the two link mechanical system is given by Equation (3.4) and (3.5) based on the design of the test model.

$$X = d - P_1 \cdot \cos \theta - P_2 \cdot \cos \beta \quad (3.4)$$

$$P_2 \cdot \sin \beta - P_1 \cdot \sin \theta = P_3 \quad (3.5)$$

where

- A = Distance from start position(equal to start position of link 1) to position of blade shaft [mm]
 X = Distance from start position of pitch mechanism to position of link 1 (same as screw linear dista
 P_1 = Length of link 1 [mm]
 P_2 = Length of link 2 [mm]
 P_3 = Distance between link 1 in upright position and blade shaft [mm]
 θ = Angle of link 1 [$^\circ$]
 β = Pitch angle [$^\circ$]

Initial position of the pitching mechanism is given by Equation (3.6). The minimum pitch angle is determined to be 46.83° , and then the distance between the center pinion and the start point of the link mechanism can be calculated. At this point θ is 0° . x_1 and x_2 can be found using Pythagoras.

$$X = 0 \quad \text{gives} \quad d = P_1 \cdot \cos \theta + P_2 \cdot \cos \beta \quad (3.6)$$

Then Equation (3.5) can be solved with respect to θ and inserted in Equation (3.4), as seen in Equation (3.7) and (3.8).

$$\theta = \sin^{-1}\left(\frac{P_2 \cdot \sin \beta - P_3}{P_1}\right) \quad (3.7)$$

$$X(\beta) = d - p_1 \cdot \cos\left(\sin^{-1}\left(\frac{P_2 \cdot \sin \beta - P_3}{P_1}\right)\right) - p_2 \cdot \cos \beta \quad (3.8)$$

Equation 3.8 gives the travelled distance from the offset point as a function of the pitch angle. The required distance to given angle is obtained. The function is plotted in Excel to determine a function with only one input, the pitch angle. In Excel it is possible to add a trend line and calculate an approximate polynomial with a function called LINEST. All values are listed in Table 3.5 including percent deviation from calculated values. The function calculated by Excel is given in Equation 3.9, and the corresponding graph is seen in Figure 3.26.

$$x(\beta) = -3.04534 \cdot 10^{-11} \cdot x^6 + 8.88851 \cdot 10^{-9} \cdot x^5 - 4.43195 \cdot 10^{-7} \cdot x^4 + -0.000106577 \cdot x^3 - 0.011183864 \cdot x^2 + 0.9 \quad (3.9)$$

Equation (3.3) is combined with the calculated function from Excel, and the only unknown is the number of step or the pulses from the stepper motor which is detected by the controller in TIA portal.

Table 3.5: Values for beta and deviation

β	$x(\beta)$	New $x(\beta)$	Percent Deviation
Beta	x(Beta)	New x(Beta)	Deviation %
0	-0,002399376	-0,002431309	1,330887221
5	5,038019144	5,038184028	0,003272781
10	10,55514027	10,55498564	-0,001464947
15	16,46214082	16,46197842	-0,000986506
20	22,67238684	22,67244342	0,000249589
25	29,10119958	29,10141455	0,000738666
30	35,66764966	35,66781263	0,0004569
35	42,2962788	42,29623694	-9,89608E-05
40	48,91863865	48,91841407	-0,000459096
45	55,47453917	55,47430421	-0,000423534
50	61,91291857	61,91286486	-8,67495E-05
55	68,19228191	68,19247189	0,000278595
60	74,28069894	74,28099805	0,000402677
65	80,15539767	80,15554885	0,000188604
70	85,80202779	85,80185586	-0,000200377
75	91,21369204	91,21332738	-0,000399786
80	96,38985172	96,38975653	-9,87574E-05
85	101,3352051	101,3356867	0,000475334
90	106,0586202	106,0584347	-0,000174907

Figure 3.26 displays the relationship between the blade angle and the linear travelled distance and the approximate function.

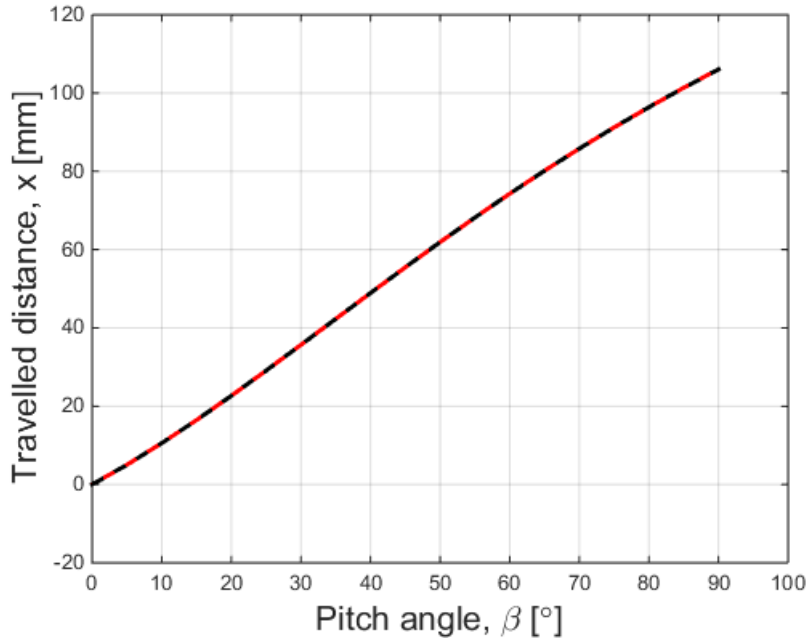


Figure 3.26: The relationship between the blade angle and the linear screw distance.

In section x, the optimized value of β is found based on the test turbine and the current wind speed above a given speed. In Excel curve fitting can be used to generate a function from the calculated parameters, as seen before. The estimated function can be seen in Equation(3.10) where the only variable is the wind speed. The Excel function LINEST was used to approximate values to obtain the estimated polynomial function. All the optimized values of β and the new values of β from the estimated function are seen in the graph in Figure 3.27.

$$\begin{aligned} \beta(v_{wind}) = & -9.24364 \cdot 10^{-6} \cdot (v_{wind})^6 + 0,000983244 \cdot (v_{wind})^5 - 0.043127738 \cdot (v_{wind})^4 \\ & + 0.998122086 \cdot (v_{wind})^3 - 12.92224067 \cdot (v_{wind})^2 + 90.59341266 \cdot (v_{wind}) - 254.5406814 \end{aligned} \quad (3.10)$$

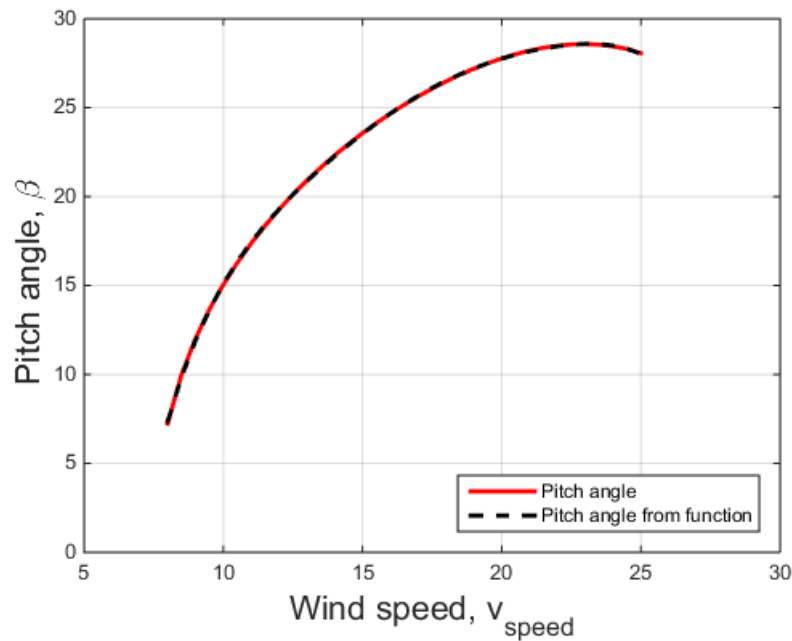


Figure 3.27: The relationship between the wind speed and a optimized pitch angle

3.2.3 Programmable Logic Controller

In order to achieve a satisfying pitch angle control of the blades, a stepper motor is controlled with a programmable logic controller (PLC) manufactured by Siemens. The control system for the Siemens ET200s PLC which is programmed in TIA Portal v12. The language used in programming the main function block is ladder logic programming language (LAD). In the ladder diagram, function calls and function blocks were added to control the motor accordingly to the flowchart. This enables monitoring of the stepper motor as it moves the slider mechanism at a given speed and with a decided torque set in the device configuration. A complete overview of the PLC program can be found in Appendix C. The step drive from Phytron was provided with a script in order to enable execution, this can be found in Appendix C.1. The flow chart of the processes used to control the stepper motor, and thus the pitch angle, is shown in Figure 3.28.

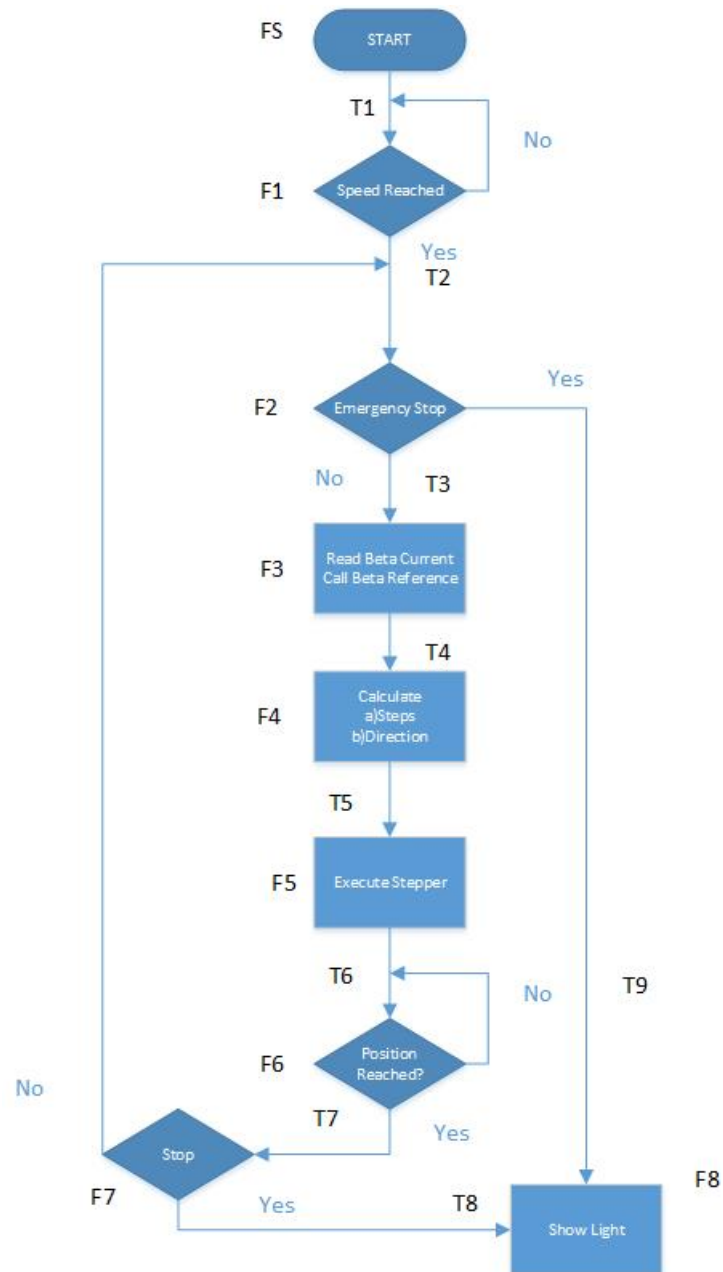


Figure 3.28: Flowchart showing the main operations of the PLC program.

As shown in Figure 3.28 the process starts by measurements of the wind speed. If it has reached a 7.0 m/s the pitching of the blades will be initiated and the control system continues to the next process. If not, the wind turbine will continue to rotate with the fixed pitch angle until the rated wind speed of 7.0 m/s is reached. Figure 3.29 show the contents of the function block F1 for the process of evaluating the wind speed measured.

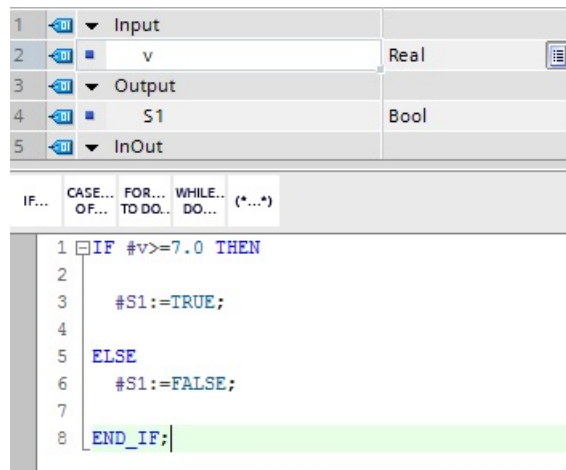


Figure 3.29: Descision block for achieved windspeed.

Further we read β_m based on the travelled distance of the slider. The calculation is shown in Equation 3.11, calculated as $\beta_{v_{wind}}$. This value gives the current angle of the blades, which is further compared to the value with the calculated β_{ref} shown in Equation 3.10.

$$\beta_m = 1.377778 \cdot dist_m \quad (3.11)$$

where the relation between mm travelled by the slider and the angle of the blades is $1.37778^\circ/\text{mm}$.

When the process of determining the deviation of the blade angle from the calculated angle β_{ref} and the current angle β_m , the steps and direction in which the stepper motor will rotate is calculated. The number of steps is found by using $dist_{ref}$ from Equation 3.9 and Equation 3.1. When the required steps have been executed and the pitch angle is in the correct position, the stepper motor stops. The function call for the rotational direction and number of pulses sent to the step drive is shown in Figure 3.30.

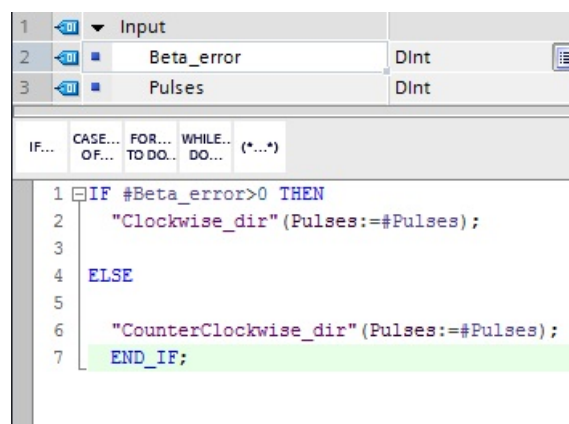


Figure 3.30: Function call for the direction and number of steps for the step drive.

The following process executes the stepper motor and monitors the position of the slider as well as the number of steps wanted. These function calls are shown in Figure 3.31 and 3.32.

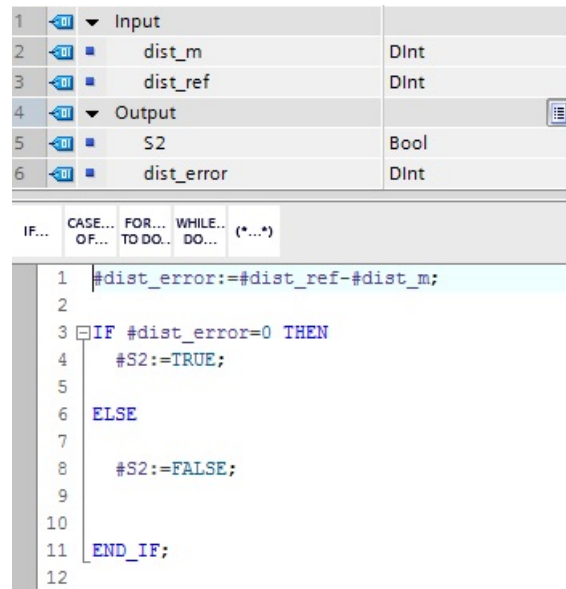


Figure 3.31: Function call that tracks the slider position.

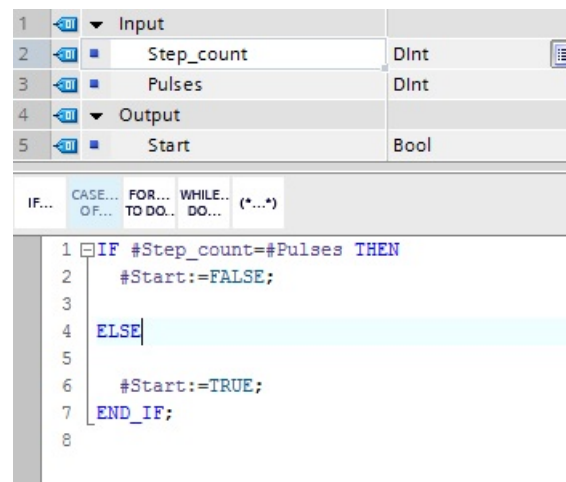


Figure 3.32: The function call which tracks when the number of steps needed to pitch the blades has been met.

The cycle time for each iteration in the control system is set to 100 ms. The networks and transitions from the programmed pitch system is shown in Table 3.7.

Table 3.6: List of networks and functions therein.

Network	Function
1	Function start. Wind speed measurement.
2	Windspeed is reached. The pitching cycle starts.
3	Checking if emergency stop. Pitch cycle if not.
4	Pitch angle as a function of wind speed is calculated.
5	Number of steps as function of pitch angle is calculated.
6	The rotational direction of the stepper and distance deviation in steps is derived.
7	The counter function showing the reduction in step deviation.
8	Stop function when correct pitch angle is achieved.
9	Emergency stop.
10	Overview of transitions to F1.
11	Overview of transitions to F2.
12	Overview of transitions to F3.
13	Overview of transitions to F4.
14	Overview of transitions to F5.
15	Overview of transitions to F6.
16	Overview of transitions to F7.
17	Overview of transitions to F8.
18	Pitching light activated.
19	Stop light activated.
20	Initiating start in 1-STEP-DRIVE script.

In the device configuration for the 1-Step-Drive from Phytron the values and settings for the digital inputs (DI) and different parameters that controls the performance of the stepper motor can be altered. The device configuration for the step drive is shown is in Table 3.7.

Table 3.7: Device configuration in PLC.

Parameter	Specification
Base frequency	400 [Hz]
Feedback value	Absolute position
Function DI0	Limit switch backward
Function DI1	Reference and limit switch forward
Input DI0	NOC
Input DI1	NOC
Limit switch	NOC
Direction of rotation	Standard
Running current	600 [mA]

The setup of the stepper motor connected to the plc is shown in Figure 3.33.

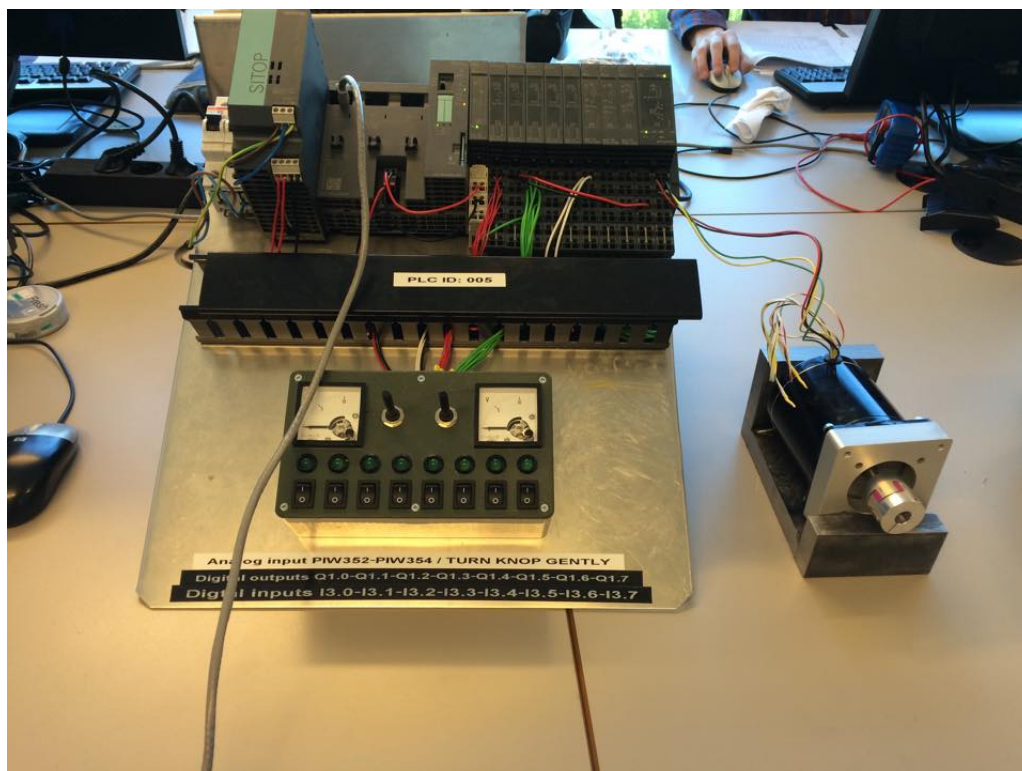


Figure 3.33: The stepper motor connected to the PLC during test runs.

Function Blocks

Organization Block (OB:

The organization blocks control the program runtime process. These blocks respond to time-based or interrupt-driven events during the runtime. Cyclic programming processing is the common type of program execution, this means that the operating system runs in cycles and communicates with

the organization block once in every loop.

Cyclic Interrupt Organization Blocks (OB35):

This block is scanning a signal for a closed loop control system. The cyclic interrupts are triggered at intervals of a given time period. This interval time is the transition from STOP to RUN.

Functions(FC):

The "function" is a logic block with no internal memory. The data used to execute the FC is stored in a local data stack and is lost after the function is executed.

Applications: Returning a function value to the calling block, for instance a math function or executing a functional feature, such as a single control function.

Function Blocks(FB):

The function block is a "function" with internal memory. This enables the block to store data locally even after execution. The parameters connected to the FB and the static variables included in the FB are all saved in the instance DB.

Applications: The function block can use embedded program code, which is executed when called by another logic block. Function blocks simplifies the programming of complex functions with frequent occurrence.

Instance Data Block (DB):

An instance data block is assigned to every function block that transfers parameters. The actual parameters and the static data of the FB are all saved in the specified DB. The variables which are declared in the FB determine the structure of the DB.

Ladder Logic Programming Language (LAD):

This language is based on the representation of circuit diagrams. Giving an easy overview of open and closed contacts, which creates a user friendly network.

Function Block Diagram Programming Language (FBD):

This language is based on graphic logic, also known as boolean algebra. This language is complex and is suitable for complex functions, such as math functions.

Statement List Programming Language (STL):

This language is text-based, where each statement represent a process.

Structured Control Programming Language (SCL):

This language is a high level text-based language. It is suitable for calculating equations, complex optimization algorithms or the management of large data volume.

3.3 Wind Turbine Design Calculations

Wind turbine design calculations are preformed to design an optimal pitch angle function for the PLC controller. The calculations are based on theory from previous courses. Some of these calculations, the shaft speed and the tip speed, are also intended to be compared to the test model.

3.3.1 Optimized β

All the design parameter from the test model form the basis for the work presented in this subsection. The procedure for wind turbine design is a multi step procedure, and all necessary parts are included here. The first step is to calculate the power coefficient (c_P) as a function of λ . For this part β is regarded as constant with the value 1. At this stage the point is to find a maximum value for c_P , while β is later utilized to lower c_P for higher wind speeds. Equation (3.12) is used to calculate the c_P according to Equation (2.3) in the theory chapter. With λ as the only variable left, the optimal value can be found using excel curve fitting. In Figure 3.34 the $c_P(\lambda)$ curve is plotted.

$$c_P = 0.5 \cdot \left(\frac{1.2}{\lambda} - 0.022 \cdot \lambda^2 - 5.6 \right) \cdot e^{-0.17 \frac{1.2}{\lambda}} \quad (3.12)$$

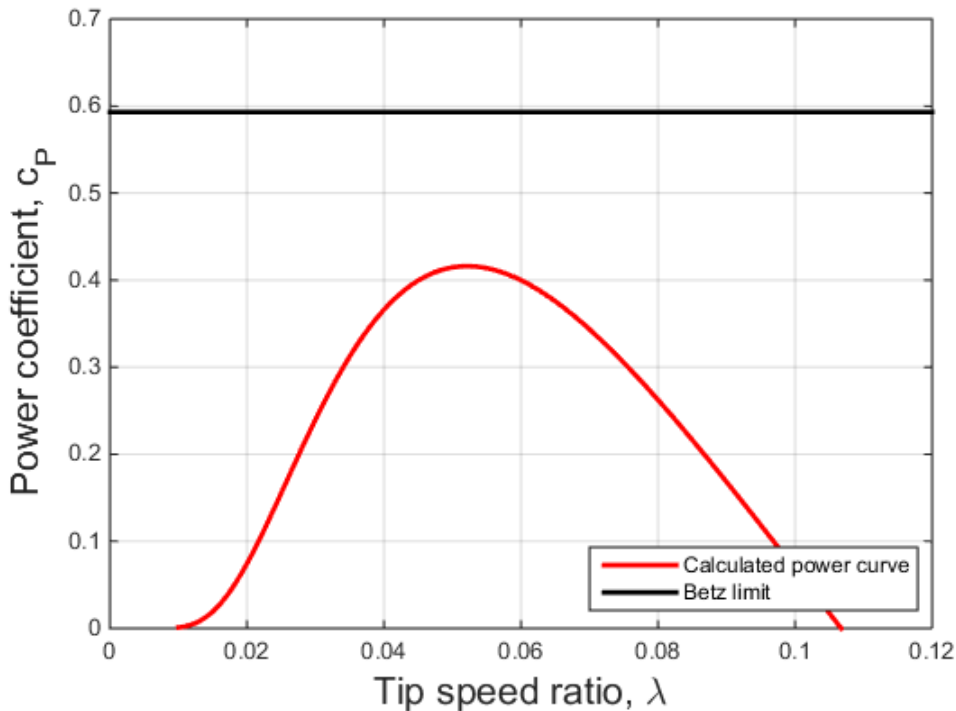


Figure 3.34: The $C_p - \lambda$ curve and the Betz limit

The goal is to find an optimized value for c_P . For obvious reasons, a negative power coefficient is not wanted. For instance a larger value then 0.107 for λ would result in a negative power coefficient. However, the goal is to optimize c_P , not use values for a marginally power output. Thus the c_P is optimized with respect to λ using the optimizing tool "Solver" in Excel. This procedure is carried out according to the test model. Ideally the c_P value should be as large as possible, and close to the theoretical maximum known as the Betz coefficient with the value 0.59. The results from the optimizing in Excel can be seen in Table 3.8.

Table 3.8: Maximum Power Coefficient

λ	r/λ	c_P
0.052	11.54	0.4161

A wind turbine with a power coefficient of 0.416 will be characterised as a good turbine, but this is calculated mathematically, so achieving these results for the test model is hard. A optimal value for λ means that the tip of the rotor blade must have a speed of 0,052 times faster than the wind speed, at any wind speed, for the turbine to operate with maximum efficiency. The next step is to calculate an optimal value for the rotational speed of the wind turbine, see Equation (3.13).

$$\Omega_{opt} = \frac{v_{design} \cdot \lambda_{opt}}{r} \quad (3.13)$$

where

$$\begin{aligned} v_{design} &= \text{Design wind speed 7.5 m/s} \\ \lambda_{opt} &= \text{Optimized value for tip speed ratio 0.052} \\ r &= \text{Radius of area swept by the rotor blades 0.6 m} \end{aligned}$$

The turbine should have a rotational speed (Ω) of 0.589 rad/s to operate at the optimal point, the design speed. It is decided that the turbine should only operate in the range of + 20% and - 40% of rotational speed. Thus the turbine can operate with a maximum c_P over a large interval of wind speeds, and still within safety limits. This allow a turbine design with rotational speed between 0.177 and 0.65 rad/s. For the highest wind speeds the rotational speed will be kept constant at maximum value, and constant at minimum value for lower wind speeds. This will result in a decreasing value for λ , and operation with a lower value for c_P . New values for λ for constant rotational speed operation will be calculated according to Equation (3.14).

$$\lambda_n = \frac{\Omega_{constant} \cdot r}{v_n} \quad (3.14)$$

where

$$\begin{aligned} \Omega_{constant} &= \text{Minimum or maximum turbine rotational speed} \\ v_n &= \text{Minimum or maximum turbine rotational speed} \end{aligned}$$

The next step is to calculate turbine operation values from cut-in wind speed to rated wind speed. For this project the cut-in wind speed is set to the lowest wind speed where the turbine start rotating. For the calculations a wind speed range from 0 to cut-out m/s, with a class width of 0.5 is studied. The power from the wind (P_{wind}) that the turbine can convert to mechanical power (P_{mech}) is given by Equation (3.15).

$$P_{mech} = c_P \cdot P_{wind} \quad (3.15)$$

Table 3.9 presents the P_{mech} the turbine can convert from P_{wind} , as well as the design parameters for the wind speed interval from cut-in to rated wind speed.

Table 3.9: Turbine design parameters from 0 m/s to rated wind speed

Wind Speed [m/s]	$P_{wind}[W]$	$\omega[rad/s]$	λ	c_P	$\beta[^\circ]$	$P_{mech}[W]$
0,5	0,0866	0,312	0,3744	-1,5304	1	-0,1325
1	0,6927	0,312	0,1872	-0,7008	1	-0,4855
1,5	2,3379	0,312	0,1248	-0,1798	1	-0,4204
2	5,5418	0,312	0,0936	0,1325	1	0,7345
2,5	10,8238	0,312	0,07488	0,3061	1	3,3137
3	18,7035	0,312	0,0624	0,3894	1	7,2833
3,5	29,7004	0,312	0,0535	0,4155	1	12,3420
4	44,3342	0,347	0,052	0,4161	1	18,4453
4,5	63,1242	0,390	0,052	0,4161	1	26,2629
5	86,5901	0,433	0,052	0,4161	1	36,0259
5,5	115,2515	0,477	0,052	0,4161	1	47,9505
6	149,6278	0,520	0,052	0,4161	1	62,2528
6,5	190,2386	0,563	0,052	0,4161	1	79,1490
7	237,6034	0,607	0,052	0,4161	1	98,8552
7,5	292,2417	0,650	0,052	0,4161	1	121,5875

For wind speeds lower than cut-in or larger than rated it is not possible to operate with λ_{opt} . The next step involves power control by adjusting the pitch angle β . According to the literature study from Chapter 2, the output power at rated speed is the maximum power that the turbine is designed to produce. Overloading may stress the wind turbine and eventually cause malfunction and breakdown of the turbine, which is especially important when considering the test model. In order to keep the rated output power constant when wind speeds increase above rated speed the pitch control is applied. The goal is to keep the power output constant from the rated wind speed to the cut-out wind speed. In Table 3.10 we see the results for the turbine design parameters for this wind speed interval.

Table 3.10: Turbine design parameters for operation during wind speeds above the rated wind speed

Wind Speed [m/s]	$P_{wind}[W]$	$\omega[rad/s]$	λ	c_P	$\beta[^\circ]$	$P_{mech}[W]$
8	354,6732	0,6933	0,0520	0,3366	7,2351	121,5875
8,5	425,4174	0,7367	0,0520	0,2631	9,9947	121,5875
9	504,9937	0,7800	0,0520	0,1942	12,0179	121,5875
9,5	593,9218	0,8233	0,0520	0,1290	13,6574	121,5875
10	692,7212	0,8233	0,0494	0,0990	15,0529	121,5875
10,5	801,9114	0,8233	0,0470	0,0758	16,2767	121,5875
11	922,0119	0,8233	0,0449	0,0578	17,3717	121,5875
11,5	1053,5423	0,8233	0,0430	0,0441	18,3655	121,5875
12	1197,0222	0,8233	0,0412	0,0336	19,2769	121,5875
12,5	1352,9711	0,8233	0,0395	0,0256	20,1194	121,5875
13	1521,9084	0,8233	0,0380	0,0197	20,9026	121,5875
13,5	1704,3539	0,8233	0,0366	0,0154	21,6341	121,5875
14	1900,8269	0,8233	0,0353	0,0124	22,3192	121,5875
14,5	2111,8471	0,8233	0,0341	0,0103	22,9623	121,5875
15	2337,9340	0,8233	0,0329	0,0090	23,5666	121,5875
15,5	2579,6071	0,8233	0,0319	0,0084	24,1346	121,5875
16	2837,3860	0,8233	0,0309	0,0082	24,6681	121,5875
16,5	3111,7901	0,8233	0,0299	0,0084	25,1685	121,5875
17	3403,3392	0,8233	0,0291	0,0088	25,6365	121,5875

For wind speeds higher than rated speed the c_P is the relationship between the rated mechanical power ($P_{mech,max}$) and P_{wind} . The pitch angle for each blade can be found, when C_P is known, by solving Equation (2.3) with respect to β . For this project the "Solver" function in Excel was used to calculate the values for β .

In order to shut down the wind turbine in a controlled manner at the cut-out wind speed there must be a control system. A brief example is given in here, and can be performed on the actual test model. This can be done by increasing the pitch angle until 90 degrees where c_P equals zero. This means that the wind does not get any attack angle on the rotor blades due to the high pitch angle. It is important not to instantly brake a wind turbine from maximum rotational speed to zero, since it most likely cause irreparable damage to the turbine. It can also be done automatic if a sensor measures continuous wind speed at cut-out speed for some time, at least 1 minute, or increasing wind speed from this point, the wind turbine must shut down to prevent damage.

Based on these calculations an optimal pitch equation was made. The reason for this is to be able to find the optimal pitch angle based on the given wind speed. Equation (3.10) in Section 3.2.2 gives the optimal pitch, and the wind speed is the only variable.

3.4 Load Considerations

This section covers considerations and observations regarding the kinematic and dynamic load on wind turbine, as well as friction. It is an important topic, and necessary to consider when designing the test model. Due to the limited amount of available material choices, the plastic material from the 3D-printer was chosen as a feasible solution. This material is lighter than steel, and some of the designed components are very expensive and difficult to be machined. The specification for this material can be seen in Appendix x. However, compare to a commercial wind turbine, the fact that it is printed in different types of plastic decreases the ability to withstand loads dramatically. When assembling the entire structure, it became clear that some parts of the construction tolerates lower loads than other parts. The plastic material from the low definition of printer are not massive, which makes it hard to tighten the parts with bolts and nuts.

3.4.1 Forces Acting on The Blades

The wind turbine is located on the roof of the school because the wind is stronger at a higher altitude, and less objects disturb the wind field of the turbine as described in Chapter 2. When the wind turbine is exposed to the wind, the load subjected to the blades, are seen in Figure 3.35. This is in the initial position of the blades at zero degree pitch. The thrust force from the wind increase with the velocity of the wind speed, until rated speed is reached, and the pitch mechanism starts to pitch the blades to the desired angle.

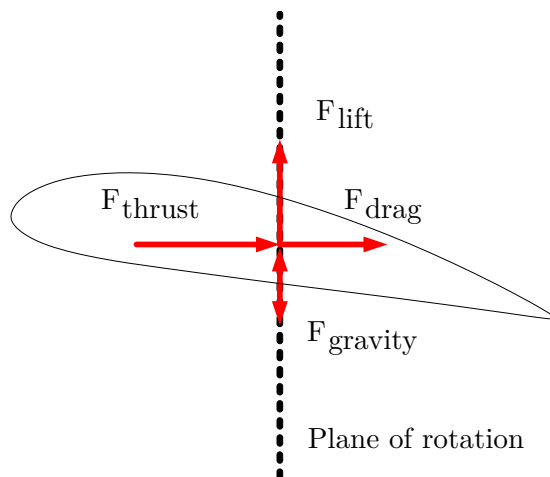


Figure 3.35: Forces acting on the turbine blades

The magnitude of the gravitational force on the blades depends on the position and orientation of the turbine blade during its 360 degree rotational movement. Thus will the gravitational force either augment or oppose the lift force. In Chapter 2, the dynamics of a wing profile was explained. However, the dynamics of wind turbines are slightly more complex than the dynamics of a simple wing because the direction of the gravitational force on the turbine blade changes with the rotation of the turbine rotor. In a simplified "theoretical" turbine operating with a single blade at constant wind force, the magnitude and direction of the lift and drag forces with respect to the aerofoil profile will be constant throughout the full 360 degrees rotation of the turbine rotor but the direction of the lift with respect to the ground will depend on the position of the rotor. The magnitude of the gravitational force on the blade will also be constant for any position of the rotor but the horizontal position of the centre of gravity of the blade with respect to the centre of the rotor will vary as the rotor turns. The result is that the net effect of these forces on the rotor torque depends on the position of the rotor, and can be summarized by the following:

- Horizontal blade: The blade is moving upwards in the opposite direction of the gravity force, which is pulling the blade down. This reduce the net lifting force acting on the blade, as well as the resulting torque on the rotor.
- Upside down horizontal: Rotated 180 degrees, the blade is still horizontal but the lifting force is in the opposite direction. This increase the net lifting force and the torque acting on the blade since the gravitational force act in the same direction as the lifting force.
- Vertical blade: When the blade is vertical, the gravitational force is perpendicular to the lifting force, and thereby has no effect on the torque. The torque is created purely due to lift.

Real life turbines have multiple blades which balance the gravitational force and cancel out the effect and the torque affecting the rotor is constant.

3.4.2 Loads Acting on The Gears

The forces acting on a straight bevel gear can be seen in Figure 3.36. As seen, the force which is normal to the middle part of the tooth face, F_n , can be split into a tangential component, F_t , and a radial component, F_r , in the normal plane of the gear tooth [28], as seen in Equation (3.16).

$$\left. \begin{aligned} F_t &= F_n \cdot \cos \alpha_n \\ F_l &= F_n \cdot \sin \alpha_n \end{aligned} \right\} \quad (3.16)$$

This radial component can again be divided into an axial force component, F_x and a radial force component, F_r perpendicular to the axis as given in Equation (3.17) and seen in Figure 3.36.

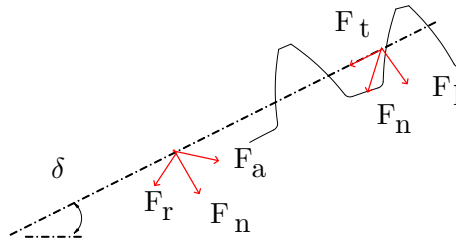


Figure 3.36: Forces acting on the bevel gears

$$\left. \begin{aligned} F_a &= F_l \cdot \sin \delta \\ F_r &= F_l \cdot \cos \delta \end{aligned} \right\} \quad (3.17)$$

Thus means that Equation (3.18) can be derived.

$$\left. \begin{aligned} F_a &= F_t \cdot \tan \alpha_n \cdot \sin \delta \\ F_r &= F_t \cdot \tan \alpha_n \cdot \cos \delta \end{aligned} \right\} \quad (3.18)$$

Figure 3.37 displays the direction of forces acting on this bevel gear construction. The relationship between the magnitude and direction can be seen in Equation (3.19).

$$\left. \begin{aligned} F_{a1} &= F_{r2} \\ F_{r1} &= F_{a2} \\ F_{t1} &= F_{t2} \end{aligned} \right\} \quad (3.19)$$

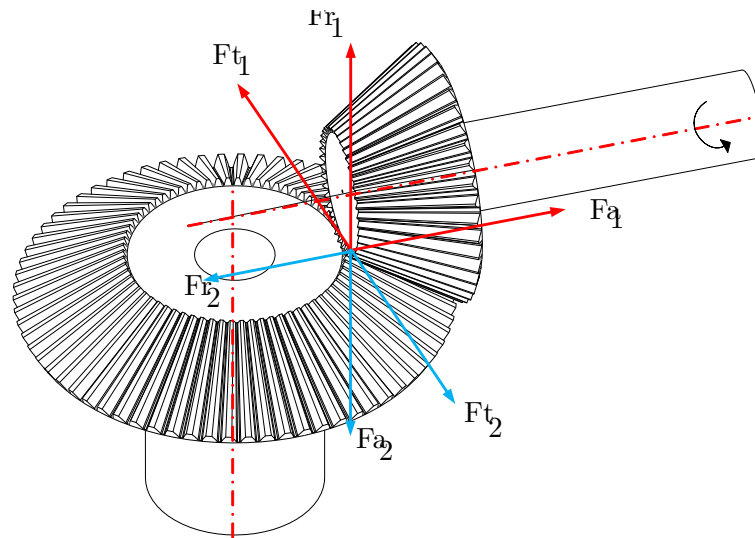


Figure 3.37: Forces acting on the bevel gears

3.4.3 Loads Acting on Other Parts

Normally is the nacelle in a wind turbine construction completely covered, but to be able to perform basic necessary maintenance tasks, it is decided not to cover the nacelle of the test model. This increase the forces subjected to the pitching system as well as other parts of the nacelle significantly. The support rig for the blades is important to support the blades, and transfer the power of the wind to the main shaft. Three bearings are included, as described before, to support the shafts of the blades and allows them to move with the least possible friction. The bearings take up forces acting on the shafts, and keeps them in place in the correct position. Forces acting on the support rig can be seen in Figure 3.38 and 3.39.

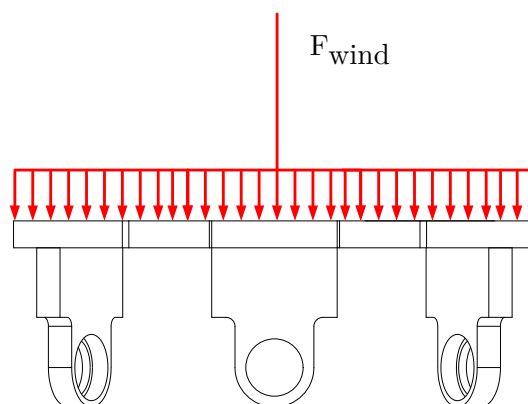


Figure 3.38: Forces acting on the support rig

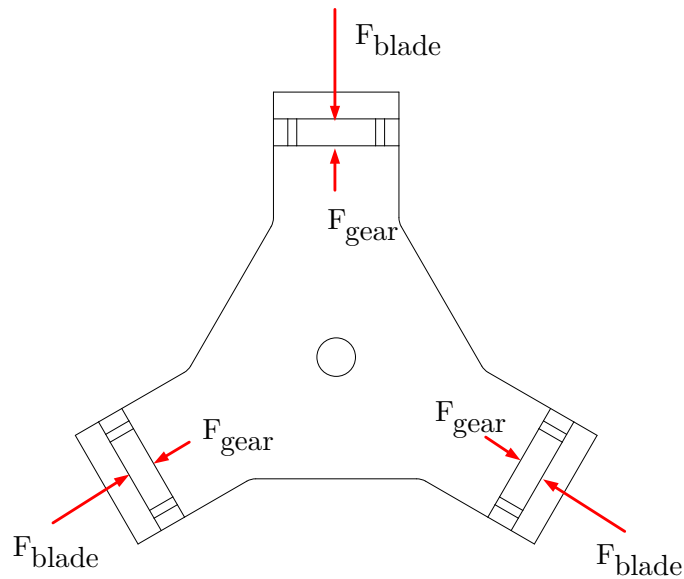


Figure 3.39: Forces acting on the support rig

Most of the parts are assembled with epoxy or another type of adhesive called locktite. This works fine when it is plastic bonded with plastic, but unfortunately it does not work very well when metal parts are bonded with plastic parts, since the adhesive is optimized for plastic materials. It was also experienced that locktite as well as epoxy worked better on plastic from the High Definition printer than than the printer with lower definition, probably due to difference in quality, density and surface structure. The main shaft is supported by bearings and mounted on the top of the tower construction. The generator is fitted directly on the main shaft without gearing, and make sure that the shaft is not moved backwards during operation. This is done in order to simplify the model, and it is believed it would be to much wear when the wind speed increase. Extra reinforcement is added during operation to reduce the risk of possible damage to the structure. Figure 3.40, displays the forces acting on the main shaft.

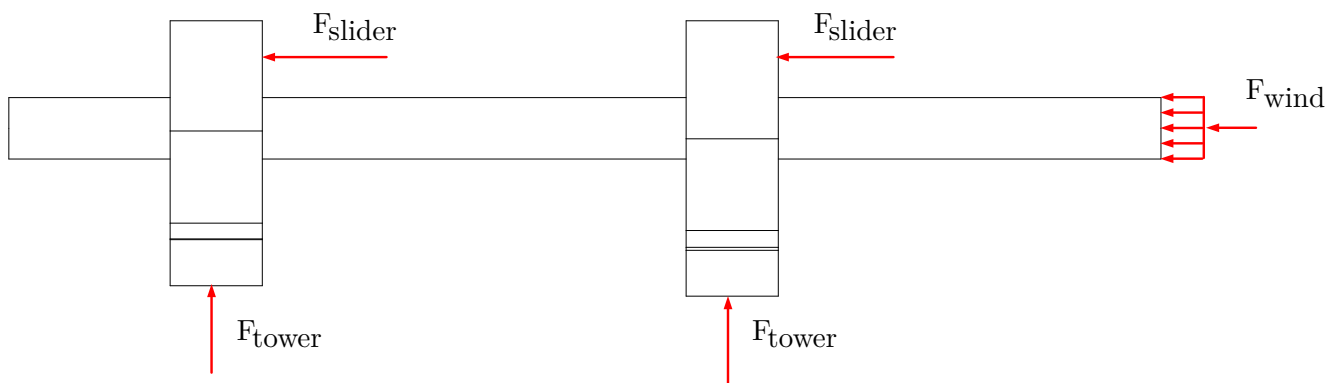


Figure 3.40: Forces acting on the tower main shaft

The tower structure should be able to withstand potentially large loads, both when standing on the ground and when standing on the top of the Stewart platform. Since the tower has no yaw

mechanism, the wind turbine must be turned manually towards the direction of the wind, to prevent large loads from behind. Extra weights is added to the bottom of the tower structure when testing to increase the vertical load and ensure the safety of the equipment. The forces acting on the tower structure can be seen in Figure 3.41.

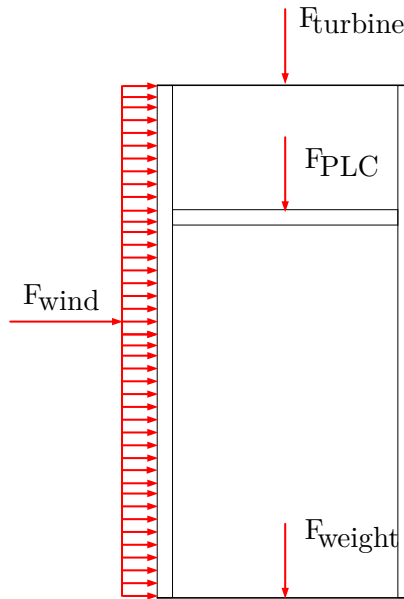


Figure 3.41: Forces acting on the tower construction

3.4.4 Friction

Friction is the force resisting the relative motion of two solid surfaces, fluid layers, and material elements sliding against each other. There is no doubt that friction can be a potential problem due to the high number of rotating and moving parts. Bearings are used to reduce friction and provide the required rotational movement. However, these bearings are low cost and requires lubrication more often to rotate optimal.

Several parts of the pitch mechanism are affected by friction. The slider should move back and forth at the same time that the main shaft is rotating. This creates a situation where bearings cannot be used since both translation movement and rotational movement is required. A small tolerance is included as well as lubrication is used to reduce the amount of friction and obtain smooth movement. The slider is attached to a metal slider mechanism to transfer the rotational movement of the stepper motor to translational movement of the slider. From testing it is seen that the amount of friction is larger for the first few seconds after activating the pitch mechanism. Also the screw connected between the stepper motor and slider creates friction when the screw rotates. However, the stepper motor can rotate faster to overcome the effect of the friction.

The gear and pinion is affected by friction, and this is perhaps the most critical friction. When the teeth is subjected to wear, they become less accurate and might miss a tooth because it is worn. This type of wear increase with increased use and the quality of the selected material. Lubrication would reduce both wear and friction. The main shaft is subjected to friction at all places it is connected to other components.

It is important to reduce the overall friction coefficient because it will reduce the cut-in speed of the turbine as well as reduce the wear, as discussed.

Chapter 4

Results and Discussion

In this chapter the results from the test model will be presented and explained in detail. The results are based on testing of the test model at the selected test site described in Section 4.1.

4.1 Testing

This section consider information regarding the test site and why the selected test site was chosen. A description of the test setup is included to give the reader an overview. The Open Platform Communications server (OPC) setup utilized to log data is explained in detail.

4.1.1 The Test Site

The main building of University of Agder has six floors, including the roof top, which contains a test site for solar panels. Behind the solar panel test site, the wind turbine is placed as seen on Figure 4.1. Since the turbine do not have yaw control incorporated in the tower construction, the rotor is moved manually to face towards the wind direction. As the wind speed increase with hight above ground, the roof is the most suitable location in the area. It is about 20 m from the ground to the roof top. The wind speed varies in the area according to [29] mean wind speed was between 1-7 m/s last year. However, Grimstad is a located close to the coast and coastal winds with higher wind speed are common.

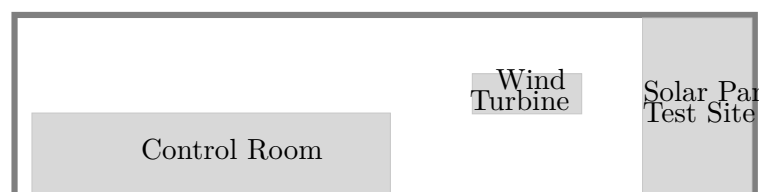


Figure 4.1: Overview of test site

The PLC, the motor and other electrical equipments are not water resistant and not covered since it need to be easy accessible for testing and validating. This means the turbine is tested only during non-raining periods to avoid damage on the equipment. Optimal conditions are wind speed from 4-12 m/s and stable weather.

4.1.2 Test Setup

In Figure 4.2, a schematic diagram of the complete test setup can be seen. The wind speed and direction is measured by an anemometer, and the retrieved data is recorded in LabVIEW and used

as an input in the PLC. A stepper motor controlled by the PLC pitch the blades according to the given wind speed. When a wind speed above rated speed is detected by the anemometer, the stepper motor pitch the blades to the calculated optimal angle given by a number of steps. The rotational shaft is connected to the generator which transfer electrical signals through the analogue signal detector (DAQ) and recorded by LabVIEW. Figure 4.3 shows the actual test site with the wind turbine on the roof top.

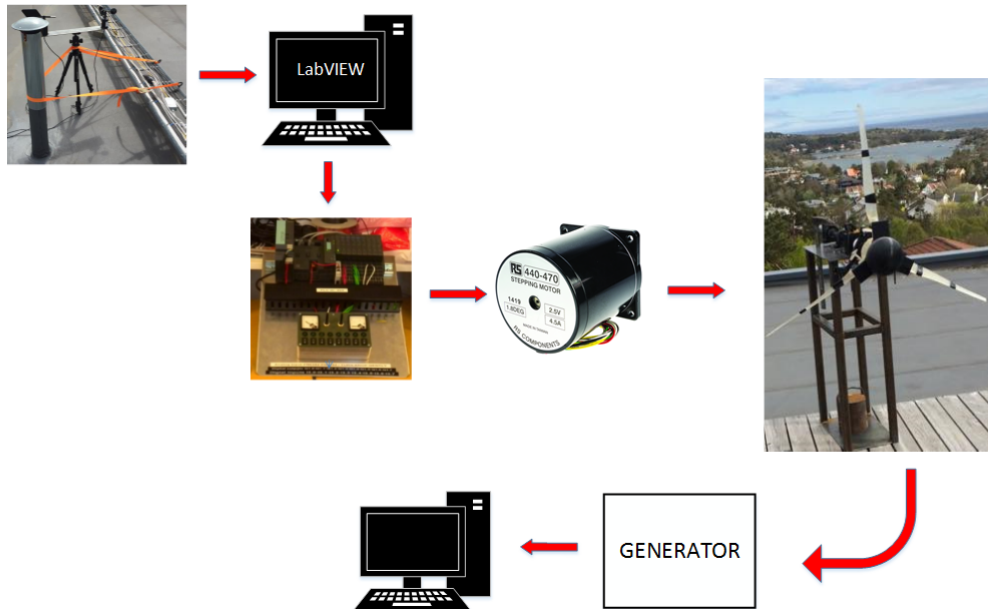


Figure 4.2: Schematic diagram of the test setup

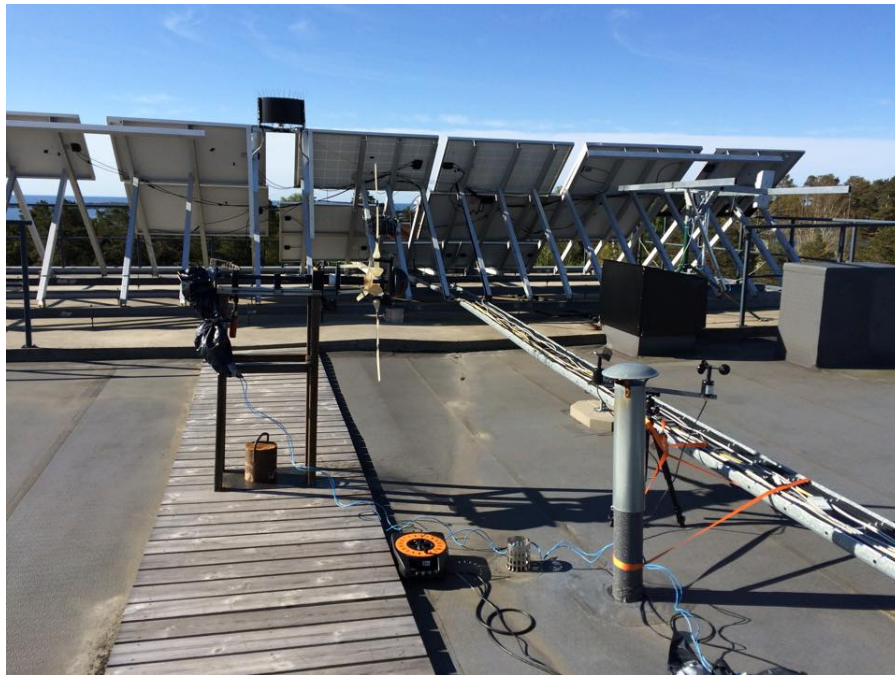


Figure 4.3: Experimental test setup

4.1.3 Logging Results

The design of the pitch controller is based on the current wind speed detected by an anemometer. To log the results from the anemometer, a LabVIEW program is developed to convert the voltage signal to current wind speed and direction of the wind. The anemometer measure wind speeds between 0 and 70 m/s and wind directions between 0 and 360 degrees equivalent to voltage from 0 to 5 volt. A conversion factor of 14 for the wind speed and 72 for the wind direction. The LabVIEW program, which also log the results from the generator, can be seen in Figure 4.4. The logging setup can be used up to rated speed, before the pitch controller is activated. This was done in order to be able log some results independent of the PLC. The program was initially developed by fellow students, but was changed to fit our setup.

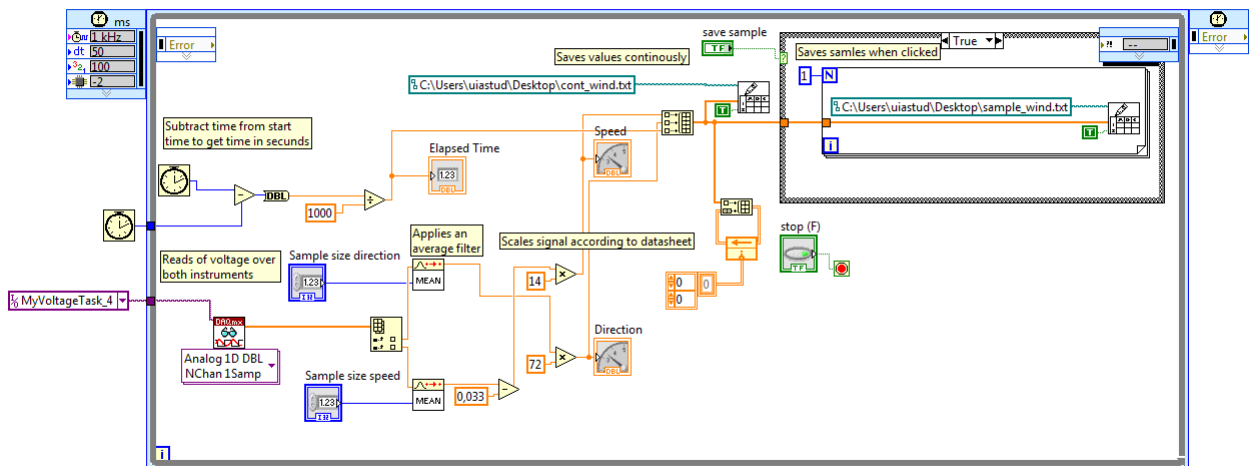


Figure 4.4: The LabVIEW program developed to log the wind measurements

Above rated speed, a different setup is required. The signals from the anemometer is sent directly into one of the analogue signal ports of the PLC. The signal is detected by the PLC, and used in the step drive setup to obtain the pitch angle based on the calculated pitch function. To log the results from the testing, a connection to an OPC server is established. It is often necessary to be able to collect, store or manage relevant data from the operation of a system, in this case the wind turbine. The Plant Information system (PI) is a set of server- and client-based software programs, designed to perform the automatic collecting, storing, visualizing and analyzing of the PI data. The OPC server is a part of the PI system as seen in Figure 4.5.

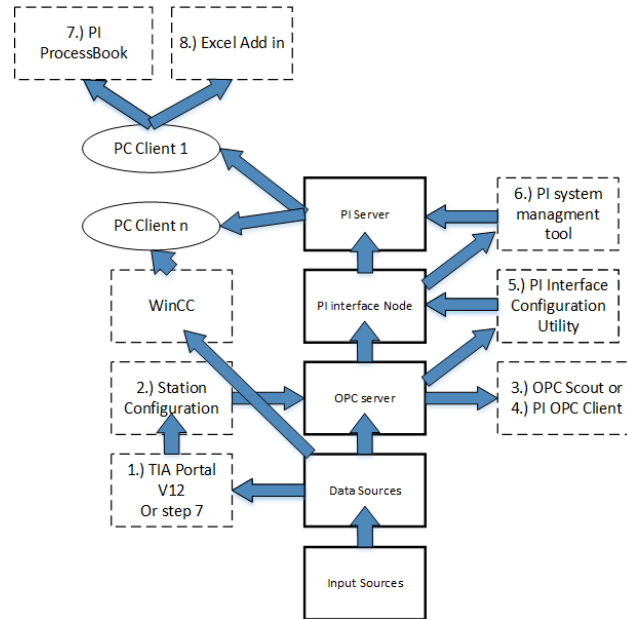


Figure 4.5: Setup of a PI system

In the setup utilized in this model, the input source is the data from the anemometer and the step drive, and the data source is the instrument that generates the data you want to monitor, in this case the PLC. A connection is made in the TIA Portal V12 to be able to send data from the PLC to an OPC server. In order to send data a new PC station needs to be included in the PLC program. The PC station will later be used as the PI interface node. The device configuration window allows to add an OPC server, and an IE general element to the station. It is important to use the correct IP-address, or else the OPC server can not communicate with the PLC. For this project 192.168.0.1 is used for this unit. A dotted highlighted blue connection is seen when the PLC is correctly connected with the OPC server. In the Station Configuration Editor an OPC Server and an IE general element is added, and the correct network card is selected for the IE general. It is important to use the same station name as in TIA Portal. The connection can be confirmed with the OPC Scout and the PI OPC Client. If the connection functions properly, the values from the PLC can be seen directly in the program.

To connect the PI Interface Node with the data source, the OPC server has to be operational and connected correctly. Another software, PI Interface Configuration Utility, has to be running before the data source can connect to the PI Server. When the PI interface is connected it will send the data to the PI Server.

A PI server need instrument tags for storing the information from the PLC, and has the same name as in the OPC client. The tags are added in the PI management tool software for every variable that is supposed to be logged and stored. In this project only a the real variable is used. A point source has to be selected, and the float32 corresponds to the real value in TIA Portal. The location and the point source also need to be specified when the tags are added. Table 4.1, displays the name, type, parameter and instrument tag of the logged variables.

Table 4.1: Tags created PI System Management Tools for logging in the PI Server

Name	Type	Parameter	Instrument Tag
step count	Float32	Steps counted	S7:[wind stepper]DB3, Real0
beta error	Float32	pitch angle error	S7:[wind stepper]DB4, Real16
beta m	Float32	Measured pitch	S7:[wind stepper]DB4, Real12
beta ref	Float32	Reference pitch	S7:[wind stepper]DB3, Real4
dist m	Float32	Measured distance	S7:[wind stepper]DB3, Real8
dist exc	Float32	Executed distance	S7:[wind stepper]DB3, Real16
disr ref	Float32	reference Distance	S7:[wind stepper]DB3, Rea20
pulses	Float32	Number of pulses	S7:[wind stepper]DB3, Real0
v	Float32	Wind speed	S7:[wind stepper]DB4, Real0

Process book is not included in this project, since the data is logged directly in Excel. The PI DataLink in connection with Microsoft Excel can do basically the same as the ProcessBook. The data is retrieved directly into a spreadsheet updated at desired intervals. The features of Excel add-in can be combined with mathematical, graphical and other functions already implemented in MS Excel.

4.2 Test Model

In this section the results obtained from testing is presented, divided in two parts, before and after activation of the pitch controller. Also improvements of the test model is discussed.

4.2.1 From Cut-in Speed to Rated Speed

After assembling the physical test model, it was subjected to different wind speeds. It is difficult to obtain the exact wind speed, because the test turbine is very dependent of the direction of the wind. From experience it was discovered that the winds speed could be as low as 3 m/s when the turbine started to rotate, while other times when the angle was slightly different the turbine started to rotate at wind speeds around 6 m/s. Figure 4.6 and 4.7 displays scattered diagrams of the obtained voltage during different wind speeds. As seen, the values varies significantly during the same wind speeds. From 5 m/s t 10 m/s, the voltage varies between 150 and 300 mV. However, all the values are low and variations during measurements are to be expected since the wind speed acting on the anemometer at a given time affects the voltage output of the generator a few seconds later. At these speeds, the pitch controller is not activated and pitch angle is kept at a constant value.

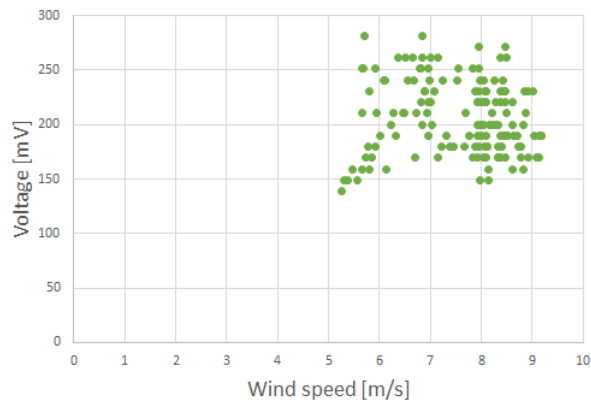


Figure 4.6: The Relationship between generated voltage and wind speed

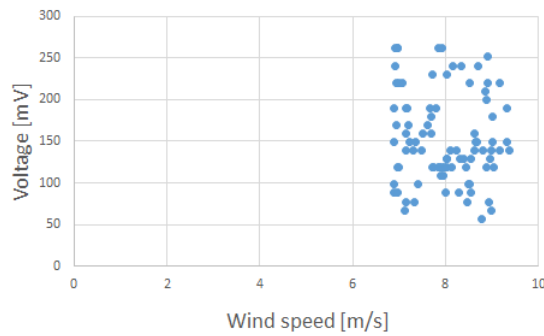


Figure 4.7: The Relationship between generated voltage and wind speed

Figure 4.8 display the voltage output of the turbine with respect to the rotation speed. These results were obtained with manually rotating the wind speed and measure the rotational speed with a tachometer. A tachometer use reflector tape and a laser beam to measure the rotation speed of the shaft.

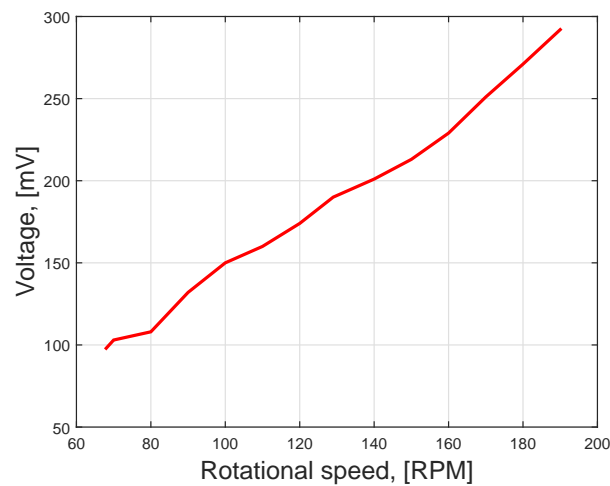


Figure 4.8: Relationship between shaft speed and voltage of the generator

As seen, the output is low and only some millivolts is generated. This is probably due to the generator, since it requires a rotational speed of 3800 RPM to generate 6 volts, and the low speed

rotational axis of the turbine hits 200 RPM at the most during manual testing.

The tip speed is measured with the tachometer in the same way as the shaft speed. Reflector tape fasten on the blade tip provides the necessary signal to measure tip speed. The relationship between voltage generated and the obtained tip speed can be seen in Figure 4.9.

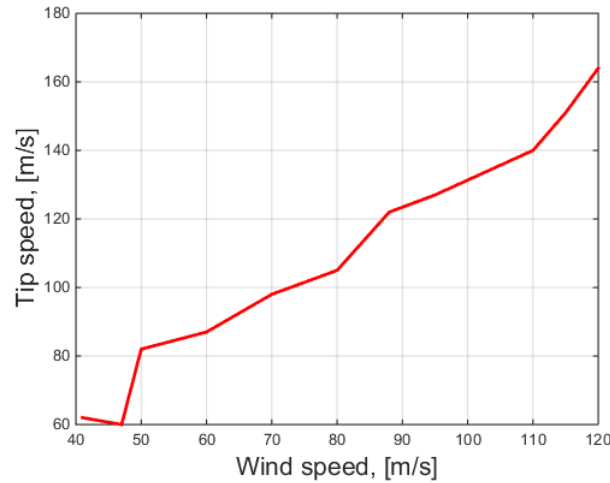


Figure 4.9: Relationship between tipshaft speed and voltage of the generator

4.2.2 The Pitch Controller

The pitch controller was tested in the mechatronics lab. In Table 4.2 the results from the pitching of the blades are and a comparison is made between the calculated input, and what the stepper motor performs. The data obtained is from the moment when pitching of the wind turbine is considered necessary. The findings show that at wind speeds from 10 m/s to 17 m/s is the wind speeds where pitching can be useful. After 17 m/s the safety of the test model is prioritized. The results obtained by running a simulation of the different wind speeds in the pitch system ladder diagram is shown in Table 4.2.

As shown in the Table 4.2 the blade angles changed after being altered by the angles that are affected by the slider mechanism which is moved translational by the stepper motor.

In the findings the observation was made that the stepper motor did control the angle of the blades as wanted. However, some problems needed addressing. While testing the pitch controller it was found that when moving the slider mechanism forward increased the rotational speed of the shaft, while moving the slider backwards reduced the rotational speed of the main main shaft, and thus affecting the voltage output from the generator.

The values given when the wind speed is varied from 7 m/s to 17 m/s is shown in Table 4.2. Here one can see how the measured values differ from the calculated ones, and where, if any losses are made from calculating the necessary pitch angle and what the stepper motor performs. From this it is obersev that the stepper motor performs. Although there is missing some variable wind speeds that the step count could continue to work from as a starting point.

Table 4.2: Test run of stepper motor in the lab.

v	Beta _{ref}	Beta _m	Beta _{error}	Dist _{ref}	Dist _m	Dist _{exc}	Step _{count}	Pulses	diff _{pulses}
7	0,6674	0,8163	-0,1488	0,644	0,5925	0,0522	79	85,96	6,96
8	7,366	10,4676	-3,1014	7,599	7,5975	0,0022	1013	1013,299	0,299
9	11,9115	17,3496	-5,4341	12,78	12,5925	0,1888	1679	1704	25
10	15,0948	22,847	-7,7522	16,582	16,5825	-0,0004	2211	2210,93	-0,07
11	17,4396	25,6163	-8,1766	19,4645	18,5925	0,872	2479	2595,27	116,27
12	19,29695	29,7496	-10,4527	21,7889	21,5925	0,1964	2879	2905	26
13	20,872	32,643	-11,7709	23,7851	23,6925	0,0926	3159	3171,35	12,35
14	22,2715	35,2366	-12,9651	25,575	25,575	0,0009	3410	3410,12	0,12
15	23,5364	36,7763	-13,2399	27,2067	26,6925	0,5142	3559	3627	68
16	24,6723	39,5146	-14,8423	28,68	28,68	0E+00	3824	3823,98	-0,02
17	25,66878	40,9096	-15,24082	29,9783	29,6925	0,2858	3959	3997	38

Setting the β value from a range of 0 to 90 deg gives the values shown in Table 4.3. This is done to test if the stepper moves the distance accordingly to what has been determined. This is proven to be correct, although one has to interfere with the script somewhat to get these values.

Table 4.3: Test run of stepper motor in the lab.

v	Beta _{ref}	Beta _m	Beta _{error}	Dist _{ref}	Dist _m	Dist _{exc}	Step _{count}	Pulses	diff _{pulses}
8	0	0	0,00	0,0024	0	0,0024	1408	0,32	-1407,68
9	10	14,54	-4,54	10,55	10,56	-0,005	1408	1407	-1
10	20	31,24	-11,24	22,67	22,68	-0,01	3024	3023	-1
11	30	49,14	-19,14	35,67	35,67	0	4756	4756	0
12	40	67,4	-27,40	48,92	48,92	0	6523	6523	0
13	50	85,31	-35,31	61,91	61,92	-0,01	8256	8255	-1
14	60	102,35	-42,35	74,28	74,28	0	9678	9904	226
15	70	118,2237	-48,22	85,8	85,8	0	11441	11440	-1
16	80	132,8144	-52,81	96,3945	96,3975	-0,003	12853	12852,61	-0,39
17	90	146,134	-56,13	106,06	106,065	-0,005		14141	14141

4.3 Verification of the Test Model

In this section it is intended to validate the test model based on hand calculations performed in Section 3.3.1. Validation is based on shaft speed and tip speed obtained from the calculations and test results from the turbine.

4.3.1 Calculations

The rotational speed was calculated based on current wind speed with parameters resembling the test model. Figure 4.10 and 4.11 shows the theoretical calculation of shaft speed versus wind speed and tip speed versus wind speed, respectively.

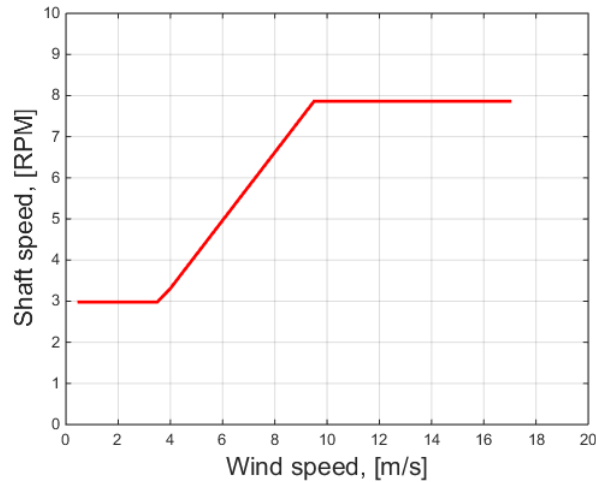


Figure 4.10: The calculated shaft speed at wind speeds from cut-in to cut-out

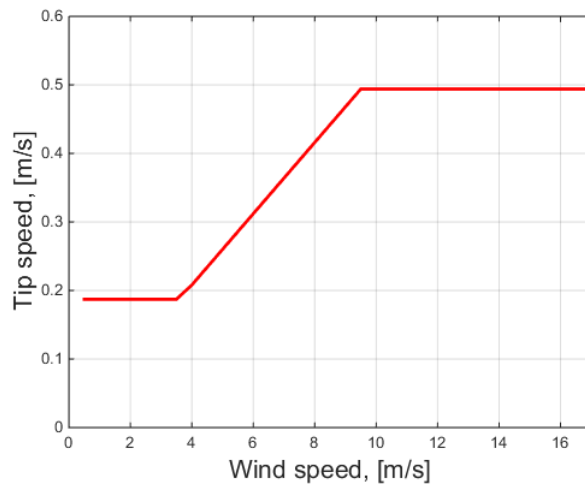


Figure 4.11: The calculated tip speed at wind speeds from cut-in to cut-out

As seen the values of tip speed and shaft speed are very low and significantly lower than values obtained during testing on the roof top. The reason for the low theoretical values are discussed below.

4.3.2 Improvement of Power Coefficient Calculations

The calculation of the power coefficient and tip speed ratio in this report is based on common theory from previous courses, as well as book sources and research articles. The problem occurs when these theories are intended for significantly larger turbines. When determining the parameters seen in Equation (??), the values are based on experimental results, and then parameter adoption is

used to determined suitable values for C_1 to C_5 .

$$c_p = C_1 \cdot (C_2 - C_3 \cdot \beta^2 - C_4) \cdot e^{C_5} \quad (4.1)$$

Today in literature, most simulation studies still use empiric curves as this [30] from 1981 or this [31] from 1983. However, as mentioned in section 2.5, the simulation software becomes more and more advance which decreases the gap between simulated results and the actual turbine. The power coefficient is determined by the tip speed ratio (TSR), which characterizes the air flow around the blades of the turbine. This number is a dimensionless parameter, calculated as the ratio between the speed of the tip of a blade and the wind speed v_w , as seen in Equation (4.1). The relation between the c_p and the TSR is non-linear and determined by the shape and the size of the blade.

$$\gamma = \frac{R \cdot \Omega}{v_w} \quad (4.2)$$

where

$$\begin{aligned} \gamma &= \text{Tip speed ratio [-]} \\ R &= \text{Radius [m]} \\ \Omega &= \text{Tip speed [m/s]} \end{aligned}$$

To calculate a more accurate TSR and power coefficient, an experimental setup is required. [cite] provides a method for calculation of γ and c_p based on a experimental setup. To obtain the γ , the wind speed is measured with an anemometer connected to a DAQ-device, and the rotational speed is estimated by measuring the current generator waveform and then calculating the fundamental frequency. However, a simple tachometer provide the rotational speed of the shaft for the experimental setup in this project. The paper propose a method for calculating the power coefficient by measuring generator voltage and current. The generator efficiency is included in the calculations and need to be estimated based on numerous parameters such as speed, current, voltage among others. If the air density also is known the value of c_p can be estimated based on a current wind speed. To obtain a curve, seen in Equation (4.3), a sufficient number of c_p values must be estimated.

$$c_p = \frac{P_{calc}}{0.5 \cdot \rho \cdot A \cdot v_w^3} \quad (4.3)$$

The simplified methodology for estimating γ and c_p has been explained. However, this does not automatically gives a realistic power coefficient curve. The dynamic performance of the blade is still unknown. In addition steady wind measurements are difficult to obtain, as well enough operating points between cut-in and cut-out speed to construct a realistic power coefficient curve. Values should optimally be measured in steady-state with stable wind and rotational speed.

4.3.3 Calculation of c_p : Test Model

To calculate the c_p on the test model, the current and the voltage from the generator must be measured. In Figure ??, the test setup with two multimeter can be seen.

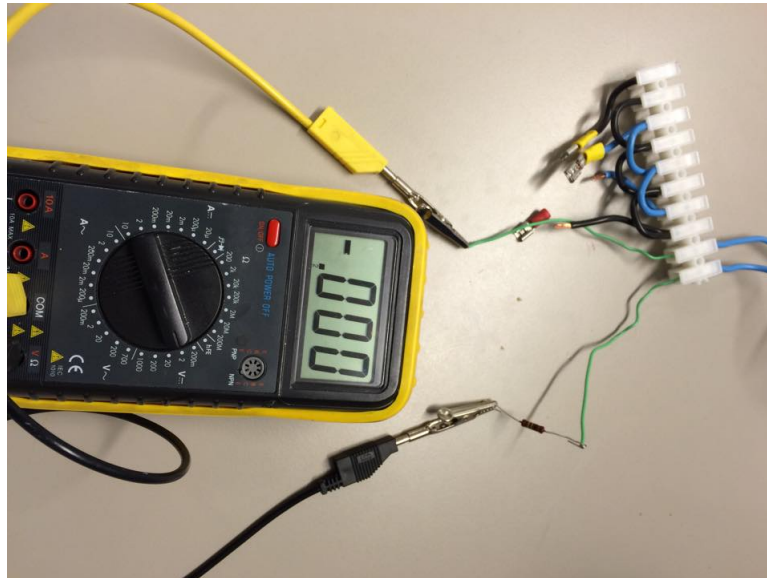


Figure 4.12: Measuring current and voltage of test model generator

Equation 4.4 is used to calculate the power with the measured voltage and current.

$$P = U \cdot I \quad (4.4)$$

It was not possible to include wind measurements from the anemometer, due to wind speeds below cut-in speed during the entire test period. From the voltage a wind speed can be estimated based on the obtained result from the earlier testing on the roof top. Rotational speed was also measured to be able to calculate the tip speed. The measured current and voltage is listed in Table 4.4. As seen the values are very low, which is most likely a consequence of too low speed on the shaft.

Table 4.4: Design Specification of Wind Turbine

Rotation speed	Current	Voltage	Power
68	0,098	0,098	0,009604
70	0,103	0,103	0,010609
80	0,108	0,108	0,011664
90	0,132	0,132	0,017424
100	0,15	0,15	0,0225
110	0,16	0,16	0,0256
120	0,174	0,174	0,030276
129	0,19	0,19	0,0361
140	0,201	0,201	0,040401
150	0,213	0,213	0,045369
160	0,229	0,229	0,052441
170	0,251	0,251	0,063001
180	0,271	0,271	0,073441
190	0,292	0,292	0,085264

Figure 4.13 displays the relationship between the calculated power from Equation 4.4 and the voltage. A small amount of power is generated from the motor.

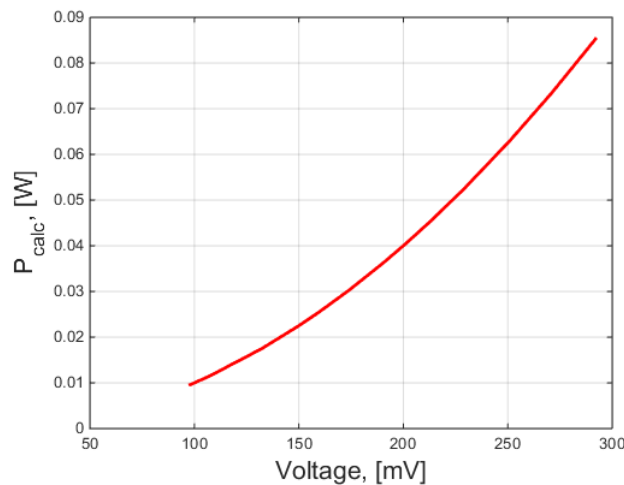


Figure 4.13: The calculated power with respect to rotational speed

The density of the air at the roof top is estimated to be 1.225 kg/m^3 . Now only different wind speeds corresponding to the shaft speed is needed to calculate values for c_p . As seen in Figure 4.14, it is difficult to conclude on a wind speed based on voltage generated. It is decided that in order to fill the complete analysis more measurements are required. More operating point above rated speed is also required to obtain an experimental c_p -curve.

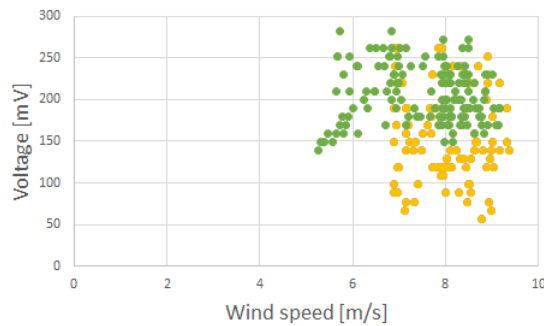


Figure 4.14: Voltage generated between 5 and 10 m/s wind speed

4.4 Improvements

There is room for improvement when it comes to the wind turbine, and a few possibilities will be listed here. The rotor area is $x \text{ m}^2$, but the surface area of the blades are much smaller. To improve the blades ability to capture more wind, the surface area could be increased or a different wing profile selected. As well as increasing the blade area, the thickness should be increased to make sure a large range of wind speed is within the safe operation area. Especially large wind gusts are a weakness with the current test model, as the blades can not handle the forces created by the wind. Improving the blades are an important part, as they are the reason that the shaft is rotating in the first place. Ideally the blades should be printed in one piece, and preferably in a different material such as glass fibre composite or similar materials.

The turbine consist of many parts, and some of them was too large for the 3D-printer. Thus the parts had to be divided in smaller parts and bonded together afterwards. This decrease the strength of the construction, and thereby the ability to withstand high loads from the wind. In general the construction should be printed in as few parts as possible, and holes fitted for bolts should be implemented in the construction before printing the parts.

4.4.1 Gearbox

The test model in this project do not include a gearbox, which means this is a direct drive. High torque, low speed input on the generator is not optimal for power production as this will produce less electricity than low torque, high speed which can be achieved with a gearbox.

In this application it is beneficial to increase the rotation speed of a drive shaft from a wind turbine to drive a dynamo generator at its optimum output voltage. The primary drive shaft from the wind turbine rotates at a relatively low speed up to around 100 RPM. This is too low to drive the dynamo directly as such as speed will only deliver around 100 mV, which is significantly less than the optimal voltage of the generator of 12 V. The practical way to match the rotation speed of the wind turbine to the generator is to increase the rotational speed by interposing a gearbox in the test model between the primary drive shaft and the current generator. A gear ratio of 20 to 1 will be sufficient to convert 100 RPM up to 2000 RPM.

For the current application, a planetary gearbox offers good torque conversion with minimum backlash and compact design. A UK based company called Reliance offers a range of small gearboxes and accessories, and their catalogue indicates that a planetary gearbox type RGP40 with a reduction ratio of 20 is a good choice. Although the gearbox specifications are given in terms of speed reduction a gear up is achieved by reversing the input and output connections. In other words

the trick is to mount the gearbox “back to front”, as it necessary to increase the speed not reduce it. The main considerations in using a gearbox are the output torque, inertia, maximum rotation speed and efficiency. Figure 4.15 displays an image of the selected gearbox.



Figure 4.15: The gearbox selected for this application [8]

Appendix A.3 provides the table of specifications for type RGP40 NEMA 17, the selected gearbox. In conclusion the overall efficiency of the gearbox is around 96 %, which means there is around 4% loss of energy on full load. The maximum rotation speed is quoted at 18000 RPM which is significantly greater than the maximum required for the wind turbine application, so the gearbox will always run within its specifications. The rotational torque is decreased by the speed conversion.

4.5 Summary of Results

The following points summarize the results:

- A pitch controlled wind turbine has been designed, and tested in various conditions. A stepper motor turn the angle of the blades.
- The friction in the system is high, perhaps too high to get proper results based on the wind speed available. Due to this some of the readings have been done by rotating the shaft manually.
- The values in our calculations have been derived from theory for larger wind turbines, and a method for calculating an experimental c_p is proposed.
- The stepper motor has not been fully automated, but function well with single pitch angle changes.
- The building and designing of the wind turbine, was a time consuming part of the project, which limited the testing period. For wind turbine testing, wind must be present. In the testing period over three weeks, the wind speeds did not reach as high as wanted. Giving a narrower list of results.

- The cut-in speed is between 3 and 5 m/s and the cut out around 17 m/s based on experience from testing without any logging of measurement and observation of the vibration of the plastic blades at higher wind speeds. With manually testing, it is possible to reach higher rotational speed because the forces of the wind due not act at the blades in the same way.
- The pitch control mechanism has not been tested outdoors in normal high wind speed conditions, therefore the values has been determined in TIA Portal. From the PLC program it was possible to withdraw important information, but how the stepper works in conterminously changing wind speeds, was not conducted.
- The power output of the wind turbine is limited by the generator. In the test model, a generator with high RPM at max voltage is used. This will effect the voltage produce, seeing as there is no gearbox involved. Implementation of a planetary gearbox is discussed in Section 4.4.

Chapter 5

Conclusion and Further Work

Wind power technology dates back centuries. Today the growing population demand more energy than ever before, simultaneously the use of fossil fuels such as oil and coal needs to be reduced in order to accommodate to the environmental challenges of our time. There are many different sources of renewable energy, however wind power is one of the most attractive resources and provides an almost unlimited source of energy. Installing wind turbines onshore causes challenges in the form of noise and visual disturbance, which makes the offshore site is a considerably more attractive location to harness the wind resources. Introducing floating offshore wind turbine, depth challenges and expensive installation and materials becomes significantly reduced. The offshore wind turbines installed during the late 90's and 2000 were limited by the ocean depths, but now the floating wind turbines take advantage of different kinds of anchoring systems and mooring lines which makes installation of offshore wind power at depths up to 600 meters possible. However, installing a floating wind turbine also requires additional calculations regarding the motion and forces acting on the turbine structure due to impact of waves and stronger winds.

In the present master thesis, the main objective was to design, build and verify a prototype model of a pitch controlled offshore wind turbine. The testing conditions required a small scale pitch controlled wind turbine. Due to limitations in production, the industry does not provide such small scale turbines. Thus, the test model had to be build and designed from draft to complete model. The pitch control mechanism would also be designed from draft using a Siemens s200es Programmable Logic Controller to control a stepper motor to rotate the blades by moving a slider mechanism. Future work include testing the model as well as the controller mounted on the Stewart platform, simulating offshore conditions.

A wind turbine with a pitch control mechanism was designed during the project. The parts of the wind turbine is mostly printed in 3D, and thereby made of lightweight plastic materials, while the rest of the components such as the main shaft, bearings and the tower construction is made of steel. The tower construction is welded together by heavy steel parts, making it a stable platform for the wind turbine. In order to change the angle of the blades the pitch mechanism was controlled by the rotations provided by a stepper motor. The stepper motor was connected to a PLC providing the number of steps required to turn the blades to the given angle based on a function with wind speed as input. The data sent and received was logged with an OPC Server. To obtain the current wind speed at all times, an anemometer measured the wind speed and provided measurements that could be used in the programming of the PLC. The PLC sends the command to the stepper motor through the step drive. Future work include to completely automate the pitch mechanism, and as the wind speed changes, a new signal from the analogue port is provided after a given time to allow the stepper motor to achieve the desired pitch angle.

A 6 V generator was mounted on the back of the platform and connected to the main shaft. In order to measure the voltage and the current generated, an analogue signal detector measured the signals and fed them into a LabVIEW program on a computer. The tip speed of the blades as well as the shaft speed was measured with a tachometer. Pitch control of the wind turbine was done by controlling a stepper motor on the PLC using a 1-step-drive from Phytron. The coding for the actuation of the stepper drive was provided by the same company. The controlling sequence was created in a ladder diagram, using function calls and function blocks in the diagram. The pitch control followed the flowchart designed, and started pitching the blades after the wind speed reached rated wind speed and above. In order to measure the results thoroughly, the pitch system handled one wind speed at the time so that the data could be logged properly.

The test model was created successfully, with a stable tower structure and functional pitch control system. However, the materials used limited the weather conditions on which the turbine could operate safely. Relatively fragile blades and plastic materials also limited the testing intervals. The programmable logic controller designed to turn the angle of the blades was achieved successfully, but only for one wind speed at the time. Some results were obtained, and improvements of the test model and the complete system were discussed in the results section. In conclusion, the systems designed and the prototype build can be considered a part of a larger and more extensive study into floating offshore wind turbines.

To improve the model, the test model should be constructed using more robust materials. Adding additional bearings and relieving the weight on the slider mechanism would reduce the friction, and should also be considered. In order to capture more wind, the blades could be re-designed with a larger surface area. Glass fibre or a similar composite material can improve the quality of the blades significantly due to reliability provided by a higher strength-to-weight ratio compared to the plastic material used with the current test model. Further improvements of the test model could be done by including a gearbox between the low speed shaft and the generator, in order to increase the input speed on the generator. This would enable the generator to produce considerably more usable energy than the current test model. The pitch control system should also be improved as suggested. More inputs, such as the rotational speed and the anemometer should be directly connected to the PLC to fully automate the process. Testing indoors with a wind tunnel or sufficient fans, improves the wind distribution and the results would be more reliable.

Bibliography

- [1] Leo H. Holthuijsen. *Waves in Oceanic and Coastal Waters*. Cambridge University Press, 2007.
- [2] Statoil. http://www.statoil.com/no/TechnologyInnovation/NewEnergy/RenewablePowerProduction/Offshore/Hywind/Downloads/Hywind_nov_2012.pdf <http://www.statoil.com/no/TechnologyInnovation/NewEnergy/RenewablePowerProduction/Offshore/HywindScotland/Pages/default.aspx>. Retrived 12.03.15, 2012.
- [3] <http://www.olavolsen.no/en/node/41>. Picture obtained online 19.05.2015.
- [4] <http://www.principlepowerinc.com/products/windfloat.html> accessed: 15.04.2015.
- [5] Takeshi Ishihara. Fukushima floating offshore wind farm - demonstration project. Pamphlet by Fukushima Offshore Wind Consortium.
- [6] Andrew Cordle and Jason Jonkman. State of the art in floating wind turbine design tools. *International Offshore and Polar Engineering Conference*, 2011.
- [7] http://www.kompetansfond.no/wp-content/uploads/Stewart_slider1.jpg. Picture obtained 19.05.2015.
- [8] Reliance Precision Limited. *Precise Motion Control Solutions* http://www.reliance.co.uk/assets/uploads/1428931960RG36_Issue_A1_Section_3_Gearboxes-Web.pdf, rg36 issue a1 edition.
- [9] Oriol Gomis. Wind power lectures. Available on Atenea, 2014.
- [10] Paul A. Lynn. *Onshore and Offshore Wind Energy*. Wiley, 2012.
- [11] Paul Gipe. *Wind Power - Renewable Energy for Home, Farm, and Business*. Chelsea Green Publishing, 2004.
- [12] Ivan Dahlberg and Haavard Froeland. Wind turbine design. Technical report, Univeristy of Agder, 2014.
- [13] Jon G. McGowan James F. Manwell and Anthony L. Rogers. *Wind Energy Explained: Theory, Design and Application*. Wiley, 2009.
- [14] Kjetil Tangen. Dynamisk respons av vindturbiner plassert offshore. Master's thesis, Faculty of Mathematics and Natural Sciences, University of Oslo, 2012.
- [15] Emrah Kulunk. *Aerodymaics of Wind Turbines, Fundamental and Advanced Topics in Wind Power*. InTech, 2011.
- [16] American wind energy association: <http://www.awea.org/Resources/Content.aspx?ItemNumber=5083&RDtoken=29819&userID=4379>. Online; accessed 17.02.2015.

- [17] David Sharpe Tony Burton, Nick Jenkins and Ervin Bossanyi. *Wind Energy Handbook*. A John Wiley and Sons, Ltd, Publication, 2 edition, 2011.
- [18] <http://www.deifwindpower.com/wind-turbine-solutions/pitch-systems>. Accessed online 15.05.2015.
- [19] F.D.and R.J Mantz. De Battista H Bianchi. *Wind Turbine Control Systems. Principles, Modelling and Gain Scheduling Design*. Springer-Verlag, 2007.
- [20] Zhe Chen Jianzhong Zhang, Ming Cheng and Xiaofan Fu. Pitch angle control for variable speed wind turbines. *Electric Utility Deregulation and Restructuring and Power Technologies*, April 2008.
- [21] Dr. Horizon Gitano-Briggs. *Small Wind Turbine Power Controllers, Wind Power*. InTech, 2010.
- [22] Qing Yu and Xiaohong Chen. Floating wind turbines. Technical report, American Bureau of Shipping, 2012.
- [23] S. Butterfield W. Musial and A. Boone. Feasibility of floating platform systems for wind turbines. *ASME Wind Energy Symposium*, 2003.
- [24] V. Diaz Casas. Mooring for floating offshore renewable energy platforms classification. *International Conference on Renewable Energies and Power Quality (ICRE PQ13)*, 2013.
- [25] Fukushima Offshore Wind Consortium. <http://www.fukushima-forward.jp/english/>.
- [26] Qing Yu and Xiaohong Chen. Floating wind turbines. Technical report, American Bureau of Shipping Corporate Offshore Technology, Renewables, 2012.
- [27] D. Stewart. A platform with six degrees of freedom. *Proceedings of the Institution of Mechanical Engineers*, 1965.
- [28] Practical information on gears - http://www.khkgears.co.jp/en/gear_technology/pdf/455-461.pdf online accessed: 15.05.2015.
- [29] http://www.yr.no/sted/Norge/Aust-Agder/Grimstad/Grimstad/detaljert_statistikk.html. Retrived 20.05.15.
- [30] J. P. Sullivan O. Wasynczuk and D. T. Man. Dynamic behavior of a class of wind turbine generators during random wind fluctuations. *Power Engineering Review*, PER-1(6):47 – 48, June 1981.
- [31] J.R Winkelman A. Murdoch and S.H Javid. Control design and performance analysis of a 6 mw wind turbine-generator. *IEEE Transactions on Power Apparatus and Systems*, 5:1340 – 1347, 1983.

Appendix A

Component Information

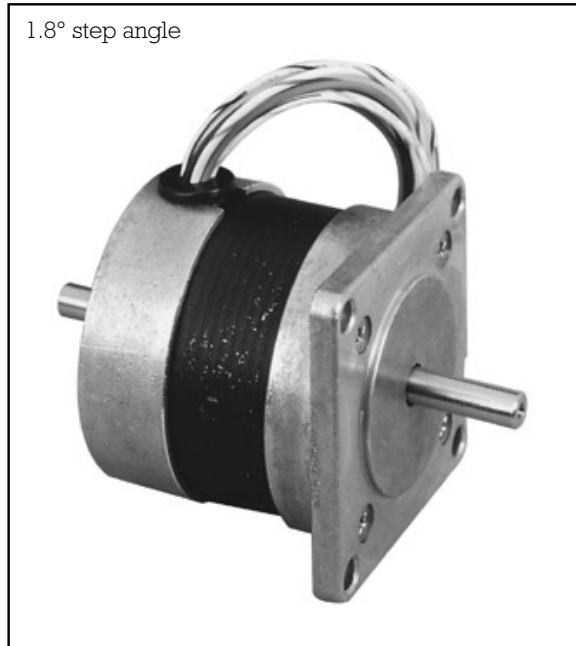
A.1 Stepper Motor



Data Sheet

Hybrid stepper motors

Size	Rear shaft	No. of wires	RS stock no.
17	No	6	440-420
	Yes		440-436
	No		191-8299
	No		191-8306
23	No	8	440-442
	Yes	8	440-458
	No	6	191-8328
	No	6	191-8334
	No	6	191-8340
	No	6	191-8356
	No	6	191-8362
	No	8	191-8378
34	Yes	8	440-464
	No	8	440-470

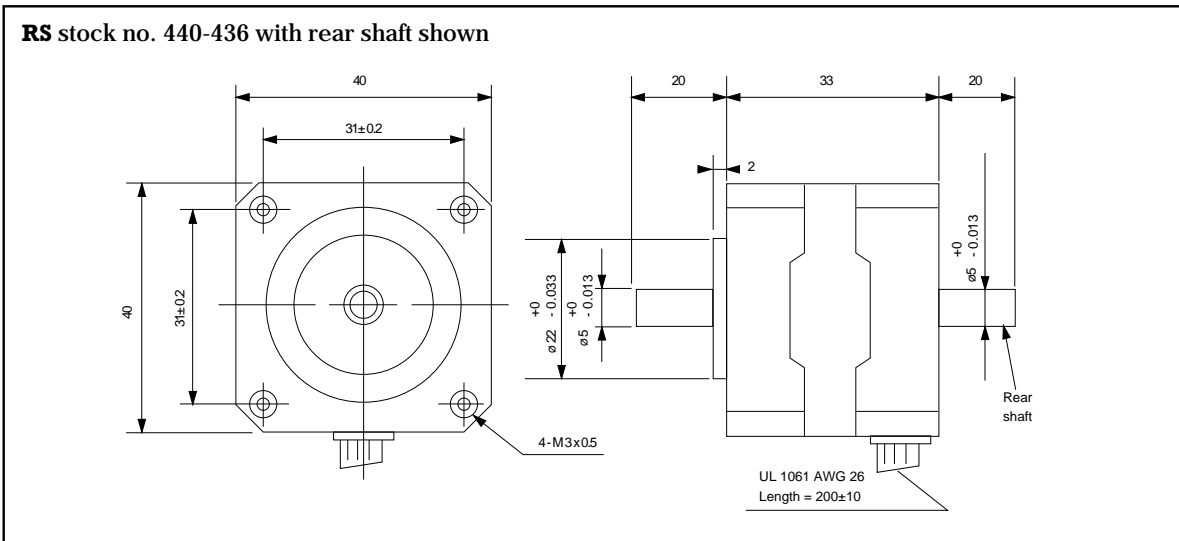


These 4 phase hybrid stepper motors are capable of delivering much higher working torques and stepping rates than permanent magnet (7.5° and 15°) types. Whilst at the same time maintaining a high detent torque even when not energised. This feature is particularly important for positional integrity. Many of the motors are directly compatible with the **RS** stepper motor drive boards (**RS** stock nos. 332-098, 342-051 and 440-240).

Size 34 motors and a number of size 23 motors are supplied in 8-lead configuration which allows the maximum flexibility when connecting to the drive boards.

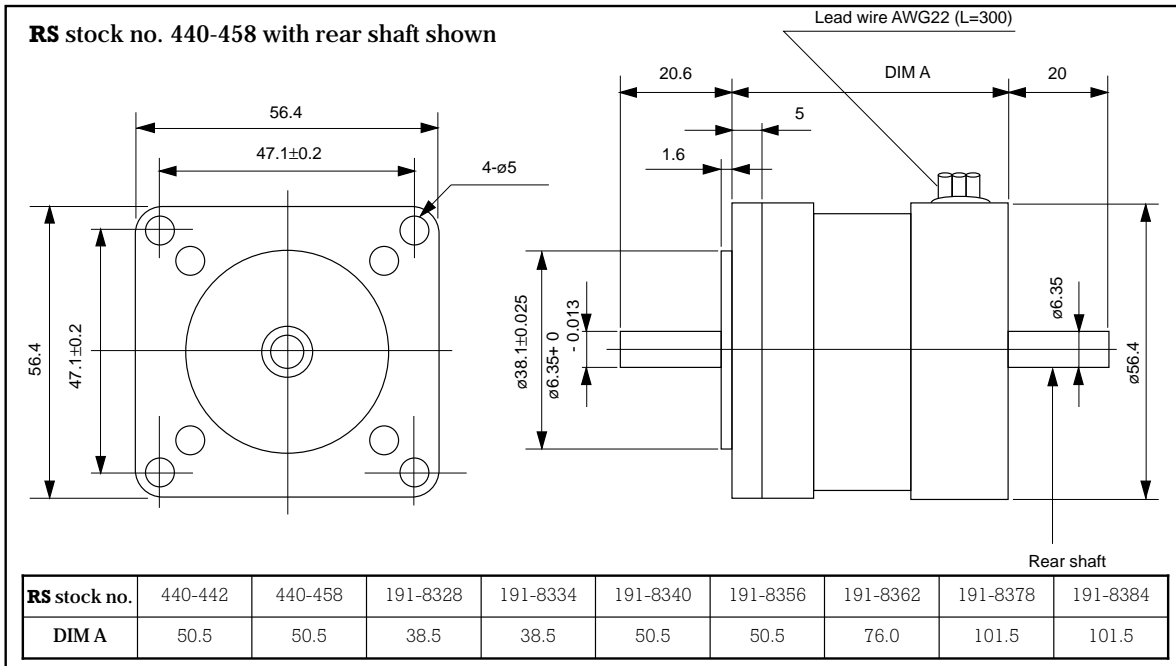
Rear extension shafts are provided on three of the motors to enable connection of other drive requirements and feedback devices.

Size 17

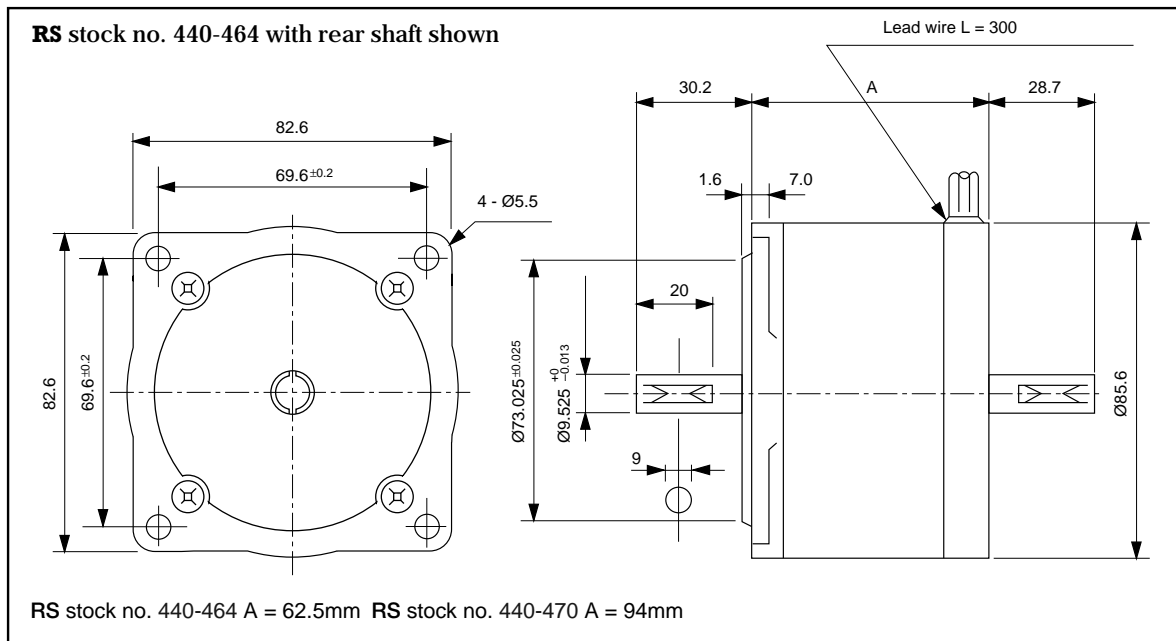


232-5749

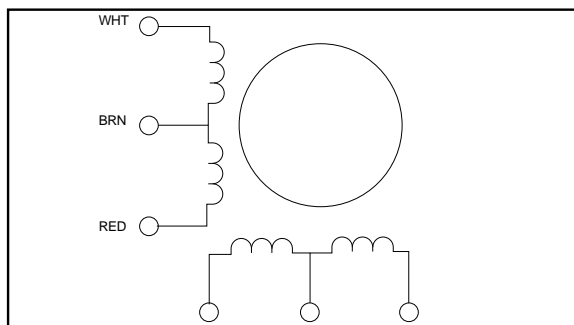
Size 23



Size 34



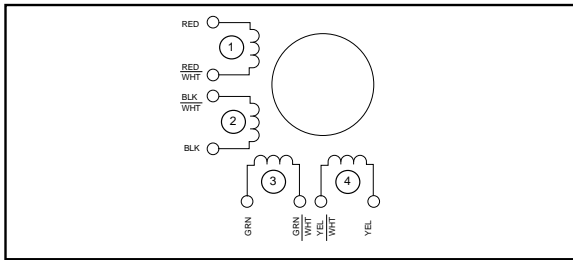
6 Wire configuration



Exciting sequence and direction of rotation when facing mounting flange end.

Step	White	Blue	Red	Yellow	Brown	CW
1	On	On			+dcV	↓
2		On	On			
3			On	On		
4	On			On		

8 Wire configuration



Exciting sequence and direction of rotation when facing mounting flange end.

Step	Red	Green	Black	Yellow	Com	CW
1	On	On			+dcV	↓
2		On	On			
3			On	On		
4	On			On		

Technical specification

RS stock no.	440-420	440-436	440-442	440-458	440-464	440-470
Rated voltage (V)	5	12	5	12	3	2.5
Rated current (I)	0.5	0.16	1	0.6	2	4.5
Resistance (Ω)	10	75	5	20	1.5	0.56
Inductance (mH)	6	36	9	32	4.5	2.8
Detent torque (mHm)	5	4	30	30	40	100
Holding torque (mNm)	70	70	500	500	1200	2200
Step angle accuracy (%)	5	5	5	5	5	5
Step angle	1.8	1.8	1.8	1.8	1.8	1.8
Insulation class	B	B	B	B	B	B

RS stock no.	191-8299	191-8306	191-8328	191-8334	191-8340	191-8356	191-8362	191-8378	191-8384
Rated voltage (V)	12	15	5	12	12	12	5.4	3.4	6
Rated current (I)	0.4	0.4	1	0.4	0.48	0.6	1.4	2.85	1.8
Resistance (Ω)	30	45	5	40	25	20	3.8	1.2	3.5
Inductance (mH)	14	22	5.7	40	33	32	6.8	1.5	7.3
Detent torque (mHm)	3.5	3.5	14.8	14.8	29.6	29.6	56.5	77.6	77.6
Holding torque (mNm)	100	100	260	260	494	494	882	1200	1200
Step angle accuracy (%)	5	5	5	5	5	5	5	5	5
Step angle	1.8	1.8	1.8	1.8	1.8	1.8	1.8	1.8	1.8
Insulation class	B	B	B	B	B	B	B	B	B

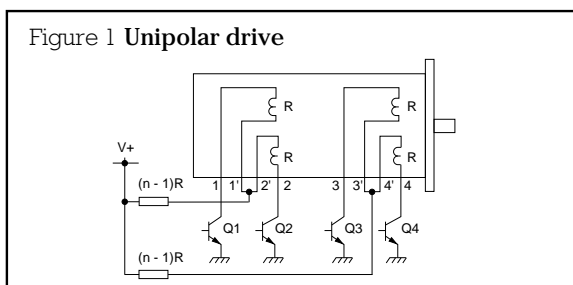
Resonance

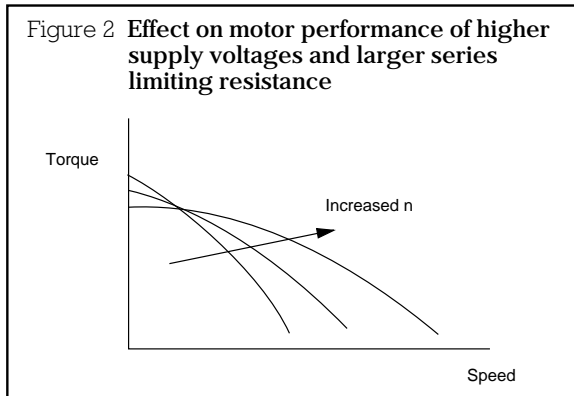
Certain operating frequencies cause resonance and the motor loses track of the drive input. Audible vibration may accompany resonance conditions. These frequencies should be avoided if possible. Driving the motor on the half step mode (see motor drive methods) greatly reduces the effect of resonance. Alternatively extra load inertia and external damping may be added to shift resonance regions away from the operating frequency.

This is commonly known as the 'Unipolar L/nr drive'. Here the current in each winding, when energised, flows in one direction only 'n', value is ≥ 1 (but not necessarily an integer) and nR is the sum of the external resistance plus the winding resistance (R). By selecting a higher value for n (ie. larger external resistance) and using a higher dc supply to maintain the rated voltage and current for each winding, improved torque speed characteristics can be obtained. Thus a 6V, 6 Ω motor (1A per phase) can be driven from a 6Vdc supply without any series resistor, in the L/R mode. Alternatively it can be driven from a 24Vdc supply using 18 Ω series resistance in the L/4R mode with much improved performance.

Motor drive methods

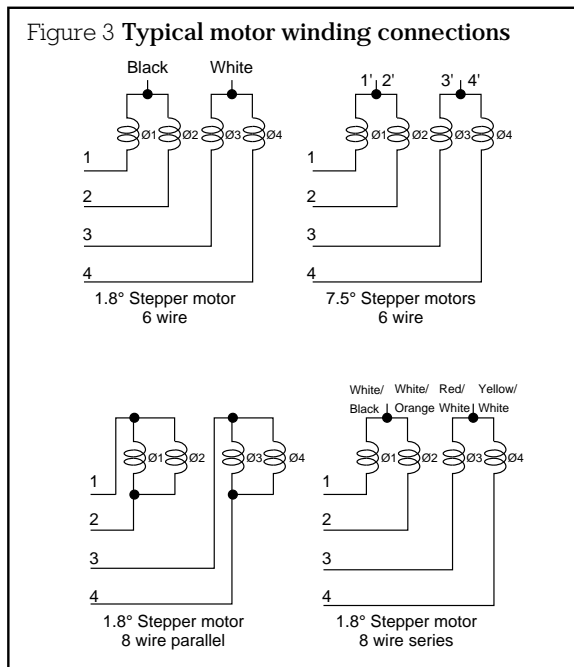
The normal way of driving a 4-phase stepper motor is shown in Figure 1.





Connection to RS bipolar stepper motor board

When the windings of the RS stepper motors are assigned (Ø1-Ø4) as shown in Figure 3, they can be connected to the board according to Figure 1.



When using 8 lead motors with coils in parallel the motor current should be set no greater than:

$$I \text{ per phase} \times \sqrt{2}$$

When using 6 lead or 8 lead motors with coils in series the motor current should be set no greater than:

$$I \text{ per phase} \times \sqrt{2}$$

Motors with 4 leads have a bipolar rating and can be used according to manufacturer's specification.

To step a motor in a particular direction a specific switching sequence for the drive transistors Q1-Q4 needs to be followed. If this sequence is in Table 1 (known as the unipolar full step mode) it results in the rotor advancing through one complete step at a time.

Table 1 Full step mode

Step No.	Q1	Q2	Q3	Q4
	ON	OFF	OFF	ON
1	ON	OFF	ON	OFF
2	OFF	ON	ON	OFF
3	OFF	ON	OFF	ON
4	ON	OFF	OFF	ON
5	ON	OFF	ON	OFF

Start position (arbitrary) →

↑ Anti-clockwise

↓ Clockwise

Above sequence repeating →

Table 2 Half step mode

Step No.	Q1	Q2	Q3	Q4
	ON	OFF	ON	OFF
1	ON	OFF	OFF	OFF
2	ON	OFF	OFF	ON
3	OFF	OFF	OFF	ON
4	OFF	ON	OFF	ON
5	OFF	ON	OFF	OFF
6	OFF	ON	ON	OFF
7	OFF	OFF	ON	OFF
8	ON	OFF	ON	OFF
9				

Start position →

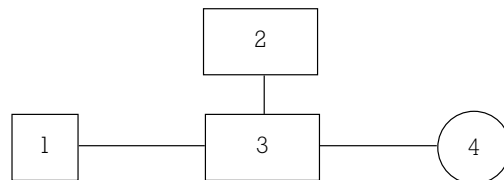
↑ Anti-clockwise

↓ Clockwise

Above sequence repeating →

Typical stepper motor control system

The operation of a stepper motor requires the presence of the following elements:



1. **A control unit.** Usually a microprocessor based unit which gives step and direction signals to the drive card. **RS** stepper motor control board (**RS** stock no. 440-098) is ideally suited for this function.
2. **Power supply.** Giving the required voltage and current for the drive card using a linear power supply.
3. **Drive card.** This converts the signals from the control unit in to the required stepper motor sequence. **RS** stock nos. 332-098, 342-051 and 440-240 are designed for the function.
4. **Stepper motor.**

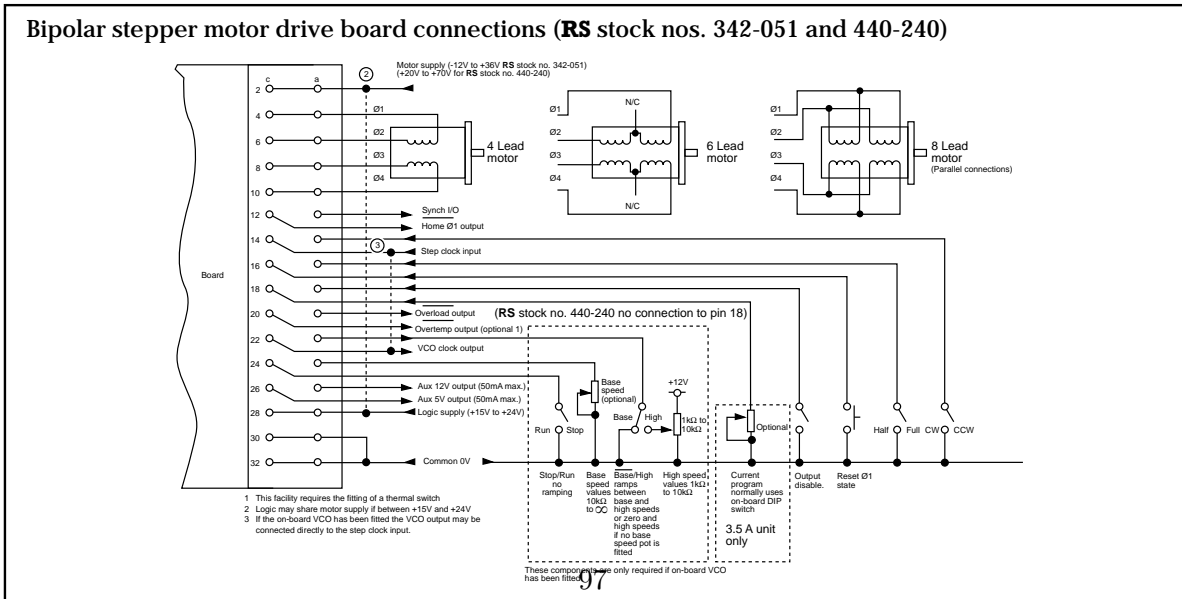
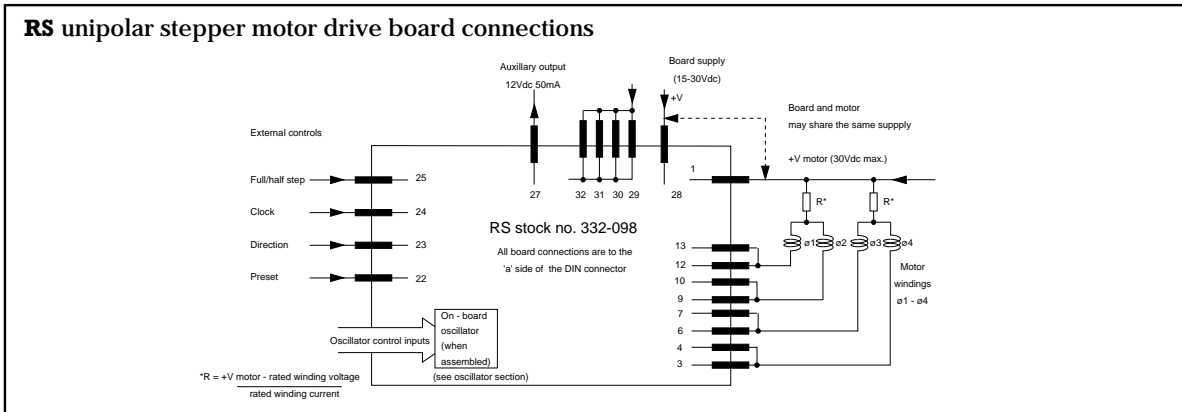
Stepper motor drive boards

For control of stepper motors **RS** has three types of stepper drive board which are suitable to drive stepper motors of various current ranges.

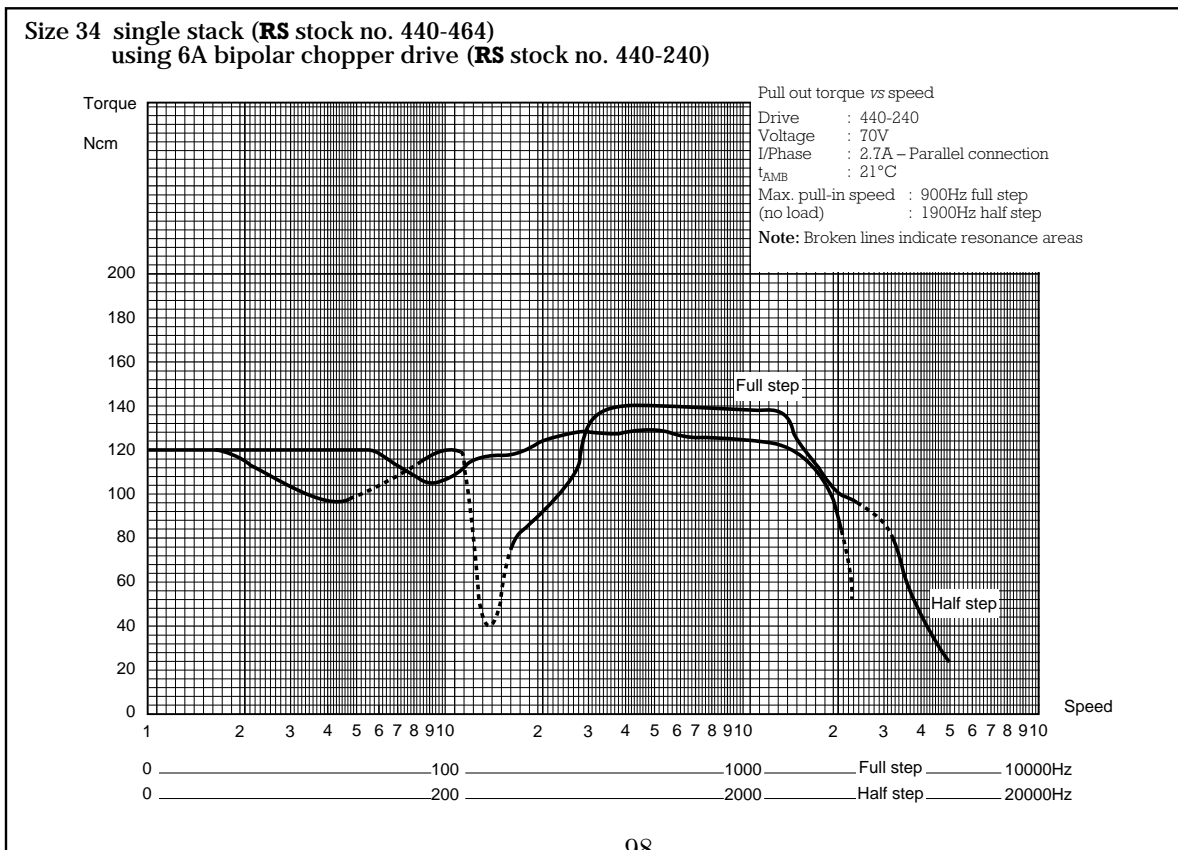
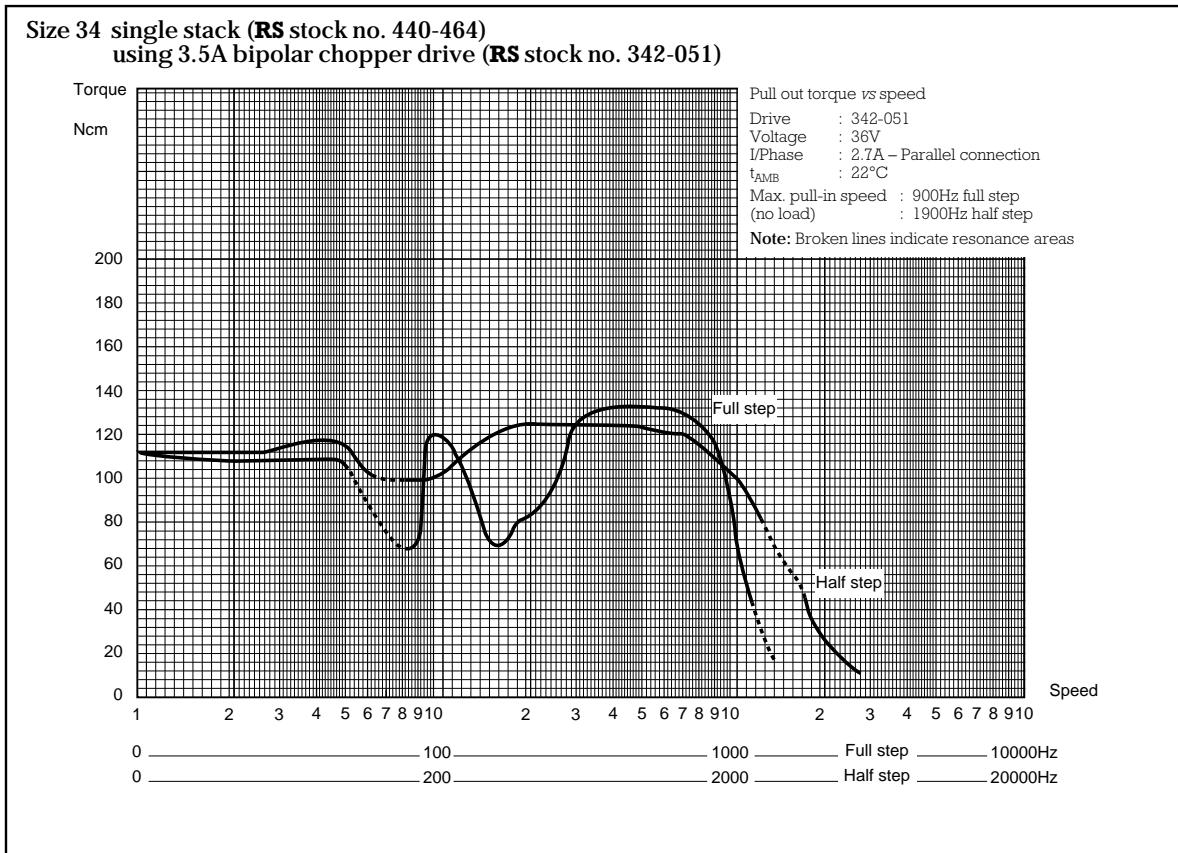
Drive board	RS stock nos.	Suitable stepper motors	Suggested wiring configuration
Unipolar 2A (RS stock no. 332-098) This drive is only suitable for applications where low speeds and low torques are required	440-420	Size 17	N/A
	440-436	Size 17	
	191-8299	Size 17	
	191-8306	Size 17	
	440-442	Size 23	
	440-458	Size 23	
	191-8328	Size 23	
	191-8334	Size 23	
	191-8340	Size 23	
	191-8356	Size 23	
Bipolar 3.5A (RS stock no. 342-051) Suitable for medium current, medium torque applications	440-442	Size 23	Series or parallel Parallel connection Series Series Series or parallel Series or parallel Series or parallel connection Series or parallel connection
	440-455	Size 23	
	191-8328	Size 23	
	191-8362	Size 23	
	191-8378	Size 23	
	191-8384	Size 23	
	440-464	Size 34	
Bipolar 6A (RS stock no. 440-240). Suitable for high current, high torque applications	191-8378	Size 23	Series or parallel Parallel Parallel connection Series or parallel connection
	191-8384	Size 23	
	440-464	Size 34	
	440-470	Size 34	

Note: Connecting a stepper motor in series will give a good low speed high torque performance.
Connecting a stepper motor in parallel will give a good high speed lower torque performance.

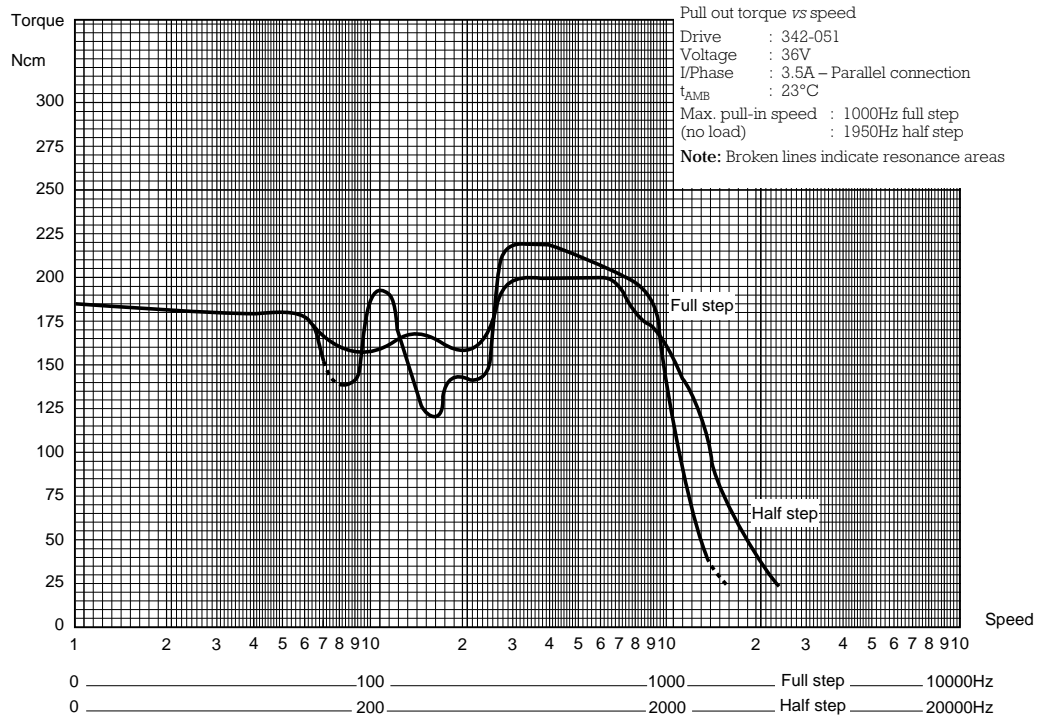
Drive board connections



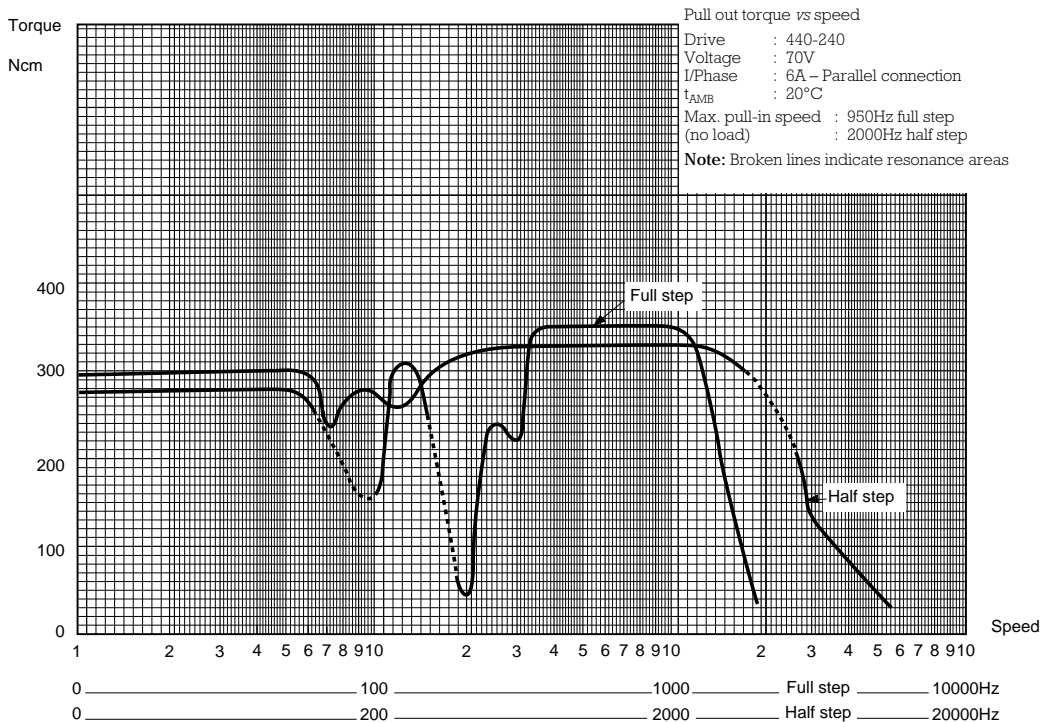
Typical drive motor speed torque curves



**Size 34 double stack (RS stock no.440-470)
using 3.5A bipolar chopper drive (RS stock no. 342-051)**



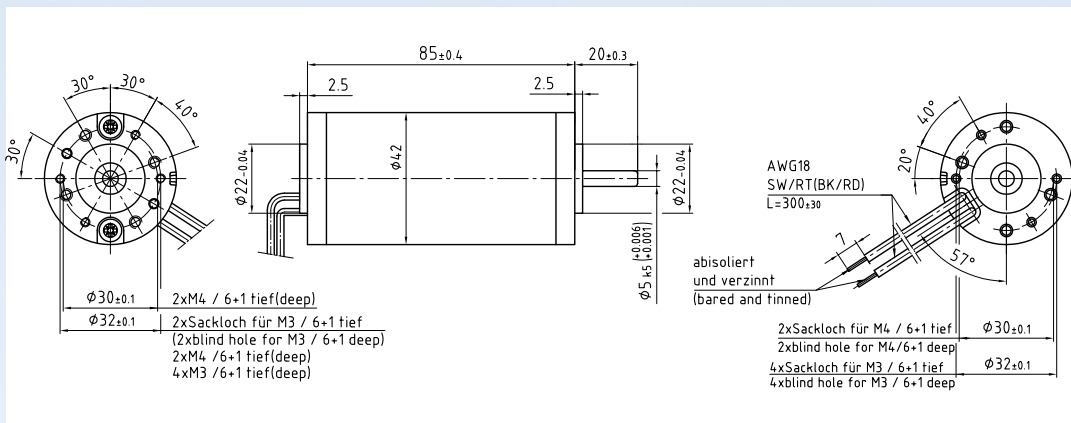
**Size 34 double stack (RS stock no.440-470)
using 6A bipolar chopper drive (RS stock no. 440-240)**



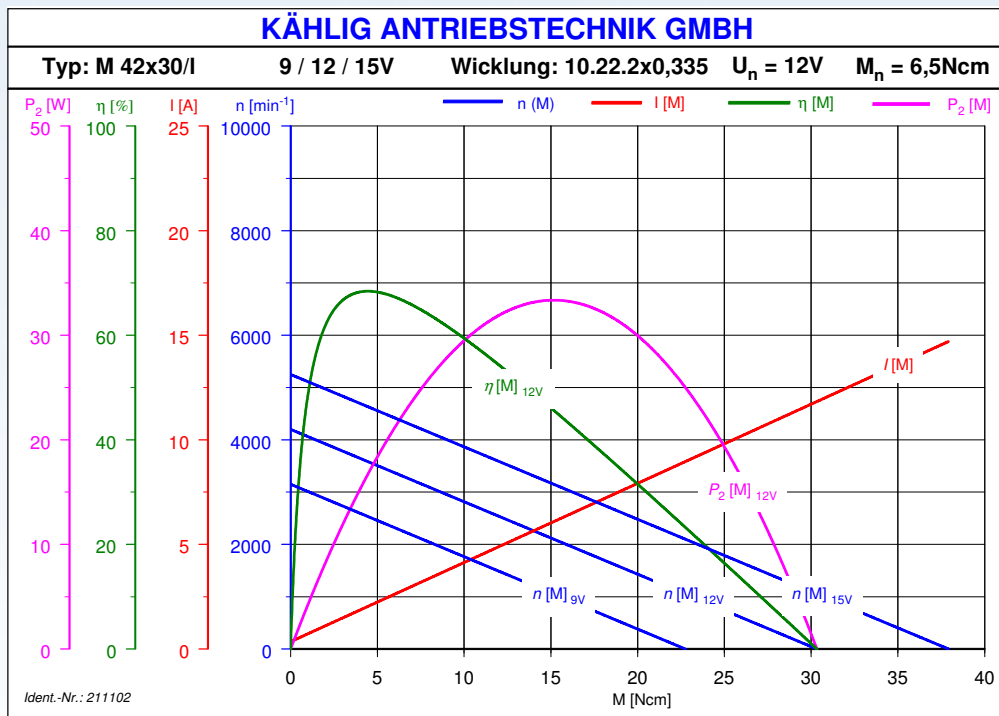
A.2 Generator

DC-Motor M42x30/I (12V) Ident-Nr. 211102

- Brushed DC motor with permanent magnet
- Ball bearings
- Lead wires
- Closed zinc-plated housing with zinc-die-cast bearing flanges
- Direction of rotation CW / CCW
- Power output in rated operation: 22,5 Watt
- Multiple combination possibilities with gears, encoders and brakes



Application on request



DC-Motor M42x30/I (12V)

Ident-Nr. 211102



excellent drives

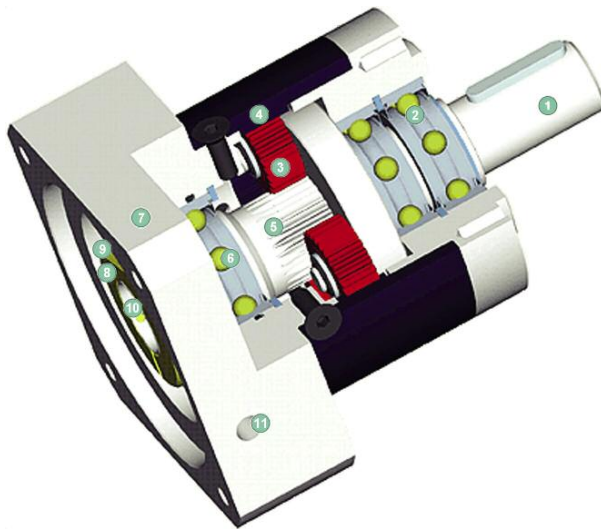
Performance

	Sign	Unit	Value	Tolerances
Rated voltage	U_N	V	12	
Rated torque ¹⁾	M_N	Ncm	6,5	
Rated speed ¹⁾	n_N	min ⁻¹	3300	±10%
Rated current ¹⁾	I_N	A	2,81	±20%
No load speed ¹⁾	n_0	min ⁻¹	4200	±15%
No load current ¹⁾	I_0	A	0,35	±50%
Rated power output ¹⁾	P_{zN}	W	22,5	
Rated power input ¹⁾	P_{1N}	W	33,7	
Rated efficiency ¹⁾	η_N	%	66,6	
Maximum power output ²⁾³⁾	P_{2max}	W	33,4	
Maximum continuous torque ²⁾³⁾	M_{max}	Ncm	6,5	
Maximum continuous current ²⁾³⁾	I_{max}	A	2,81	
Maximum speed ¹⁾³⁾	n_{max}	min ⁻¹	10000	
Stall torque ¹⁾	M_H	Ncm	30,3	
Stall current ¹⁾	I_H	A	11,8	
Demagnetization current	I_E	A	31,7	
Connecting resistance ¹⁾	R	Ω	1,01	
Armature resistance ¹⁾	R_A	Ω	0,61	±5%
Armature inductance [1 kHz] ¹⁾	L_A	mH	0,61	
Rise of speed-characteristic ¹⁾	k_D	min ⁻¹ /Ncm	138,5	
Torque constant ¹⁾	k_M	Ncm/A	2,6	
Voltage constant ¹⁾	k_E	V/10 ³ min ⁻¹	2,9	
Friction torque ¹⁾	M_R	Ncm	-0,9	
Mechanical time constant ¹⁾	T_M	ms	8,7	
Electrical time constant ¹⁾	T_e	ms	0,6	
Rotor inertia	J_R	gcm ²	100	
Maximum case temperature ²⁾	ϑ_G	°C	80	
Starting voltage ¹⁾	U_A	V	2	
Permissible axial shaft loads ³⁾	F_{axial}	N	40	
Permissible radial shaft loads ³⁾	F_{radial}	N	100	
Protection class DIN VDE 0530			IP 40	
Duty cycle DIN VDE 0530			S1	
Insulation class DIN VDE 0530			E	
Lifetime at rated torque [h] ¹⁾			3000	
Ambient temperature			-30°C to +40°C	
Bearing			2 ball bearings	
Interference suppression			optional	

1) ϑ_w Winding temperature ≈ 20°C 2) $\Delta\vartheta_w$ allowable = 100K
 3) The operating at maximum levels reduces the lifespan

Stand: 8. Oktober 2014 – changes reserved

A.3 Gearbox



RGP40, RGP60

- standard backlash (RGP40 from <math><22^\circ</math>)
(RGP60 from <math><18^\circ</math>)
- high output torque
- novel motor clamp system
- high efficiency (up to 96%)
- ratios $i=3, \dots, 512$
- low noise
- high quality
- any mounting position
- easy motor mounting
- lifetime lubrication
- direction of rotation equidirectional

- 1 Output shaft**
High strength one piece planet carrier and output shaft
- 2 Output shaft bearing**
Deep groove ball bearings with contact seals
- 3 Planet gear**
Precision zero helix angle gear with optimised profile modifications and crowning, case hardened and hard finished by honing
- 4 Housing with integrated ring gear**
Ring gear case hardened for high load capacity, minimum wear, consistent backlash
- 5 Sun gear**
Precision machined optimised gear profile, case hardened and honed for higher load capacity, low noise, minimum wear and consistent backlash
- 6 Bearing for sun gear**
High speed, deep groove ball bearings eliminating thrust loads from thermal expansion, whilst providing exact sun gear position for easy mounting
- 7 Motor adaptor plate**
Allows matching up of the gear head with NEMA 17 and 23 motors, made from aluminium for enhanced thermal conductivity (other adaptors and motors on request)
- 8 Clamping ring**
Balanced ring suitable for high rpm, made from steel to allow greater clamping forces for safe torque transfer
- 9 Clamping screw**
High strength steel with special low pitch thread to generate a greater clamping force
- 10 Motor shaft clamp**
Multiple closed slot precision clamping system for improved reliability
- 11 Assembly hole**
Access hole for the clamping screw



RGP40 NEMA 17

Planetary Gearboxes

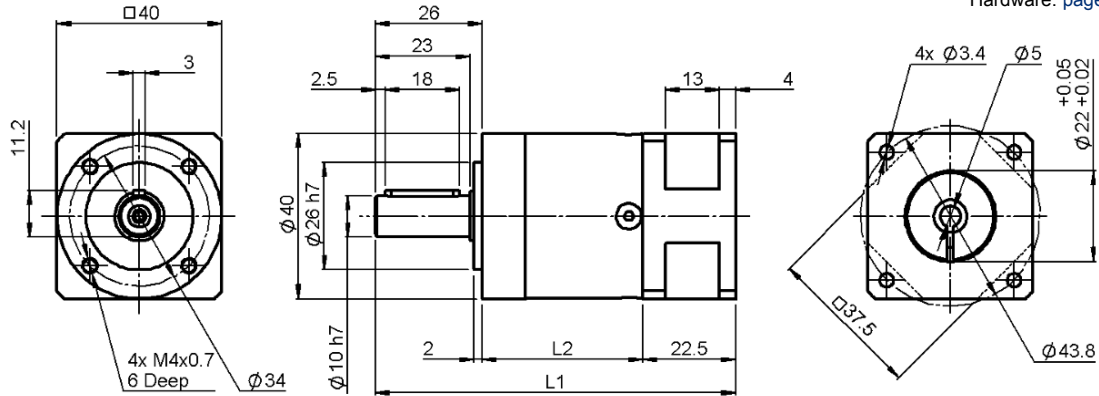
All dimensions in mm

Associated Products

Reliance Cool Muscle: [page 2-2](#)

Couplings: [page 8-1](#)

Hardware: [page 13-1](#)



Part number selection table

Example Part No:- RGP40 - 60 - NEMA17																								
Basic Part Number	Ratio	Stage	L1	L2	Output Torque		Inertia	Efficiency ⁽⁶⁾ with full load																
			mm	mm	Nm ⁽²⁾	Nm			kgcm ²	%														
RGP40	3	1	87.5	39	11	17.6	0.031	98																
	4				15	24			0.022	98														
	5				14	22					0.019	98												
	7				8.5	13.6							0.018	97										
	8				6	10									0.017	96								
	10				5	8											0.016	95						
RGP40	9	2	100.5	52	16.5	26	0.030	97																
	12				20	32			0.029	96														
	15				18	29					0.023	96												
	16				20	32							0.022	96										
	20				20	32									0.019	96								
	25				18	29											0.019	95						
	32				20	32													0.017	95				
	40				18	29															0.016	94		
	64				7.5	12																	0.016	86
RGP40	60	3	113	64.5	20	32	0.029	92																
	80				20	32			0.019	90														
	100				20	32					0.019	89												
	120				18	29							0.029	87										
	160				20	32									0.016	86								
	200				18	29											0.016	82						
	256				20	32													0.016	81				
	320				18	29															0.016	76		
	512				7.5	12																	0.016	48

Gearboxes



Technical information

Specification	Unit	RGP40	Stage
Backlash	arcmin	<15	1
		<19	2
		<22	3
Torsional stiffness	Nm/arcmin	1.0	1
		1.1	2
		1.0	3
Weight	kg	0.35	1
		0.45	2
		0.55	3
Lifetime ⁽³⁾	h	30,000	
Radial load for 20,000h ⁽⁴⁾	N	200	
Axial load for 20,000h ⁽⁴⁾	N	200	
Running noise ⁽⁵⁾	dB(A)	58	
Maximum input speed	rpm	18,000	
Input speed at >50% torque		5,000	
Operating temperature	max °C	90	
	min °C	-25	
Motor mounting clamp torque	M2.5	Nm	
Lubrication		Greased for life	
Degree of protection		IP54	

⁽¹⁾ Gearboxes for use with NEMA motors are supplied with a motor output shaft bush

⁽²⁾ Emergency stop torque equals twice nominal torque, maximum 500 times

⁽³⁾ Based on nominal torque and output shaft speed 100 rpm

⁽⁴⁾ Based on output shaft speed 100 rpm, centrally positioned along shaft

⁽⁵⁾ Distance 1 metre, idle running, input speed 3,000 rpm, ratio 5

⁽⁶⁾ Degree of efficiency at nominal output torque, reference temperature 70°C at 1,000 rpm

? Technical support

- Product overview - see [page 3-3](#)
- Technical information - see [pages T3-1 to T3-3](#)
- Section view - see [page 3-4](#)
- For detailed duty cycle and life calculation, please contact us
- Gearbox complements the Reliance Cool Muscle servo system - see [page 2-2](#)
- For system design information when using the RGP40 series with Reliance Cool Muscle, please contact us

i Features and options

- Gearbox may be used in any mounting orientation
- Housing material: Steel - black
- Input and output flanges material: Aluminium - untreated
- Optional smooth output shaft if required
- Other motors may be utilised, please contact us



Appendix B

Material and Printer Specification

B.1 High Definition Printer

Productive, high-capacity ProJet® 3500 professional printers



The widest applications range: concept models, verification models, pre-production, digital manufacturing

Easy connectivity and high productivity with high resolution and accuracy

ProJet 3510 SD

The affordable ProJet 3510 SD prints high-quality, durable plastic parts for engineering and mechanical design applications, including functional testing, form and fit verification, rapid prototyping, design communication, rapid tooling and more. This office-friendly 3D printer delivers exceptional parts on demand.

AFFORDABILITY • QUALITY • EASE-OF-USE

ProJet 3510 HDPlus

The ProJet 3510 HDPlus offers the flexibility to choose between three resolution modes to print concept models, verification prototypes and patterns for pre-production and digital manufacturing. Just connect to the printer to create extremely fine-featured plastic parts with greater output.

RESOLUTION *Plus* • PARTS SIZE *Plus* • FLEXIBILITY *Plus*

ProJet 3510 HD

The ProJet 3510 HD prints precision, durable plastic parts ideal for functional testing, design communication, rapid manufacturing, rapid tooling and more. With a choice in materials and selectable print resolutions, this office-friendly, easy-to-use 3D printer is packed with features that help you maximize your return on investment (ROI).

HIGH DEFINITION • PRECISION • PRODUCTIVITY

ProJet 3500 HDMax

The high-capacity ProJet 3500 HDMax offers greater productivity, especially with the high-speed printing mode, and larger high-definition prints for the production of functional plastic parts. Users also benefit from increased throughput, part size, feature detail and quality only possible with ProJet printers.

Max THROUGHPUT • Max DEFINITION • Max VOLUME

VisiJet® M3 Materials for ProJet SD & HD Printers

The VisiJet line of plastic materials offers numerous capabilities to meet a variety of commercial applications. 3D Systems' ProJet 3500 3D printers use VisiJet M3 materials to build accurate, high-definition models and prototypes for proof of concept, functional testing, master patterns for moldmaking, and direct investment casting. Vertical markets for the ProJet 3500 line include transportation, energy, consumer products, recreation, healthcare and education. Toughness, high temperature resistance, durability, stability, watertightness, biocompatibility and castability are a few of the key attributes you will find within the VisiJet M3 materials line. Parts can be drilled, glued, painted, plated, etc. Support material offers easy, non-hazardous post-processing and preserves delicate features.

Properties	Condition	VisiJet M3-X	VisiJet M3 Black	VisiJet M3 Crystal	VisiJet M3 Proplast	VisiJet M3 Navy	VisiJet M3 Techplast	VisiJet M3 Procast	VisiJet® S300
Composition		----- UV Curable Plastic -----							Wax Support Material
Color		White	Black	Natural	Natural	Blue	Gray	Dark Blue	White
Bottle Quantity		2 kg	2 kg	2 kg	2 kg	2 kg	2 kg	2 kg	2 kg
Density @ 80 °C (liquid)	ASTM D4164	1.04 g/cm ³	1.02 g/cm ³	1.02 g/cm ³	1.02 g/cm ³	1.02 g/cm ³	1.02 g/cm ³	1.02 g/cm ³	N/A
Tensile Strength	ASTM D638	49 MPa	35.2 MPa	42.4 MPa	26.2 MPa	20.5 MPa	22.1 MPa	32 MPa	N/A
Tensile Modulus	ASTM D638	2168 MPa	1594 MPa	1463 MPa	1108 MPa	735 MPa	866 MPa	1724 MPa	N/A
Elongation at Break	ASTM D638	8.3 %	19.7 %	6.83 %	8.97 %	8 %	6.1 %	12.3 %	N/A
Flexural Strength	ASTM D790	65 MPa	44.5 MPa	49 MPa	26.6 MPa	28.1 MPa	28.1 MPa	45 MPa	N/A
Heat Distortion Temperature @ 0.45MPa	ASTM D648	88 °C	57 °C	56 °C	46 °C	46 °C	46 °C	N/A	N/A
Ash Content		N/A	N/A	N/A	0.01 %	0.01 %	0.01 %	0.01 %	N/A
Melting Point		N/A	N/A	N/A	N/A	N/A	N/A	N/A	60 °C
Softening Point		N/A	N/A	N/A	N/A	N/A	N/A	N/A	40 °C
USP Class VI Certified*		No	No	Yes	No	No	No	No	N/A
ProJet Compatibility		SD, HD	SD, HD	SD, HD	SD, HD	SD, HD	SD, HD	HD	SD, HD
Description		ABS-like Plastic	High strength & flexibility plastic	Tough Plastic, Translucent	Plastic, Natural	Plastic, Blue	Plastic, Gray	Castable Plastic	Non-toxic wax material for hands-free melt-away supports

DISCLAIMER: It is the responsibility of each customer to determine that its use of any VisiJet® material is safe, lawful and technically suitable to the customer's intended applications. The values presented here are for reference only and may vary. Customers should conduct their own testing to ensure suitability for their intended application.



VisiJet M3-X



VisiJet M3 Crystal



VisiJet M3 Proplast



VisiJet M3 Black



VisiJet M3 Navy



VisiJet M3 Techplast



VisiJet M3 Procast

ProJet® 3500 SD & HD

Professional 3D Printers



3DSYSTEMS®

Extend Innovation. Extend Production. Extend Choices.



ProJet 3510 SD

ProJet 3510 HD

ProJet 3510 HDPlus

ProJet 3500 HDMax

Printing Modes	HD - High Definition - -	HD - High Definition - UHD - Ultra High Definition -	HD - High Definition - UHD - Ultra High Definition XHD - Xtreme High Definition	HD - High Definition HS - High Speed UHD - Ultra High Definition XHD - Xtreme High Definition
Net Build Volume (xyz)				
HD Mode	11.75 x 7.3 x 8" (298 x 185 x 203 mm)	11.75 x 7.3 x 8" (298 x 185 x 203 mm)	11.75 x 7.3 x 8" (298 x 185 x 203 mm)	11.75 x 7.3 x 8" (298 x 185 x 203 mm)
HS Mode	-	-	-	11.75 x 7.3 x 8" (298 x 185 x 203 mm)
UHD Mode	-	5 x 7 x 6" (127 x 178 x 152 mm)	8 x 7 x 6" (203 x 178 x 152 mm)	11.75 x 7.3 x 8" (298 x 185 x 203 mm)
XHD Mode	-	-	8 x 7 x 6" (203 x 178 x 152 mm)	11.75 x 7.3 x 8" (298 x 185 x 203 mm)
Resolution				
HD Mode	375 x 375 x 790 DPI (xyz); 32µ layers	375 x 375 x 790 DPI (xyz); 32µ layers	375 x 375 x 790 DPI (xyz); 32µ layers	375 x 375 x 790 DPI (xyz); 32µ layers
HS Mode	-	-	-	375 x 375 x 790 DPI (xyz); 32µ layers
UHD Mode	-	750 x 750 x 890 DPI (xyz); 29µ layers	750 x 750 x 890 DPI (xyz); 29µ layers	750 x 750 x 890 DPI (xyz); 29µ layers
XHD Mode	-	-	750 x 750 x 1600 DPI (xyz); 16µ layers	750 x 750 x 1600 DPI (xyz); 16µ layers
Accuracy (typical)	0.001-0.002 inch per inch (0.025-0.05 mm per 25.4 mm) of part dimension. Accuracy may vary depending on build parameters, part geometry and size, part orientation, and post-processing.			
E-mail Notice Capability	Yes	Yes	Yes	Yes
Tablet/Smartphone connectivity	Yes	Yes	Yes	Yes
5-Year Printhead Warranty	Optional	Standard	Standard	Standard
Build Materials	VisiJet M3-X VisiJet M3 Black VisiJet M3 Crystal VisiJet M3 Proplast VisiJet M3 Navy VisiJet M3 Techplast -	VisiJet M3-X VisiJet M3 Black VisiJet M3 Crystal VisiJet M3 Proplast VisiJet M3 Navy VisiJet M3 Techplast VisiJet M3 Procast	VisiJet M3-X VisiJet M3 Black VisiJet M3 Crystal VisiJet M3 Proplast VisiJet M3 Navy VisiJet M3 Techplast VisiJet M3 Procast	VisiJet M3-X VisiJet M3 Black VisiJet M3 Crystal VisiJet M3 Proplast VisiJet M3 Navy VisiJet M3 Techplast VisiJet M3 Procast
Support Material	VisiJet S300	VisiJet S300	VisiJet S300	VisiJet S300
Material Packaging	Build and support materials In clean 4.41 lbs (2 kg) bottles (machine holds up to 2 with auto-switching)			
Electrical	100-127 VAC, 50/60 Hz, single-phase, 15A; 200-240* VAC, 50 Hz, single-phase, 10A			
Dimensions (WxDxH)				
3D Printer Crated	32.5 x 56.25 x 68.5 in (826 x 1429 x 1740 mm)	32.5 x 56.25 x 68.5 in (826 x 1429 x 1740 mm)	32.5 x 56.25 x 68.5 in (826 x 1429 x 1740 mm)	32.5 x 56.25 x 68.5 in (826 x 1429 x 1740 mm)
3D Printer Uncrated	29.5 x 47 x 59.5 in (749 x 1194 x 1511 mm)	29.5 x 47 x 59.5 in (749 x 1194 x 1511 mm)	29.5 x 47 x 59.5 in (749 x 1194 x 1511 mm)	29.5 x 47 x 59.5 in (749 x 1194 x 1511 mm)
Weight				
3D Printer Crated	955 lbs, 434 kg	955 lbs, 434 kg	955 lbs, 434 kg	955 lbs, 434 kg
3D Printer Uncrated	711 lbs, 323 kg	711 lbs, 323 kg	711 lbs, 323 kg	711 lbs, 323 kg
ProJet® Accelerator Software	Easy build job set-up, submission and job queue management ; Automatic part placement and build optimization tools ; Part stacking and nesting capability ; Extensive part editing tools ; Automatic support generation ; Job statistics reporting tools			
Print3D App	Remote monitoring and control from tablet, computers and smartphones			
Network Compatibility	Network ready with 10/100 Ethernet interface			
Client Hardware Recommendation	1.8 GHz with 1GB RAM (OpenGL support 64 mb video RAM) or higher			
Client Operating System	Windows XP Professional, Windows Vista, Windows 7			
Input Data File Formats Supported	STL and SLC	STL and SLC	STL and SLC	STL and SLC
Operating Temperature Range	64-82 °F (18-28 °C)	64-82 °F (18-28 °C)	64-82 °F (18-28 °C)	64-82 °F (18-28 °C)
Noise	< 65 dBa estimated (at medium fan setting)			
Certifications	CE	CE	CE	CE

* Requires small external transformer supplied by 3D Systems in the provided country kit.



UK
Tel: +44 1442 282 600
info@3dsystems-europe.com

USA
Tel: +1 803.326.3900
moreinfo@3dsystems.com

**Germany, Scandinavia,
Eastern Europe, Middle East**
Tel: +49 6151 357 0
info@3dsystems-europe.com

Asia-Pacific
Melbourne Tel: +61 3 9819 4422
Sydney Tel: +61 2 9516 5571
3dprinters.asiapac@3dsystems.com

Warranty/Disclaimer: The performance characteristics of these products may vary according to product application, operating conditions, material combined with, or with end use. 3D Systems makes no warranties of any type, express or implied, including, but not limited to, the warranties of merchantability or fitness for a particular use.

© 2015 by 3D Systems Inc. All rights reserved. Specifications subject to change without notice. ProJet, VisiJet, 3D Systems and the 3D Systems logo are registered trademarks of 3D Systems, Inc. Windows is a registered trademark of Microsoft Corporation.

B.2 Standard Definition Printer

Dimension 1200es™

Think in 3D and give your ideas new Dimension.



Print large, durable 3D models right in your office.

See your designs come to life with the Dimension SST 1200es and BST 1200es 3D Printers. They turn 3D CAD files into functional, durable 3D models that you can not only discuss but test.

The large build capacity of Dimension 1200es 3D Printers gives you the room to print models at the size you need. And they're simple to operate: Just click "print" to prep the CAD file and print the model, then remove the support material to reveal your design in three dimensions.

Bundle & Save

Order the Dimension 3D Print Pack and you'll get everything you need to start printing 3D models affordably – as soon as you unbox it.

You get a:

- Dimension 1200es SST 3D Printer
- SCA-1200 support removal system
- Startup supply of materials

Learn more about Dimension 1200es at stratasys.com

Dimension 1200es™



Print 3D models that are big, tough and functional.

Print models in production-grade thermoplastic.

Dimension 1200es 3D Printers use ABS*plus*™ modeling material, a production-grade thermoplastic that is durable enough to perform virtually the same as production parts. Models printed with Dimension 3D Printers have customer-proven toughness – from commercial sprayers tested at pressures up to 60 psi, to final parts on M1 tanks normally machined in aircraft-grade aluminum

At the core of every model: FDM® Technology.

Stratasys FDM (Fused Deposition Modeling) technology is the foundation for all Dimension 3D Printers. Models are printed from the bottom up with precisely deposited layers of modeling and support material. There's no waiting for models to "cure" — they're ready for support removal right from the printer. The SST 1200es uses Soluble Support Technology which dissolves the supports in a water-based solution. The BST 1200es uses Breakaway Support Technology in which the supports are simply snapped off to reveal the final model. Then, models can be drilled, tapped, sanded and painted.

A tool for today's fast-track product development.

You'll dramatically improve your product development process with Dimension 1200es 3D Printers. They print models that help you check form, fit and function, and correct errors, before your product goes into production. And they're versatile enough to produce functional models, molds, patterns, customized tools and fixtures. To shorten product development cycles and accelerate time-to-market, start with Dimension 1200es 3D Printers — and bring your ideas to life.

Stratasys | www.stratasys.com | info@stratasys.com

7665 Commerce Way
Eden Prairie, MN 55344
+1 888 480-3548 (US Toll Free)
+1 952 937-3000 (Intl)
+1 952 937-0070 (Fax)

2 Holtzman St.,
Science Park, PO Box 2496
Rehovot 76124, Israel
+972 74 745-4000
+972 74 745-5000 (Fax)

Local Street Address
City, State, Zip
Phone #
Fax #

© 2013 Stratasys Inc. All rights reserved. Stratasys, Stratasys logo, For a 3D World, FDM, FDM Technology, ABS*plus*, Fused Deposition Modeling, Dimension, Dimension BST, Dimension SST, Print Pack and Catalyst are trademarks or registered trademarks of Stratasys Inc. and/or its subsidiaries or affiliates and may be registered in certain jurisdictions. All other trademarks belong to their respective owners. Dim1200esSellSheet-INTL-ENG-1013

Product Specifications

Model material:

ABS*plus* in ivory, white, black, red, olive green, nectarine, fluorescent yellow, blue or gray

Support material:

Soluble Support Technology (SST) or Breakaway Support Technology (BST)

Build size:

254 x 254 x 305 mm (10 x 10 x 12 in)

Layer thickness:

.254 mm (.010 in) or .330 mm (.013 in) of precisely deposited ABS*plus* model and support material

Workstation compatibility:

Windows Vista®

Network connectivity:

Ethernet TCP/IP 10/100Base-T

Size and weight:

838 x 737 x 1143 mm (33 x 29 x 45 in)
148 kg (326 lbs)

Power requirements:

110–120 VAC, 60 Hz, minimum 15A dedicated circuit; or 220–240 VAC 50/60 Hz, minimum 7A dedicated circuit

Regulatory compliance: CE/ETL

Special facility requirements: None

Appendix C

Programmable Logic controller

C.1 Step-script

1	L	4800	//Ref position 0	4800
2	T	"Data_block_1".DB_VAR		%DB1.DB0
3	L	1		1
4				
5	T	%DB1.DBB0		%DB1.DBB0
6				
7	L	0	//Delete limit switch etc.	0
8	T	%DB1.DBB5		%DB1.DBB5
9	T	%DB1.DBW6		%DB1.DBW6
10				
11	SET			
12				
13	R	%DB1.DBX5.0	//Set Soft-Limit	%DB1.DBX5.0
14	R	%DB1.DBX5.1	//Set Soft-Limit Plus	%DB1.DBX5.1
15				
16	S	%DB1.DBX5.2	//Set pulse enable DRV_EN	%DB1.DBX5.2
17	R	%DB1.DBX4.0	//Set 'Relative incremental' operation mo	%DB1.DBX4.0
18	R	%DB1.DBX4.1	//Set 'Relative incremental' operation mo	%DB1.DBX4.1
19	R	%DB1.DBX4.2	//Set 'Relative incremental' operation mo	%DB1.DBX4.2
20	R	%DB1.DBX4.3	//Reserve bit = 0	%DB1.DBX4.3
21	R	%DB1.DBX4.4	//Start backwards delete DIR_M	%DB1.DBX4.4
22	R	%DB1.DBX4.6	//delete STOP	%DB1.DBX4.6
23	R	%DB1.DBX4.7	//delete reduction factor R	%DB1.DBX4.7
24				
25	L	"Data_block_1".DB_VAR	//Write 8 Byte to the 1-STEP-DRIVE	%DB1.DB0
26	T	"DW1_OUT":P		%QD400:P
27	L	"Data_block_1".DB_VAR_1		%DB1.DB4
28	T	"DW2_OUT":P		%QD404:P
29				
30	L	"DW1_IN":P	//Read 8 Byte from 1-STEP-DRIVE	%ID400:P
31	T	"Data_block_1".DB_VAR_2		%DB1.DB8
32	L	"DW2_IN":P		%ID404:P
33	T	"Data_block_1".DB_VAR_3		%DB1.DB12
34				
35	A	"Start"	//Detect flank of the start impulse and s	%M30.0
36	AN	%DB1.DBX12.0	//Set if STS_JOB is deleted	%DB1.DBX12.0
37	S	%DB1.DBX4.5		%DB1.DBX4.5
38				
39	A	%DB1.DBX12.0	//Wait on STS_JOB	%DB1.DBX12.0
40	R	%DB1.DBX4.5	//Reset Start DIR_P, the traversing start	%DB1.DBX4.5
41	R	"Start"	//Delete start impulse	%M30.0
42				
43				
44				
45				
46				

C.2 Step-drive

1 1-STEP-DRIVE-5A-48V

1.1 Short Overview



Fig. 1: 1-STEP-DRIVE Module

1-STEP-DRIVE-5A-48V is a stepper motor controller with integrated power stage. It is specially developed for application in the decentralized SIMATIC ET 200[®]S peripheral system.

2 phase stepper motors in the 200 W power range up to 5 A_{PEAK} with a supply voltage from 24 to 48 V_{DC} can be controlled by this module. Beside the high precision positioning up to 1/512 micro step in operating/incremental mode, the 1-STEP-DRIVE can be applied in velocity control mode. Two parameterizable digital inputs are available for limit or reference switches, too.

The most important characteristic features of the 1-STEP-DRIVE:

- 2 phase stepper motor controller with integrated power stage for SIMATIC ET 200[®]S
- 200W power range up to 5A_{PEAK} at 24-48V_{DC}
- Up to 1/512 micro step
- Maximum starting frequency 510 kHz

1-STEP-DRIVE Module

- Operating modes:
 - + Reference point approach
 - + Relative incremental mode (relative positioning)
 - + Absolute incremental mode (absolute positioning)
 - + Velocity control mode
 - + Set home position
- Support of linear and modulo axes (rotary axes)
- Function and active level of the IN0 and IN1 digital inputs can be configured
- Type of the feedback value can be set in the feedback interface (residual distance, position or frequency)
- Power stage parameter setting after starting the system and during operation: e.g.: run, stop, boost current, step resolution, current delay time, etc.
- Online power stage diagnostics
- STEP[®]7 programming

1.2 Overview of the Data Interfaces

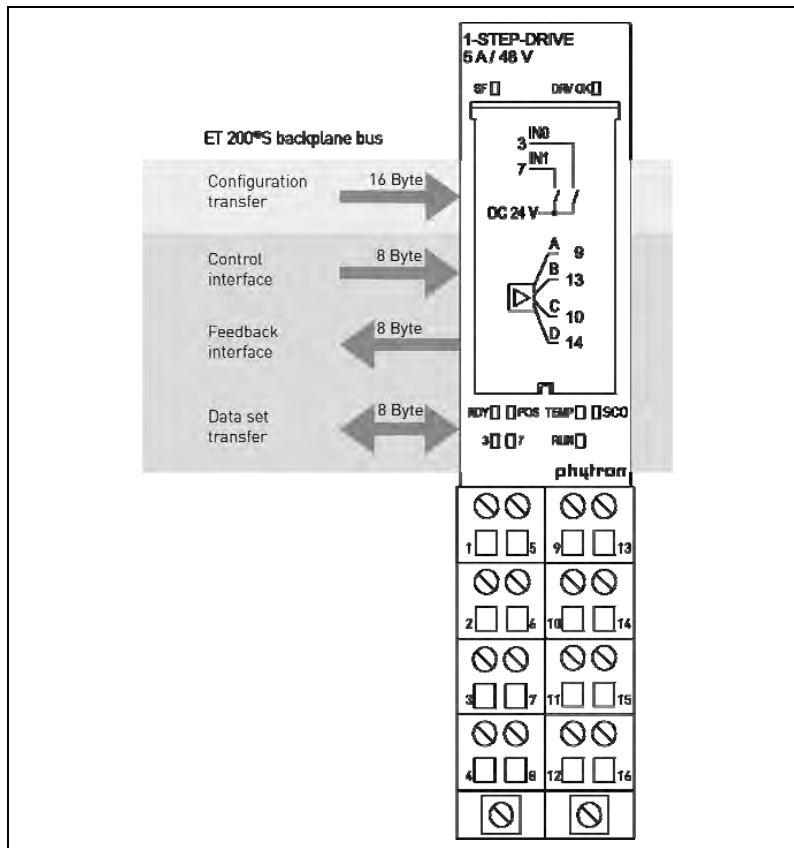


Fig. 2: Data bus

Configuration transfer: Configuration of the module with STEP[®]7: all 1-STEP-DRIVE parameters can be set by mouse click and transmitted (16 Byte). See chap. 6.

Control / Feedback interface: So called parameter assignment jobs can synchronize with the clock of the control and feedback interface to be transmitted and status be read (e.g.: base frequency F_b , multiplier, ramp definition ...). See chap. 7.1 and 7.2.

Data set transfer: If there is no transfer instruction, the complete parameter set of the power stage can be transferred from the user program into the 1-STEP-DRIVE module (e.g.: run current, stop current, step resolution, etc.). Reading of the data set and status inquiry are independent of the transfer job, writing is only possible at motor standstill. See chap. 7.3.

1-STEP-DRIVE Module

1.3 Directives and Standards

CE Mark	With the declaration of conformity and the CE Mark on the product the manufacturer certifies that the product complies with the requirements of the relevant EC directives. The unit, described here, can be used anywhere in the world.
EC Machinery Directive	The drive system, described here, is not a machine in the sense of the EC Machinery Directive (2006/42/EC), but a component of a machine for installation. They have no functional moving parts, but they can be part of a machine or equipment. The conformity of the complete system in accordance with the machine guideline is to be certified by the manufacturer with the CE marking.
EC EMC Directive	<p>The EC Directives on electromagnetic compatibility (89/336/EEC) applies to products that can cause electromagnetic interference or whose operation can be impaired by such interference.</p> <p>The power stage's compliance with the EMC Directive cannot be assessed until it has been installed into a machine or installation. The instructions provided in "Installation" must be complied with to guarantee that the ZMX⁺ is EMC compliant when fitted in the machine or installation and before use of the device is permitted.</p>
Standards for safe operation	<p>EN 60204-1: 1998-11: Electrical equipment of machines, degree of pollution 2 must be observed</p> <p>EN 60529: IP Degree of protection</p>
Standards for observing the EMC limit values	<p>EN 61000-6-2:2005 / EN 61000-6-4:</p> <p>EMC Immunity for industrial environments</p>
Standards for measuring methods of observing EMC limit values	<p>EN 55011 class B: Noise field and voltage measuring</p> <p>EN 61000-4-2...6,11 Emission standard test</p>
Standards for environmental tests	<p>EN 60068-2-6: Vibration, sinusoidal</p> <p>EN 60068-2-27/29: Vibration and shock resistance</p>

4 Technical Data

4.1 Mechanical Data

Type	SIMATIC ET 200 [®] S plastic housing
Dimensions	30 x 81 x 50 mm (W x H x D)
Weight	80 g
Mounting	Pluggable in SIMATIC ET 200 [®] S terminal modules
Mounting position	Optional (power loss see chap. 5.2)

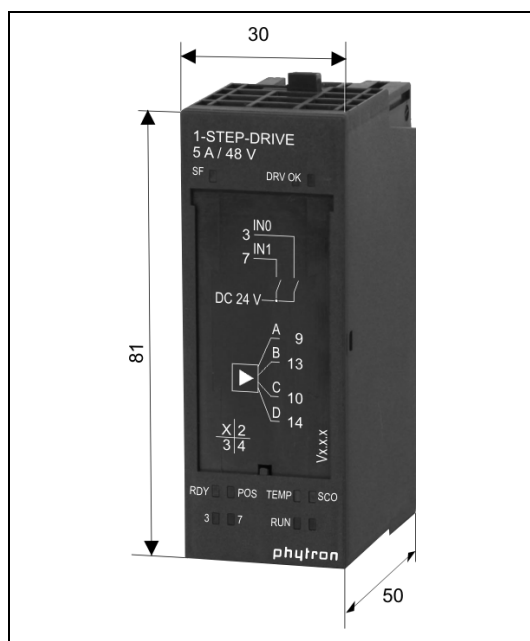


Fig. 5: Dimensions

1-STEP-DRIVE Module

4.2 Features

Features	
Stepper motors	Suitable for bipolar control of 2 phase stepper motors with 4, (6) or 8 lead wiring
Superior main station	SIMATIC ET 200 [®] S
Power supply	24 to 48 V _{DC} Nominal voltage: 48 V _{DC}
Phase current	5 A _{PEAK}
Motor current adjustment	20 mA increments
Step resolutions	Full step, half step, 1/2.5, 1/4, 1/5, 1/8, 1/10, 1/16, 1/20, 1/32, 1/64, 1/128, 1/256, 1/512 micro step
Maximum step frequency	510,000 steps/sec
Physical resolution	Approx. 102,400 positions per revolution (0.0035°/step). An encoder with a counter should be considered for very fine positioning.
Chopper frequency	18, 20, 22 or 25 kHz selectable Patented Phytron chopper technology for a minimal heat loss in the motor and smooth rotation
Current consumption (max.)	3 A _{DC} at 5 A _{PEAK}
Mechanical output power	Up to the 200 W range
Nominal power of the motor voltage supply	150 W
Cable length - motor	Shielded: 50 m max.
Cable length - digital inputs	Shielded: 100 m max.

<p>Diagnostic LEDs</p>	<ul style="list-style-type: none"> • SF (group error) • DRV OK (power stage ready) • RDY (module ready) • POS (traversing job) • 3 (IN0 digital input active) • 7 (IN1 digital input active) • TEMP (over temperature > 85°C) • SCO (over current > 10 A) • RUN (Motor is running)
<p>Operating modes of the controller</p>	<ul style="list-style-type: none"> • Relative Positioning • Move to a reference point • Absolute Positioning • Revolution mode • Reference setting
<p>Security modes</p>	<p>Security modes, such as e.g. Safe Torque Off (STO) from IEC 61508-2 are not directly compatible</p>
<p>Mechanism of the communication via backplane bus</p>	<p>Synchronous: control interface, feedback interface</p> <p>Asynchronous – PLC in STOP mode: Base parameterizing</p> <p>Asynchronous – PLC in RUN mode: Data set transfer</p>
<p>Support of linear and modulo axes (rotary axes)</p>	<p>yes</p>
<p>Hardware error detection</p>	<ul style="list-style-type: none"> • Over current, > 10 A spike at the power stage • Over temperature at the power stage T > 85 °C
<p>Refresh rate</p>	<p>2 ms</p>

1-STEP-DRIVE Module

Interfaces	
Analog outputs	A, B, C, D for a 2 phase stepper motor
Digital inputs	<p>2 configurable digital inputs IN0 and IN1: 0 signal: -30 to 5 V with 2 mA max. (quiescent current) 1 signal: 11 to 30 V with 9 mA typical Input delay: 4 ms</p> <p>IN0: External stop Limit switch towards forward / reverse External release of momentum</p> <p>IN1: Reference switch and also limit switches towards forwards / reverse Limit switch configurable to open / close</p>
Backplane bus and module supply	Backplane bus of the ET 200 [®] S Module supply via ET 200 [®] S power module
Communication and Programming	
Programming	via STEP [®] 7
Control interface (synchronous)	<p>Parameter assignments:</p> <ul style="list-style-type: none"> • Base frequency F_b • Multiplier i (ramp) • Multiplier n (start-stop) <p>Positioning:</p> <ul style="list-style-type: none"> • Move to a reference point • Set home position • Relative incremental mode (relative positioning) • Absolute incremental mode (absolute positioning) • Revolution mode • Reference setting

<p>Feedback interface (synchronous)</p>	<p>Configurable:</p> <ul style="list-style-type: none"> • Residual distance • Absolute Positioning • Velocity <p>Also included in the feedback:</p> <ul style="list-style-type: none"> • Position reached • Parameterization error • Power stage error • Limit switch causes a stop
<p>Data set transfer to the 1-STEP-DRIVE (asynchronous while CPU RUN)</p>	<p>Parameterizing the 1-STEP-DRIVE power stage:</p> <ul style="list-style-type: none"> • Step resolution (1/1, 1/2,...1/512) • Preferred direction of rotation • Run current (20 mA increments) • Stop current(20 mA increments) • Boost current(20 mA increments) • Current delay time 1...1000 ms • Chopper frequency 18...25 kHz • Switching frequency overdrive 1... 40 kHz • ODIS behavior
<p>Data set transfer to the 1-STEP-DRIVE (asynchronous)</p>	<p>Diagnostics</p> <p>Feedback of the following driver parameters(asynchronous) to the main station</p> <ul style="list-style-type: none"> • Power stage parameters • Home position • Error (short circuit, over temperature, parameterizing error)

1-STEP-DRIVE Module

5 Installation

Following modules/components are necessary for the connection of the 1-STEP-DRIVE:

- ET 200[®]S station in a S7 system with DP-Master
- 24–48 V_{DC} supply
- Applicable terminal modules:

Terminal modules	Order number	Terminals
TM-E30S46-A1	6ES7193-4CF40-0AA0	screw with AUX1
TM-E30C46-A1	6ES7193-4CF50-0AA0	spring with AUX1
TM-E30S44-01	6ES7193-4CG20-0AA0	screw without AUX1
TM-E30C44-01	6ES7193-4CG30-0AA0	spring without AUX1

- Applicable power modules:

Power module for ET 200 [®] S	Order number
DC 24V-48V with diagnostics	6ES7138-4CA50-0AB0 SIMATIC DP
DC 24V-48V, AC 24-230V with diagnostic and protection	6ES7138-4CB11-0AB0 SIMATIC DP

- 1-STEP-DRIVE-5A–48V
- 2 phase stepper motor up to 5 A_{PEAK}
- Shield contact element
- The necessary wiring material

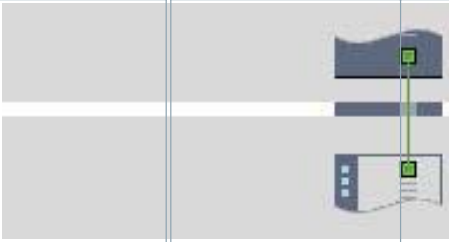
C.3 Complete program

Totally Integrated Automation Portal			
Pitch_system			
Project			
Name:	Pitch_system	Creation time:	3/3/2015 2:40:38 PM
Last change	5/19/2015 6:29:06 PM	Author:	student
Last modified by:	student	Version:	
Comment:			
Operating system			
Name	Description		
Operating system	Microsoft Windows 7 Professional		
Version of the operating system	6.1.7601.65536		
Operating system service pack	Service Pack 1		
Version of the Internet Explorer	9.10.9200.16660		
Computer name	STUDENT-PC		
User name	student-PC\student		
Installation path of the TIA Portal	C:\Program Files\Siemens\Automation\Portal V12		
Components			
Name	Version	Release	
SIMATIC S7 PLCSIM - S7 PLCSIM Single SetupPackage (S7_PLCSIM_V12)	V12.0	V12.00.00.00_33.29.00.01	
S7 PLCSIM Single SetupPackage - SIMATIC S7 PLCSIM V12 V12.0 (S7_PLCSIM_V12)	V12.0	V12.00.00.00_34.33.00.01	
Compatibility Check Tool TIA - TIACOMP CHECK Single SetupPackage V11.0 + SP1 (TIACOMP CHECK)	V11.0 + SP1	K11.00.02.00_01.01.00.02	
Totally Integrated Automation Portal V12 - TIA Portal Single SetupPackage V12.0 (TIAP12)	V12.0	V12.00.00.00_33.29.00.01	
TIA Portal Single SetupPackage - HM All Editions Single SetupPackage V12.0 (TIAP12)	V12.0	V12.00.00.00_33.29.00.01	
TIA Portal Single SetupPackage - HM NoBasic Single SetupPackage V12.0 (TIAP12)	V12.0	V12.00.00.00_33.29.00.01	
TIA Portal Single SetupPackage - Hardware Support Base Package 0 V12.0 (TIAP12)	V12.0	V12.00.00.00_27.01.00.01	
TIA Portal Single SetupPackage - STEP 7 Single SetupPackage V12.0 (TIAP12)	V12.0	V12.00.00.00_33.29.00.01	
TIA Portal Single SetupPackage - Hardware Support Base Package 02 V12.0 (TIAP12)	V12.0	V12.00.00.00_27.01.00.01	
TIA Portal Single SetupPackage - Hardware Support Base Package 03 V12.0 (TIAP12)	V12.0	V12.00.00.00_27.01.00.01	
TIA Portal Single SetupPackage - Support Base Package TO-01 V12.0 (TIAP12)	V12.0	V12.00.00.00_27.01.00.01	
TIA Portal Single SetupPackage - Support Base Package TO-02 V12.0 (TIAP12)	V12.0	V12.00.00.00_27.01.00.01	
TIA Portal Single SetupPackage - Hardware Support Base Package WCF-01 V12.0 (TIAP12)	V12.0	V12.00.00.00_27.01.00.01	
TIA Portal Single SetupPackage - TIACOMP CHECK Single SetupPackage V12.0 (TIAP12)	V12.0	V12.00.00.00_33.29.00.01	
TIA Portal Single SetupPackage - TIA Tour Single SetupPackage V12.0 (TIAP12)	V12.0	V12.00.00.00_33.29.00.01	
TIA Portal Single SetupPackage - Simatic Single SetupPackage V12.0 (TIAP12)	V12.0	V12.00.00.00_33.29.00.01	
TIA Portal Single SetupPackage - WinCC Single SetupPackage V12.0 (TIAP12)	V12.0	V12.00.00.00_33.29.00.01	

Totally Integrated Automation Portal		
Name	Version	Release
SIMATIC HMI License Manager Panel Plugin	11.0.2.0	K11.0.2.0_33.25.0.4
Automation Access Control Component	4.0	K04.00.01.00_01.01.00.01
SIMATIC Colour Editor	5.1.15	K05.01.15.02_01.01.00.01
SIMATIC HMIProvider	7.0	K07.00.01.00_01.01.00.01
License Logon Interface	4.0	K04.00.03.00_01.01.00.02
SIEMENS OPC	3.8	K03.08.00.03_01.02.00.01
SIMATIC WinCC OPC Alarm & Events Server	3.8	K03.08.00.03_01.02.00.01
SIMATIC WinCC OPC Data Access Server	3.8	K03.08.00.03_01.02.00.01
SIMATIC WinCC OPC Historical Data Access Server	3.8	K03.08.00.03_01.02.00.01
SIMATIC WinCC OPC XML Client	3.8	K03.08.00.03_01.02.00.01
PCS7 Common Classes	7.3	V07.03.00.00_01.01.00.01
PlcSimPlus32	1.0	V01.00.00.00_01.01.00.01
SIMATIC HMI ProSave	10.0.0.0	V10.0.0.0_33.25.0.4
SIMATIC HMI Symbol Library	12.0	V12.0.0.0_33.25.0.4
SIMATIC HMI Touch Input	6.2.2.1	K6.2.2.1_1.2.0.5
SIMATIC Runtime Interfaces	2.1	K02.01.00.01_01.03.00.01
SIMATIC Version View	1.7.5.0	K1.7.5.0_1.2.0.1
SIMATIC Common Services	5.3.12.0	K5.3.12.0_2.2.0.1
SIMATIC Device Drivers	8.3	K08.03.01.00_01.02.00.01
SIMATIC Event Database	5.5.3.0	05.05.03.00_01.11.00.01
SIMATIC GRAPH-Visualisierung	5.2.2.0	K5.2.2.0_1.2.0.1
SIMATIC GSD CONTROL	3.5.3.0	K3.5.3.0_1.1.0.1
SIMATIC GSD Interpreter	2.3.2.0	K2.3.2.0_11.1.0.1
SIMATIC Interface Editor	5.4.13.0	K5.4.13.0_4.4.0.1
SIMATIC Extended Interfaces	5.4.4.0	K5.4.4.0_1.2.0.1
SIMATIC LanguageSupportTool	5.8.0.0	V5.8.0.0_2.2.0.1
SIMATIC Condition Editor	5.4.4.0	K5.4.4.0_2.1.0.1
SIMATIC NCM	05.05.00.00	V5.5.0.0_25.5.0.1
SIMATIC Process Diagnosis Base	5.3.9.0	K05.03.09.00_01.02.00.01
SIMATIC Process Diagnosis Database	5.3.6.1	K05.03.06.01_01.01.00.01
SIMATIC Runtime Manager	8.0	T8.0.0.0_01.36.0.2
SIMATIC DIAGNOSTIC REPEATER GUI CTRL	5.2.1.0	K5.2.1.0_1.1.0.1
SIMATIC Grid Control	2.5.4.0	K2.5.4.0_1.1.0.1
SIMATIC S7-Status-OCX	5.3.8.0	K5.3.8.0_1.3.0.1
SIMATIC Technological Parameter Assignment	5.3.8.0	K5.3.8.0_1.3.0.1
SIMATIC X-Ref Control	5.2.5.0	K5.2.5.0_4.2.0.1
SIMATIC Asset Manager	2.2	K02.02.01.00_01.14.00.01
SIMATIC SCL Compiler	5.3.6.0	K05.03.06.00_01.03.00.01
SeCon	2.0	K02.00.00.01_01.16.00.01
SIMATIC Security Control	1.1	K01.01.01.00_01.05.00.01
SIMOTION OPC File Manager	1.1.0.0	V01.01.00.00_02.00.02.00
SIMATIC Station Observer	7.1	K07.01.01.01_01.01.00.01
SIMATIC SCS	7.1	K07.01.05.00_01.27.00.01
SIMATIC WinCC Common Archiving	7.1	K07.01.02.00_01.43.00.01
WinCC Runtime Advanced Simulator	12.0.0.0	V12.0.0.0_33.25.0.4
Products		
Name	Version	Release
SIMATIC S7 PLCSIM V12	12.00.0000	V12.00.00.00_34.33.00.01
SIMATIC S7 PLCSIM	V12.0	V12.00.00.00_33.39.00.01
SIMATIC STEP 7 Professional	V11.0 + SP2	K11.00.02.00_02.08.00.01
SIMATIC STEP 7 Professional	V12.0	V12.00.00.00_33.29.00.01
SIMATIC WinCC Basic	V12.0	V12.00.00.00_33.29.00.01

Totally Integrated Automation Portal		
Name	Version	Release
FORDM		
Automation License Manager	V5.2 + Upd1	K05.02.00.01_01.02.00.02
S7-PLCSIM	V5.4 + SP5 + Upd2	K05.04.05.02_01.01.00.02
SIMATIC ProSave	V10.0	V10.0.0.0_33.25.0.4
S7-GRAPH Professional 2010	V5.3 + SP6	K5.3.6.0_7.2.0.1
S7-PCT	V2.1	V02.01.00.00_01.29.00.01
S7-SCL Professional 2010	V5.3 + SP5 + HF1	K05.03.05.01_01.02.00.02
SIMATIC NET PC Software	V8.0 + SP1	V08.00.01.00_41.60.00.09
STEP 7	V5.5	V5.5.0.0_25.6.0.1
WinCC Runtime	V7.0 + SP2	K07.00.02.00_01.37.00.03
WinCC Configuration	V7.0 + SP2	K07.00.02.00_01.37.00.03
WinCC OPC Server	V3.8 + HF3	K03.08.00.03_01.02.00.01
SIMATIC WinCC Smart Tools	V7.0 + SP2	K07.00.02.00_01.37.00.03

Totally Integrated Automation Portal			
Pitch_system			
PLC_1 [IM151-8 CPU]			
PLC_1			
General			
Name	PLC_1	Author	student
Comment		Rack	0
Slot	2		
General\Catalog information			
Short designation	IM 151-8 PN/DP CPU	Description	Work memory 128KB; 0.3ms/1000 instructions; PROFINET interface; S7 communication (loadable FBs/FCs); PROFINET IO controller; supports RT/IRT; 3 ports; PROFINET CBA; PROFINET CBA Proxy; transport protocol TCP/IP, UDP and ISO-on-TCP; data record routing; firmware V2.7; expansion with maximum 63 modules of ET 200S range; also available as SIPLUS module with order number 6AG1 151-8AB00-4AB0.
Order number	6ES7 151-8AB00-0AB0	Firmware version	V2.7
General\Identification & Maintenance			
Plant designation		Location identifier	
PROFINET interface [X1]\General			
Name	PROFINET interface_1	Author	student
Comment			
PROFINET interface [X1]\General\Catalog information			
Short designation	PROFINET interface	Description	
Order number		Firmware version	
PROFINET interface [X1]\Ethernet addresses\Interface networked with			
Subnet:	PN/IE_1		
PROFINET interface [X1]\Ethernet addresses\IP protocol			
IP address:	192.168.0.1	Subnet mask:	255.255.255.0
Use router	False		
PROFINET interface [X1]\Ethernet addresses\PROFINET			
PROFINET device name	plc_1	Converted name:	plcxb1d0ed
Device number:	0		
PROFINET interface [X1]\Time synchronization\NTP mode			
Enable time synchronization via NTP server	Enable time synchronization via NTP server		IP addresses
Server 1	0.0.0.0	Server 2	0.0.0.0
Server 3	0.0.0.0	Server 4	0.0.0.0
Update interval	10s		
PROFINET interface [X1]\Advanced options\Interface options			
Call the user program if communication errors occur	False	Support device replacement without exchangeable medium	True
PROFINET interface [X1]\Advanced options\Real time settings\IO communication			
Send clock:	1.000		
PROFINET interface [X1]\Advanced options\Real time settings\Synchronization			
Sync domain:	Sync-Domain_1	Synchronization role:	Unsynchronized
RT class:	RT,IRT		

Totally Integrated Automation Portal								
PROFINET interface [X1]\Advanced options\Real time settings\Real time options								
Calculated bandwidth for cyclic IO data:	0.000							
PROFINET interface [X1]\Advanced options\Port [X1 P1]\General								
Rack	1	Name	Port_1					
Comment								
PROFINET interface [X1]\Advanced options\Port [X1 P1]\Port interconnection\Local port:								
Local port:	PLC_1\PROFINET interface_1 [X1]\Port_1 [X1 P1]	Medium:	Copper					
Cable name:	---							
								
PROFINET interface [X1]\Advanced options\Port [X1 P1]\Port interconnection\Partner port:								
Alternative partners	False	Partner port:	Any partner					
Medium:		Cable length:						
		Signal delay [µs]:						
PROFINET interface [X1]\Advanced options\Port [X1 P1]\Port options\Activate								
Activate this port for use.	True							
PROFINET interface [X1]\Advanced options\Port [X1 P1]\Port options\Connection								
Transmission rate / duplex:	Automatic	Monitor	False					
Enable autonegotiation	True							
PROFINET interface [X1]\Advanced options\Port [X1 P1]\Port options\Boundaries								
End of detection of accessible devices	False	End of topology discovery	False					
End of the sync domain	False							
PROFINET interface [X1]\Advanced options\Port [X1 P1]\Diagnostics addresses\Diagnostics addresses								
Start address	2046							
PROFINET interface [X1]\Diagnostics addresses\Diagnostics addresses								
Start address	2047							
IO address overview								
outputs	true							
inputs	true							
outputs	true							
Type	AddrFrom	AddrTo	Module	PIP	DP	PN	Rack	Slot
true	true	true	true	true	true	true	true	true
Startup								
Startup if preset configuration does not match actual configuration	True							
Startup after POWER ON	Warm restart							
Startup\Monitoring time for								
Ready message from modules	100x 100 ms		Parameter transfer to modules					
			100x 100 ms					

Totally Integrated Automation Portal			
Cycle			
Cycle monitoring time	150ms	Cycle load due to communication	20%
Size of the process image input:	128	Size of the process image output:	128
OB85 call if I/O access error occurs	No OB85 call		
Clock memory			
Memory byte	0		
Clock memory\Clock memory			
Clock memory	False		
Retentive memory\			
Number of memory bytes starting at MB 0	16	Number of S7 timers starting at T 0	0
Number of S7 counters starting at C 0	8		
\Time-of-day interrupts\			
OB number	Priority	Activated	Interval
OB 10:	2	False	None
			Start time
			1994-01-01 00:00:00.000
\Time-delay interrupts\			
OB number	Priority	Process image partition(s)	
OB 20:	3	None	
\Cyclic interrupts\			
OB number	Priority	Interval	
OB 35:	12	100	ms
\Hardware interrupts\			
OB number	Priority		
OB 40:	16		
\Interrupts for DPV1\			
OB number	Priority		
OB 55:	2		
OB 56:	2		
OB 57:	2		
\Asynchronous error interrupts\			
OB number	Priority		
OB 82:	26		
OB 83:	26		
OB 85:	26		
OB 86:	26		
OB 87:	26		
Diagnostics system			
Report cause of STOP	True	Number of alarms in the diagnostics buffer	500
Anchor (System diagnostics)			
The feature Report system error is not available			
Time of day			
Correction factor	0ms		
Operating mode			
	Test mode	Max. cycle time for test functions	5ms

Totally Integrated Automation Portal			
Protection\			
Level of protection	No protection		
Protection\Password for read/write access			
Password	••••••••	Confirm password	••••••••
System diagnostics\General			
Activate system diagnostics for this PLC	False		
Parameter			
Interference frequency suppression	50Hz	Bus length	<= 1 m
Parameter\Reference junctions			
Reference junctions	False	Slot number	0
Channel number	0		
Web server			
Activate web server on this module	False		
Web server\Automatic update			
Enable	False	Update interval	0s
Web server\ParameterWebServerLanguagesMenu			
ParameterWebServerLanguagesMenu was not filled by one ACF			
Web server\ParameterWebServerDisplayClassOfMessagesMenu			
ParameterWebServerDisplayClassOfMessagesMenu was not filled by one ACF			
Anchor (ParameterCommunicationMenu)			
The TreeNode ParameterCommunicationMenu was not filled by some ACF			
Anchor (AddressesOverviewMenu)			
The AddressesOverviewMenu was not filled by some ACF			
Web server\Languages			
Web server language	Active	Assign project language	
German	False		
English	False		
French	False		
Spanish	False		
Italian	False		
Japanese	False		
Chinese (simplified)	False		

Totally Integrated Automation Portal		
Web server\Display class of the alarm		
Display class	Active	
0	True	
1	True	
2	True	
3	True	
4	True	
5	True	
6	True	
7	True	
8	True	
9	True	
10	True	
11	True	
12	True	
13	True	
14	True	
15	True	
16	True	

Pitch_system / PLC_1 [IM151-8 CPU] / Program blocks

CounterClockwise_dir [FC1]

CounterClockwise_dir Properties

General

Name	CounterClockwise_dir	Number	1	Type	FC
Language	STL				

Information

Title		Author		Comment	
Family		Version	0.1	User-defined ID	

Name	Data type	Offset	Comment
▼ Input			
Pulses	DInt		
Output			
InOut			
Temp			
▼ Return			
CounterClockwise_dir	Void		

Network 1: Start moving in Backward/Counter-clockwise direction

```

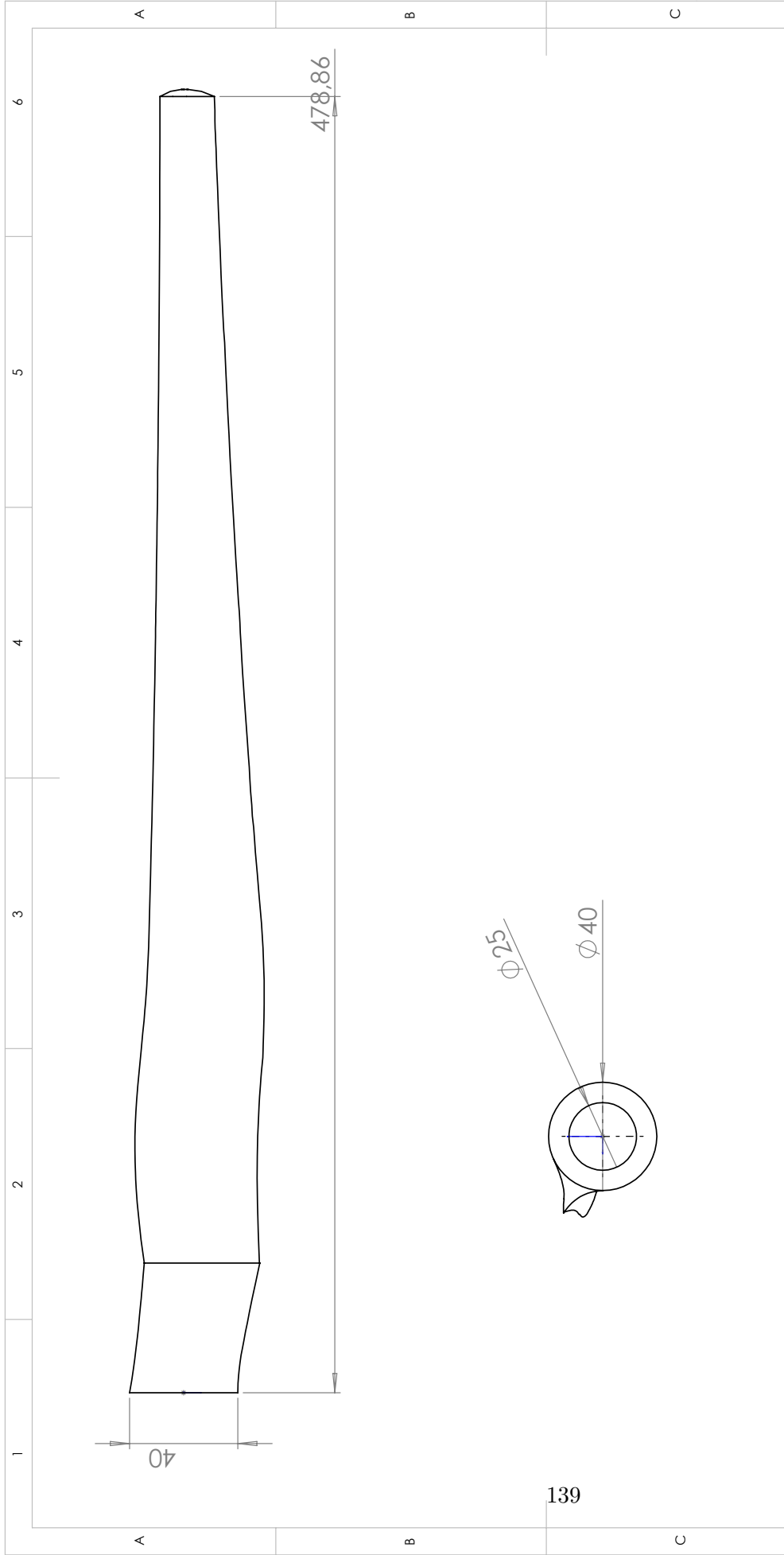
0001      L      "Tag_2"                //Ref position 0 Number of pulses
0002      T      "Data_Block_1".DB_VAR
0003      L      1
0004
0005      T      %DB1.DBB0
0006
0007      L      0                      //Delete limit switch etc.
0008      T      %DB1.DBB5
0009      T      %DB1.DBW6
0010
0011      SET
0012
0013      R      %DB1.DBX5.0            //Set Soft-Limit - Backward direction
0014      R      %DB1.DBX5.1            //Set Soft-Limit Plus - Forward direction
0015
0016      S      %DB1.DBX5.2            //Set pulse enable DRV_EN
0017      R      %DB1.DBX4.0            //Set 'Relative incremental' operation mode
0018      R      %DB1.DBX4.1            //Set 'Relative incremental' operation mode
0019      R      %DB1.DBX4.2            //Set 'Relative incremental' operation mode
0020      R      %DB1.DBX4.3            //Reserve bit = 0
0021      R      %DB1.DBX4.5            //Start Clockwise delete DIR_P
0022      R      %DB1.DBX4.6            //delete STOP
0023      R      %DB1.DBX4.7            //delete reduction factor R
0024
0025      L      "Data_Block_1".DB_VAR //Write 8 Byte to the 1-STEP-DRIVE
0026      T      "DW1_OUT":P
0027      L      "Data_Block_1".DB_VAR_1

```

Totally Integrated Automation Portal			
0028	T	"DW2_OUT":P	
0029			
0030	L	"DW1_IN":P	//Read 8 Byte from 1-STEP-DRIVE
0031	T	"Data_Block_1".DB_VAR_2	
0032	L	"DW2_IN":P	
0033	T	"Data_Block_1".DB_VAR_3	
0034			
0035	A	"Start"	//Detect flank of the start impulse and start
	DIR_P		
0036	AN	%DB1.DBX12.0	//Set if STS_JOB is deleted
0037	S	%DB1.DBX4.4	//Start Counterclockwise delete DIR_M
0038			
0039	A	%DB1.DBX12.0	//Wait on STS_JOB
0040	R	%DB1.DBX4.4	//Reset Start DIR_M, the traversing starts
0041	R	"Start"	//Delete start impulse
0042			
0043			
0044			
0045			
0046			
0047			
Symbol	Address	Type	Comment
"Data_Block_1"	%DB1	Block_DB	
"Data_Block_1".DB_VAR	%DB1.DBDO	DWord	
1	1	Int	
%DB1.DBB0	%DB1.DBB0	Byte	
0	0	Int	
%DB1.DBB5	%DB1.DBB5	Byte	
%DB1.DBW6	%DB1.DBW6	Word	
%DB1.DBX5.0	%DB1.DBX5.0	Bool	
%DB1.DBX5.1	%DB1.DBX5.1	Bool	
%DB1.DBX5.2	%DB1.DBX5.2	Bool	
%DB1.DBX4.0	%DB1.DBX4.0	Bool	
%DB1.DBX4.1	%DB1.DBX4.1	Bool	
%DB1.DBX4.2	%DB1.DBX4.2	Bool	
%DB1.DBX4.3	%DB1.DBX4.3	Bool	
%DB1.DBX4.6	%DB1.DBX4.6	Bool	
%DB1.DBX4.7	%DB1.DBX4.7	Bool	
"DW1_OUT":P	%QD400:P	DWord	
"Data_Block_1".DB_VAR_1	%DB1.DBD4	DWord	
"DW2_OUT":P	%QD404:P	DWord	
"DW1_IN":P	%ID400:P	DWord	
"Data_Block_1".DB_VAR_2	%DB1.DBD8	DWord	
"DW2_IN":P	%ID404:P	DWord	
"Data_Block_1".DB_VAR_3	%DB1.DBD12	DWord	
"Start"	%M30.0	Bool	
%DB1.DBX12.0	%DB1.DBX12.0	Bool	
%DB1.DBX4.5	%DB1.DBX4.5	Bool	
%DB1.DBX4.4	%DB1.DBX4.4	Bool	
"Tag_2"	%MD4	DInt	

Appendix D

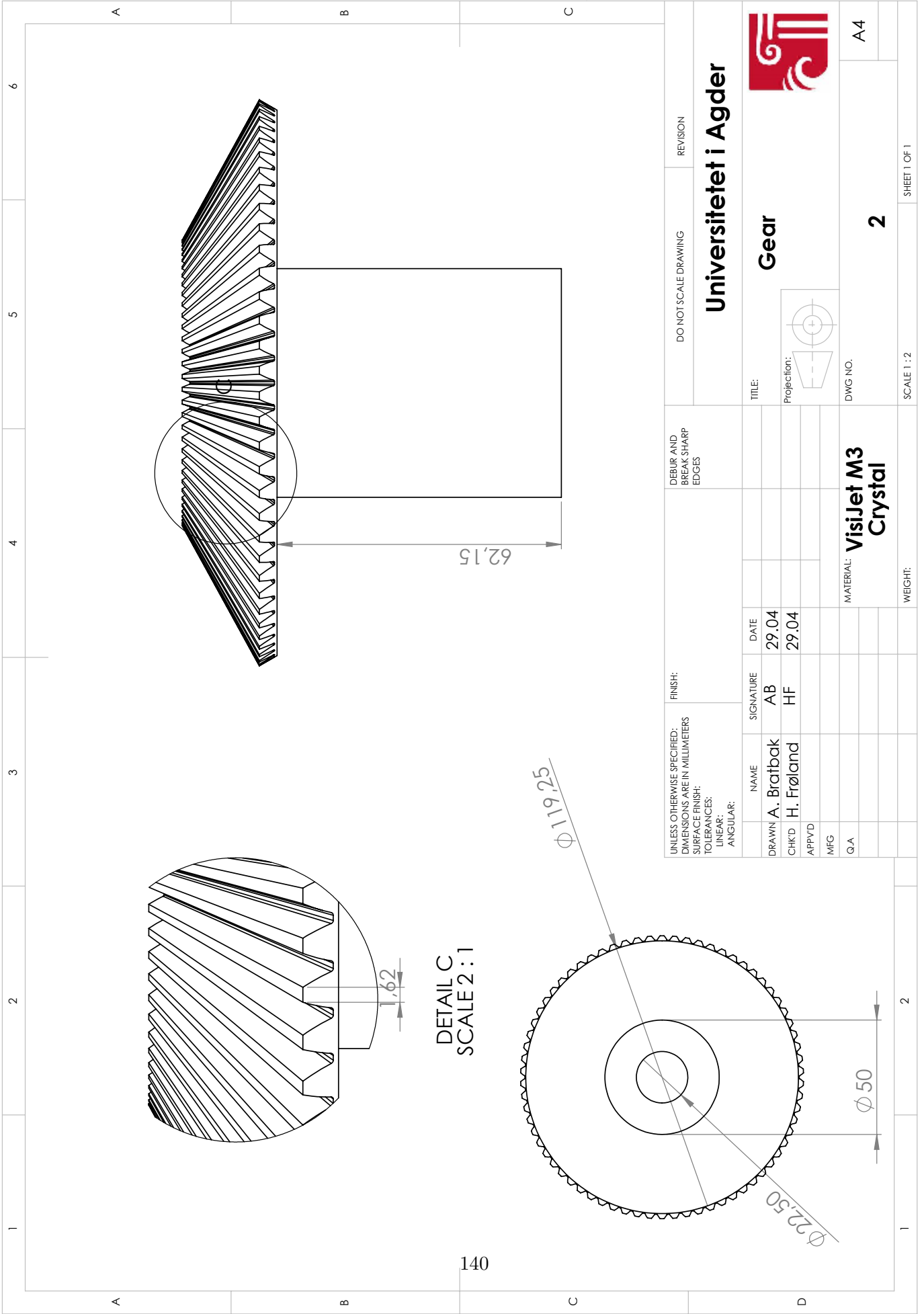
Technical Drawings



UNLESS OTHERWISE SPECIFIED: DIMENSIONS ARE IN MILLIMETERS		FINISH:		DEBUR AND BREAK SHARP EDGES		DO NOT SCALE DRAWING		REVISION	
SURFACE FINISH:									
TOLERANCES:									
LINEAR:									
ANGULAR:									
DRAWN	A. Bratbak	SIGNATURE	AB	DATE	29.04	TITLE:		Blade	
CHK'D	H. Frøland	SIGNATURE	HF	DATE	29.04	Projection:			
APP'VD						DWG NO.		1	
MFG						MATERIAL:		VisiJet M3 Crystal	
Q.A.						WEIGHT:		A4	
						SCALE:1:2		SHEET 1 OF 1	




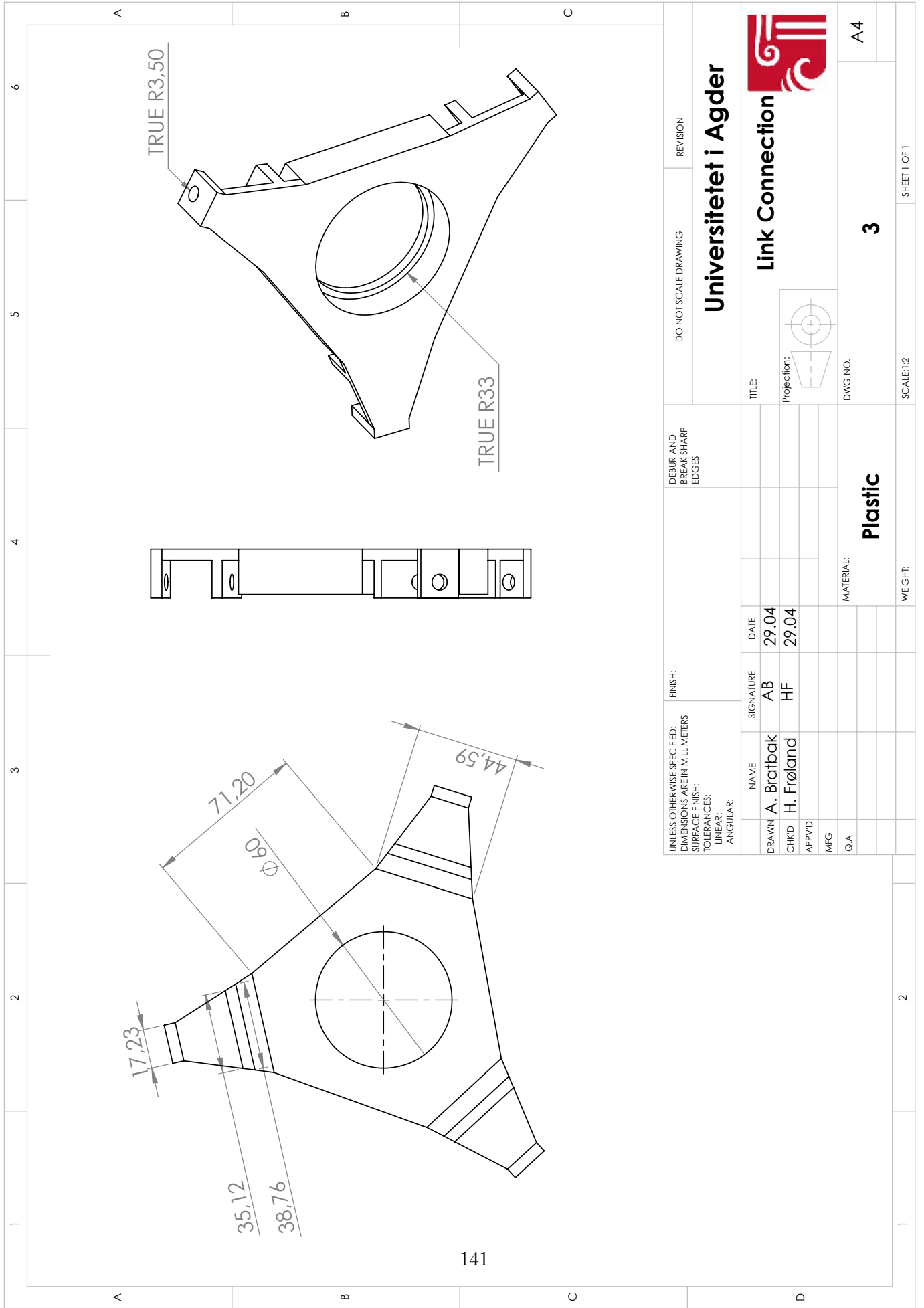
Universitetet i Agder





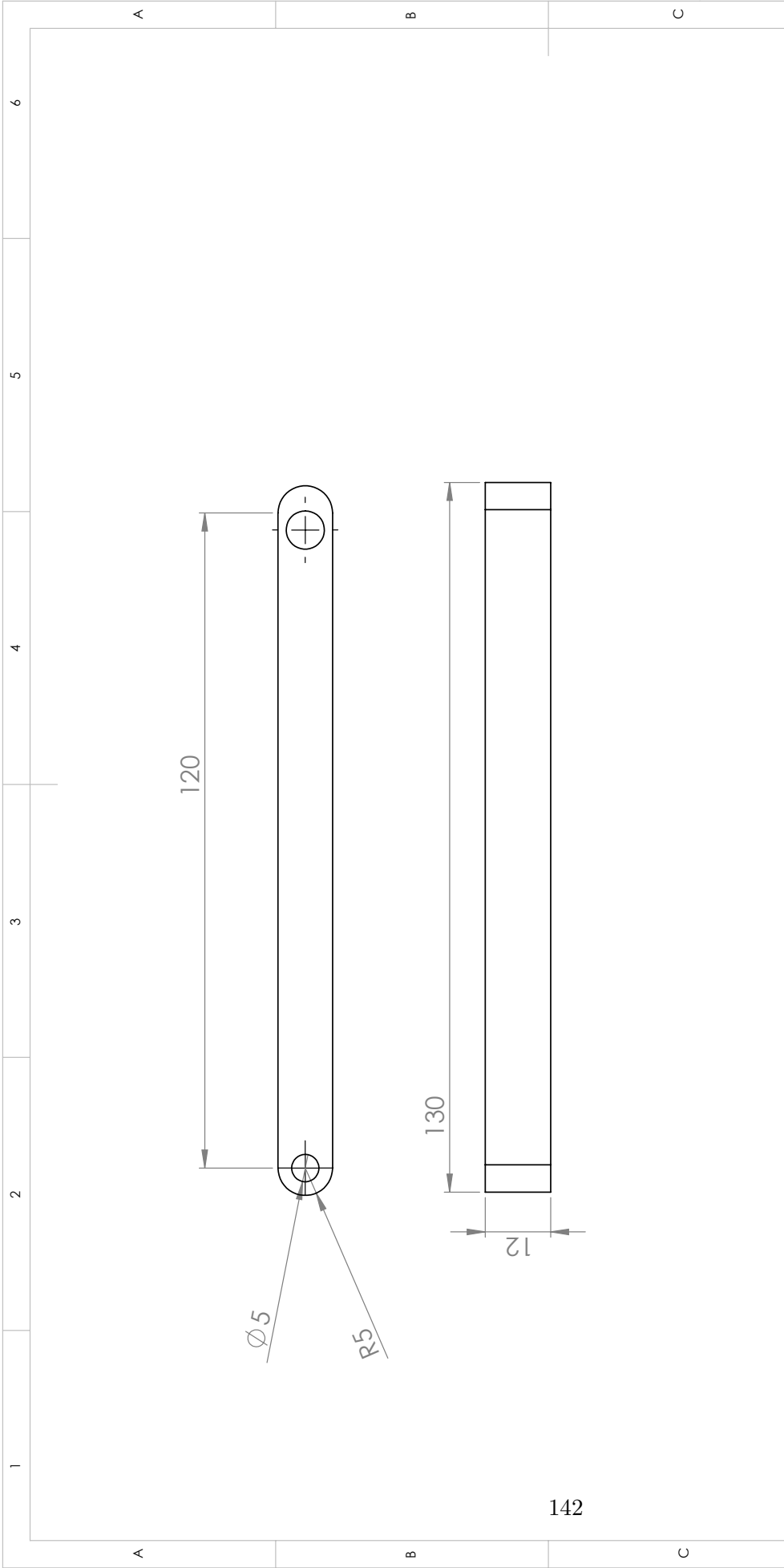
DETAIL C
SCALE 2 : 1

140

UNLESS OTHERWISE SPECIFIED: DIMENSIONS ARE IN MILLIMETERS		FINISH:		DEBUR AND BREAK SHARP EDGES		DO NOT SCALE DRAWING		REVISION	
SURFACE FINISH:		SIGNATURE		DATE		Universitetet i Agder  Gear TITLE:			
TOLERANCES:		AB		29.04					
LINEAR:		HF		29.04					
ANGULAR:									
DRAWN	NAME	MATERIAL: VisiJet M3 Crystal		DWG NO. 2		A4			
CHK'D	A. Bratbak	WEIGHT:		SCALE 1 : 2		SHEET 1 OF 1			
APP'VD	H. Frøland								
MFG									
Q.A.									



UNLESS OTHERWISE SPECIFIED: DIMENSIONS ARE IN MILLIMETERS		FINISH:		DEBUR AND BREAK SHARP EDGES		DO NOT SCALE DRAWING		REVISION		
SURFACE FINISH:		SIGNATURE				TITLE:				
TOLERANCES:		NAME	SIGNATURE	DATE			Universitetet i Agder			
LINEAR:		A. Bratbak	AB	29.04			Link Connection			
ANGULAR:		H. Frøland	HF	29.04					A4	
		APPV'D							3	
		MFG					Projection:		DWG NO.	
		Q.A.					MATERIAL:		3	
							Plastic		SCALE:1:2	
							WEIGHT:		SHEET 1 OF 1	
									1	
									2	



142

UNLESS OTHERWISE SPECIFIED: DIMENSIONS ARE IN MILLIMETERS		FINISH:		DEBUR AND BREAK SHARP EDGES		DO NOT SCALE DRAWING		REVISION	
SURFACE FINISH:		SIGNATURE				TITLE:		Universitetet i Agder	
TOLERANCES:		DATE				Projection:		Link Part 1	
LINEAR:		29.04				DWG NO.		4	
ANGULAR:		29.04				MATERIAL:		VisiJet M3 Crystal	
DRAWN	A. Bratbak	AB							
CHK'D	H. Frøland	HF							
APP'VD									
MFG									
Q.A.									
						WEIGHT:		SHEET 1 OF 1	
								A4	



1

2

6

5

4

3

2

1

A

B

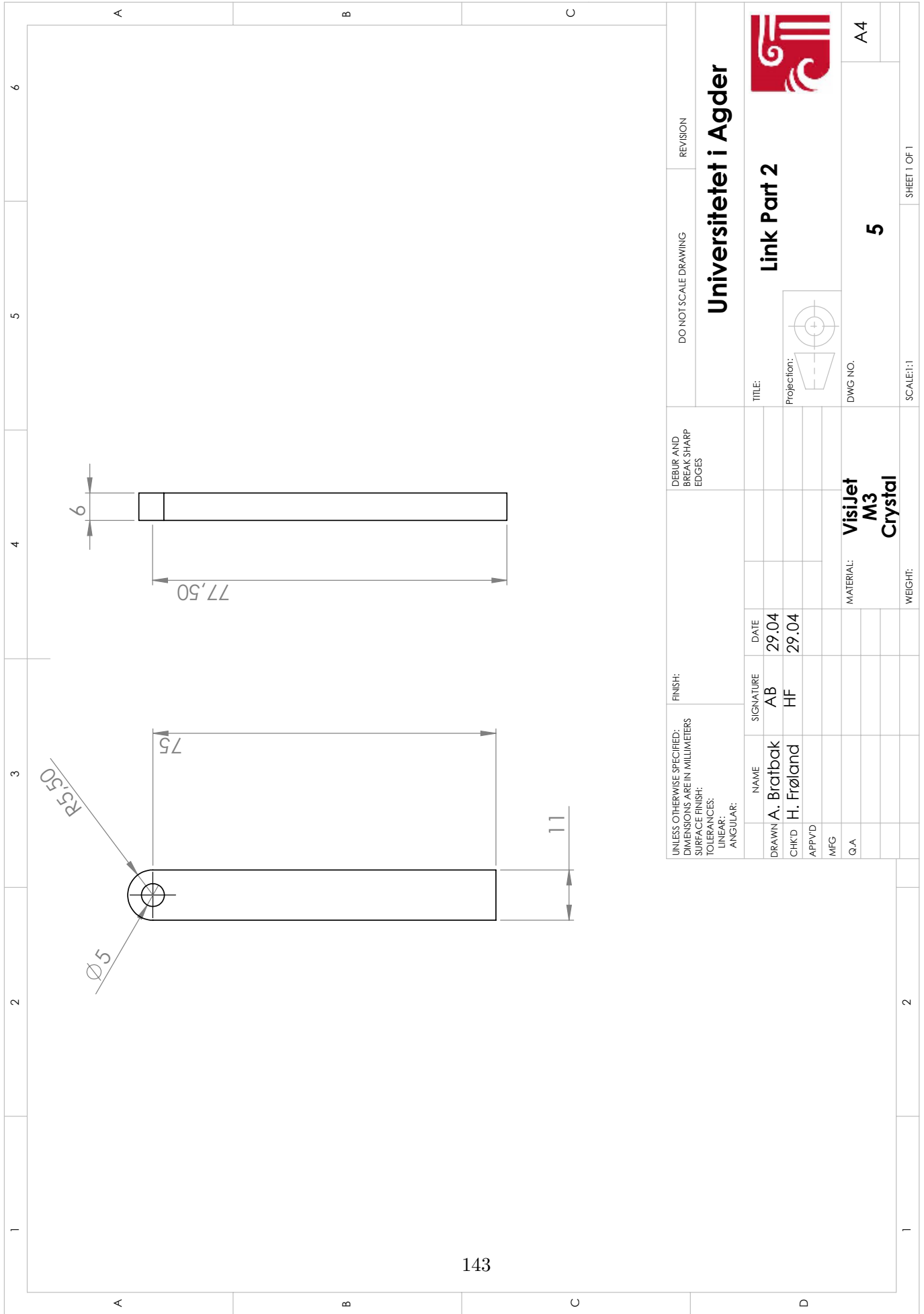
C

A

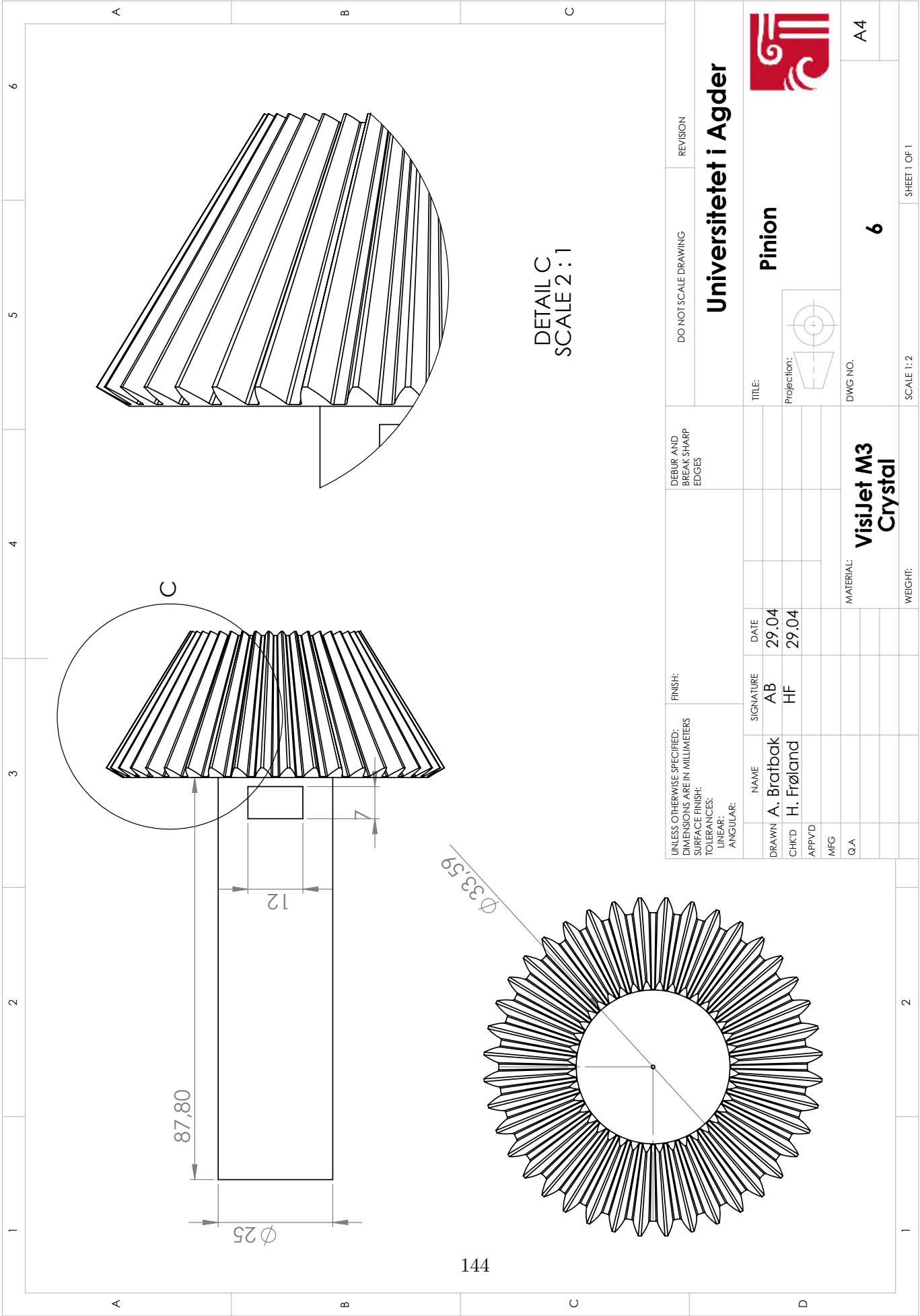
B

C

D

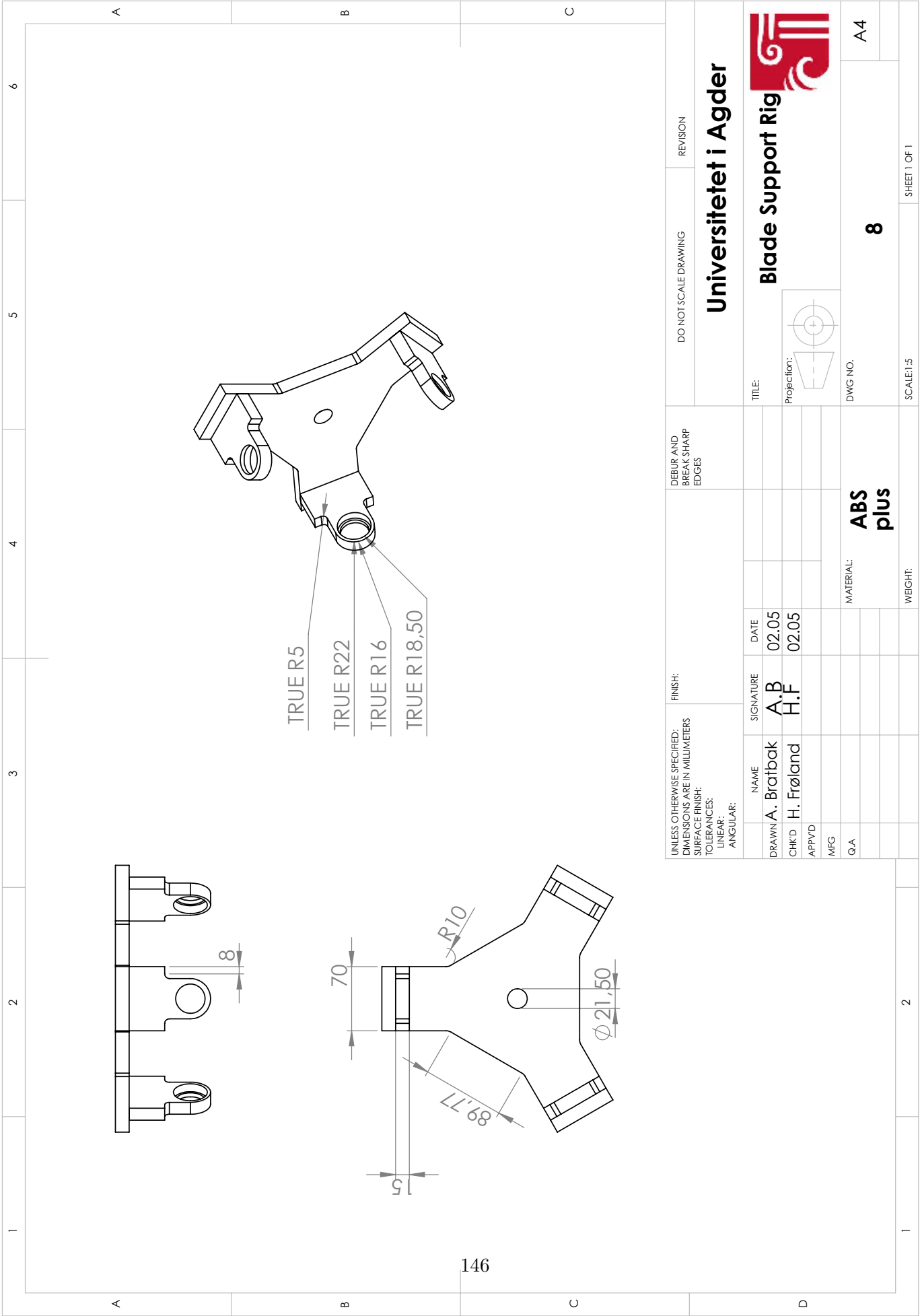


UNLESS OTHERWISE SPECIFIED: DIMENSIONS ARE IN MILLIMETERS		FINISH:		DEBUR AND BREAK SHARP EDGES		DO NOT SCALE DRAWING		REVISION		
SURFACE FINISH:		SIGNATURE				TITLE:		Universitetet i Agder		
TOLERANCES:		NAME	SIGNATURE	DATE			Link Part 2		A4	
LINEAR:		DRAWN	AB	29.04			Projection:		5	
ANGULAR:		CHK'D	HF	29.04			DWG NO.		5	
		APP'VD							SCALE: 1	
		MFG							SHEET 1 OF 1	
		Q.A.					MATERIAL:		A4	
							VisiJet M3 Crystal		5	
							WEIGHT:		SHEET 1 OF 1	



UNLESS OTHERWISE SPECIFIED: DIMENSIONS ARE IN MILLIMETERS		FINISH:		DEBUR AND BREAK SHARP EDGES		DO NOT SCALE DRAWING		REVISION	
SURFACE FINISH:		SIGNATURE				TITLE:		Universitetet i Agder	
TOLERANCES:		DATE				Projection:		Pinion	
LINEAR:		29.04				DWG NO.		6	
ANGULAR:		29.04				MATERIAL:		VisiJet M3 Crystal	
DRAWN		NAME				WEIGHT:		A4	
CHK'D		A. Bratbak				SCALE 1:2		SHEET 1 OF 1	
APP'VD		H. Frøland							
MFG									
Q.A									

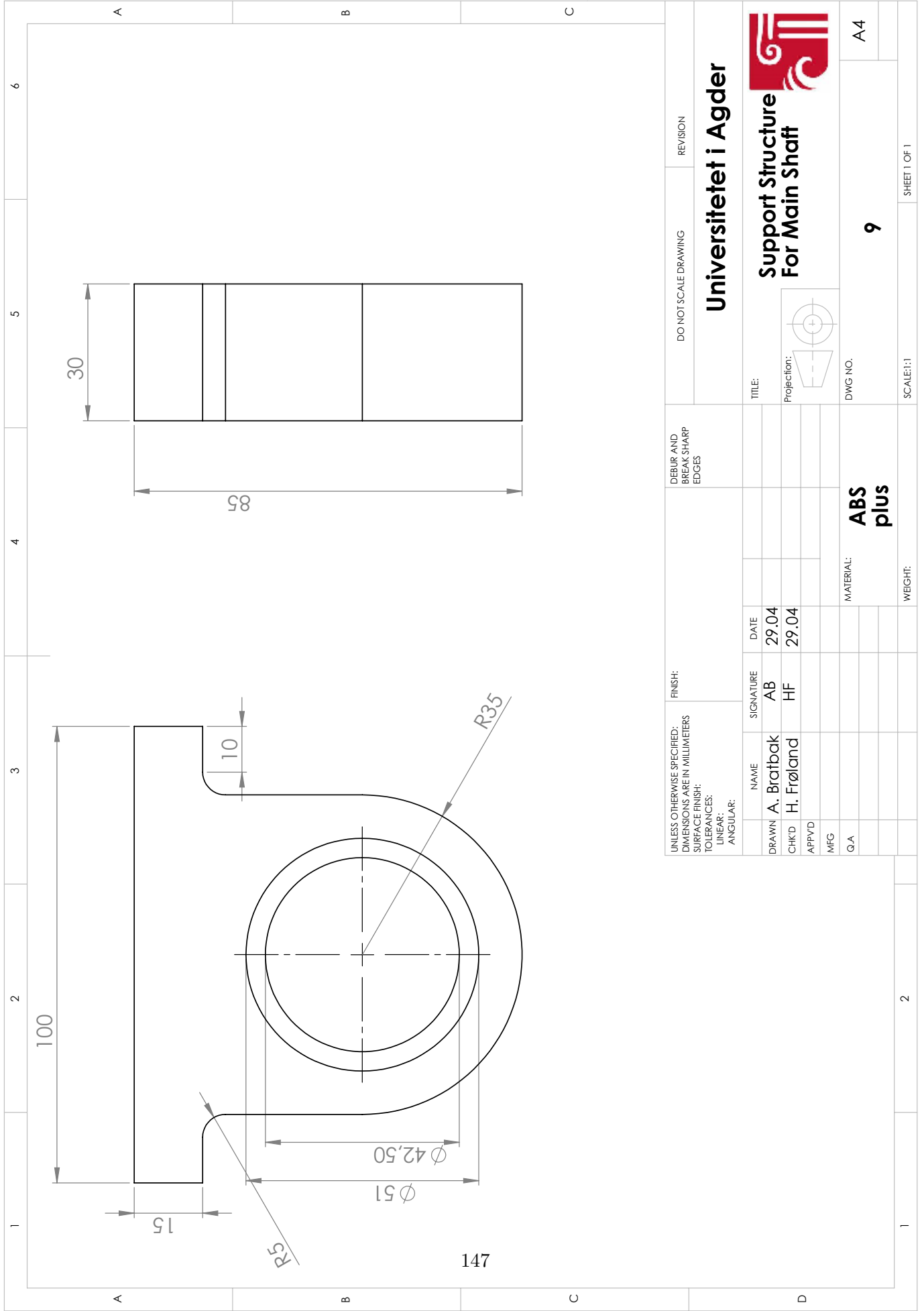




146

UNLESS OTHERWISE SPECIFIED: DIMENSIONS ARE IN MILLIMETERS		FINISH:		DEBUR AND BREAK SHARP EDGES		DO NOT SCALE DRAWING		REVISION	
SURFACE FINISH:		DRAWN		DATE		TITLE:		Universitetet i Agder	
TOLERANCES:		A.B		02.05		Projection:		Blade Support Rig	
LINEAR:		H.F		02.05		DWG NO.		8	
ANGULAR:		NAME		SIGNATURE		MATERIAL:		A4	
		A. Bratbak		A.B		ABS			
		H. Frøland		H.F		plus			
		APPVD				WEIGHT:		SCALE: 1:5	
		MFG						SHEET 1 OF 1	
		Q.A							



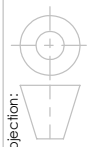


UNLESS OTHERWISE SPECIFIED: DIMENSIONS ARE IN MILLIMETERS		FINISH:		DEBUR AND BREAK SHARP EDGES		DO NOT SCALE DRAWING		REVISION	
SURFACE FINISH:									
TOLERANCES:									
LINEAR:									
ANGULAR:									
DRAWN	NAME	SIGNATURE	DATE	MATERIAL: ABS plus		DWG NO. 9		TITLE: Support Structure For Main Shaft	
CHK'D	A. Bratbak	AB	29.04						
APP'VD	H. Frøland	HF	29.04						
MFG									
Q.A.									
				WEIGHT:		SCALE: 1:1		SHEET 1 OF 1	

Universitetet i Agder



Support Structure
For Main Shaft



A4